Winter 12-23-2010

An integrated approach for phytate degradation and recovery of myo-inositol and phosphate as valued-added products from the by-products of corn ethanol industry

Jun Dang
University of Nebraska-Lincoln, jun.dang@huskers.unl.edu

An integrated approach for phytate degradation and recovery of myo-inositol and phosphate as valued-added products from the by-products of corn ethanol industry

By

Jun Dang

A DISSERTATION

Presented to the Faculty of
The Graduate College at the University of Nebraska
In Partial Fulfillment of Requirements
For the Degree of Doctor of Philosophy

Major: Engineering
(Chemical and Biomolecular Engineering)

Under the Supervision of Professor Hossein Noureddini

Lincoln, Nebraska
December, 2010

An integrated approach for phytate degradation and recovery of myo-inositol and phosphate as valued-added products from the by-products of corn ethanol industry

Jun Dang, Ph.D.

University of Nebraska, 2010

Adviser: Hossein Nouredddini

An integrated process was developed to hydrolyze the phytates in light steep water (LSW) and to simultaneously isolate inorganic phosphate (Pi) and myo-inositol products. The proposed integrated process is helpful in resolving the environmental and nutritional concerns in the use of corn gluten feed (CGF) in the animal diets. This process comprised of partial and total hydrolysis of LSW and intermediate anion exchange separation technique. The phytates in LSW were initially degraded to negatively charged myo-inositol phosphates ($InsP_2$ – $InsP_5$). The optimized experimental parameters for the partial hydrolysis of LSW were determined to be 2 h hydrolysis with 1 FTU *A. niger*/g substrate at 35 ℃. The negatively charged species of the partially hydrolyzed substrate were separated on a strong base anion exchange resin. The negatively charged species, retained by the resin, were eluted with 1M NaCl solution and were subjected to complete hydrolysis with *E. coli*, *A. niger*-derived phytases and their respective combinations. The maximum amount of myo-inositol released from the anion exchange column was detected after 48 h reactions catalyzed by 100 FTU *E. coli*, 150 FTU *E.coli*, and 150 FTU the combination of *A. niger* and *E. coli*. The time course of Pi released showed a similar trend to that of myo-inositol and the released Pi reached a

maximum amount after 48 h incubation at the enzyme loadings for which the maximum concentration of myo-inositol were reached.

An isocratic HPLC method was developed for routine analysis of myo-inositol and Pi. For myo-inositol, the limit of detection (LOD) was 0.01 mg/ml, and the limit of quantification (LOQ) was 0.04 mg/ml. The linear range of this method for myo-inositol was 0-20 mg/ml. The HPLC method is also a fast method for Pi quantification in the hydrolysate. The linear range of this method for Pi was 0-10 mg/ml. The LOD and LOQ were 0.05 and 0.17 mg/ml, respectively.

A size-exclusion chromatography packed was developed for isolating and purifying myo-inositol and Pi, from the mixture with *E.coli* phytase and Cl^-.

I dedicate this dissertation to my dearly beloved parents.

ACKNOWLEDGEMENTS

I would like to express my special gratitude to my advisor, Dr. Hossein Noureddini, for his guidance and support during my doctorate's study. I would also like to express my special thanks to Dr. Gustavo Larsen, Dr. Dennis D. Schulte, and Dr. Kevin Van Cott for serving on my supervisory committee and their help.

Thanks to Jongwon Byun, Mostafa Fatemi, and Hunter Flodman for their assistance during my experiments.

I also thank all professors and staff members in the Department of Chemical & Biomolecular Engineering that I have had the opportunity to interact with during my studies here.

Special thanks to Yinhuan Yuan for his encouragement and help during this dissertation writing.

TABLE OF CONTENTS

LIST OF TABLES

LIST OF FIGURES

Preface

The use of bioethanol as an alternative fuel helps to reduce greenhouse gas emissions, relieve energy crises and promote energy security. As a result, corn based bioethanol production has increased dramatically during the past two decades in the United States. According to the U.S. Department of Energy, bioethanol production has risen from 175 million gallons in 1980 to 10.6 billion gallons in 2009 [1]. With current planning of expansion in capacity and construction of new plants, this trend will continue. At least 15 billion gallons production is expected by 2015 [1].

Meanwhile, the ethanol production has increasingly become a low-profit process in recent years. The industry's current profit is mainly from the co-product, subsidies and tax waivers [2] and is facing profitability challenges due to significant increases in corn grain prices other expenditures (e.g. enzymes, yeast, chemicals, electricity, water, labor etc) [3]. To facilitate for the economic viability of this industry, one feasible approach is to optimize the use of the co-products of the process by increasing the quality of the co-products and by producing more value-added co-products [2, 3].

Dry-milling and wet-milling are the two main ethanol production processes and account for about 82 and 18% of the current ethanol production, respectively, producing distillers dried grains with solubles (DDGS) and corn gluten feed (CGF) as the major co-products [3]. CGF and DDGS contain important nutrients and high levels of phosphorous (P) (0.9-1.1%; DM basis) [4], which is much higher than that needed in animal diets (0.25 to 0.35%; DM basis) [5]. Moreover, the P in CGF and DDGS is mainly in phytate

form which can not be digested by nonruminant animals such as poultry and swine, leaving significant amounts of phytate P in their excreta. This phytate P-rich manure serves as a source of phosphorous and potentially could cause P pollution in soil and surface water resources [5-7]. Moreover, to guarantee the skeletal integrity and growth performance of swine and poultry, inorganic P supplements are also added into their diets which result in an added P in the animal excrete and further environmental concerns [8]. Phytates, also known as antinutrients, can strongly bind to divalent minerals (Ca^{2+}, Mg^{2+}, Zn^{2+} and Fe^{2+}), starch, and proteins, preventing their assimilation through the digestive system of nonruminant animals [9]. Thus, both nutritional and environmental problems are likely to occur when animals are fed with CGF and DDGS diets, compromising the quality of CGF and DDGS as an animal feed.

This research aims to eliminate the environmental and nutritional problems in the use of CGF and DDGS as animal feed, which are caused by phytate content. Moreover, as phytate is the main storage of myo-inositol and P, which are of great value and highly marketed products, the phytate in CGF and DDGS can provide a good source for the production of myo-inositol and P. The profits gained from myo-inositol and P can largely improve the industry's economic viability.

A previous study in this lab studied the P distribution in the dry- and wet –milling process. The WS stream, which is further processed to form DDGS, contains the whole of the P content of the starting corn. Light steep water (LSW), the intermediate stream to form CGF, contains most of the P entering the wet-milling process. Therefore, the objectives of this study include:

1) Explore the feasibility of reducing phytates in CGF and DDGS via enzymatic hydrolysis of LSW and WS.
2) Completely degrade phytate in the LSW and isolate myo-inositol and P as value-added products.
3) Develop analytical and separation methods for myo-inositol and P.

This dissertation includes 7 chapters. Chapter 1 introduced the current status of corn ethanol industry, the challenges it met, and the environmental and nutritional problems associated with the use of CGF and DDGS as the animal feeds. A literature review of phytate was also given in this chapter. In chapter 2, the feasibility of reducing phytates in CGF and DDGS via enzymatic hydrolysis of LSW and WS was studied. In chapter 3, chemical precipitation methods were tried to remove the phosphate released in chapter 2. Based on these studies, in chapter 4, an integrated process was developed to hydrolyze the phytates in light steep water and to simultaneously isolate inorganic phosphate (Pi) and myo-inositol products. To carry out routine analysis of myo-inositol and Pi, a HPLC method was developed and documented in chapter 5. In chapter 6, an approach of size exclusion chromatography was developed to isolate myo-inositol and Pi. Suggestions of future works were given in chapter 7.

Reference

[1] RFA., 2010. Ethanol industry outlook. Available from: http://www.ethanolrfa.org/page/objects/pdf/outlook/RFAoutlook2010_fin.pdf?nocdn=1

[2] Kale, A., Zhu, F.Y., Cheryan, M., 2007. Separation of high-value products from ethanol extracts of corn by chromatography. Ind. Crop. Prod. 26, 44-53.

[3] RFA., 2008. Ethanol industry outlook. Available from: http://www.ethanolrfa.org/page//objects/pdf/outlook/RFAoutlook2008_fin.pdf?nocdn=1

[4] Myer, B. and Hersom, M. Corn Gluten Feed for Beef Cattle. University of Florida IFAS extension. Available from: http://edis.ifas.ufl.edu/pdffiles/AN/AN20100.pdf.

[5] EPA., 1998. National water quality inventory: 1996 Report to Congress. EPA841-R-97- 008, Office of Water, Washington, DC. June.

[6] Parry, R., 1998. Agricultural phosphorous and water quality: a US Environmental Protection Agency perspective. J. Environ. Qual. 27, 258-261.

[7] Sharpley, A., Daniel, T. C., Sims, J. T., Pote, D. H., 1996. Determining environmentally sound phosphorus levels. J. Soil Water Conserv. 51, 160-166.

[8] Selle, Peter H., Ravindran, V., 2007. Microbial phytase in poultry nutrition. Anim. Feed. Sci.Tech. 135, 1-41.

[9] Ravindran, V., Bryden, W. L. and Kornegay, E. T., 1995. Phytates: occurrence, bioavailability and implications in poultry nutrition. Poult. Avian. Biol. Rev. 6, 125-143.

Chapter 1

Introduction

1.1 Overview of the Ethanol production

The ethanol industry is the fastest growing renewable energy industry in the U.S. and the ethanol production has increased dramatically since 2000. Ethanol production in 2001 increased by 8.5% from the previous year, while it increased more than 550% in 2009 compared with the year 2000 [1]. As of December 2009, 200 ethanol plants have been constructed with a production capacity of 10.6 billion gallons, which represents 8% of the gasoline supply [1]. An additional 16 ethanol plants with 1.4 billion gallons of new capacity are being built to meet the rising demand of ethanol created by the Renewable Fuel Standard (RFS) [1]. The RFS was part of the Energy Independence and Security Act of 2007 and mandated a gradual increase in the country's use of renewable fuels to 36 billion gallons in 2022 [2].

The growth in ethanol production is driven by the factors of environmental and health concerns, energy security, and economics. With a high octane rating of 106, the ethanol is used as the oxygenate replacement of methyl tertiary butyl ether (MTBE) and lead in the gasoline which are both associated with environmental and health problems [3]. The ethanol is primarily blended with gasoline at the 10% and 85% level to form E10 and E85 [4]. In the U.S. almost 80% of all gasoline sold contains ethanol [1]. E10 can be used in current high-compression engines without any modifications and keeps them

running smoothly. E85 is considered as a replacement of gasoline. It is used in flexible-fuel vehicles such as many light trucks, minivans, and SUV produced since 1996 in the U.S. According to the National Ethanol Vehicle Coalition, there were more than 8 million flexible-fuel vehicles in the U.S. as of 2009 [5]. Both E10 and E85 are cleaner-burner fuel than straight gasoline, as the combustion of ethanol only produces the carbon dioxide (CO_2) and water as the end products. The ethanol fuels reduce the emission of harmful pollutants such as carbon monoxide (CO), fine particulate matter (PM), and volatile organic compounds (VOC) [6]. Because the CO_2 emitted during ethanol combustion is harvested by the plants from the atmosphere, which is converted into carbohydrates through photosynthesis and metabolic pathways, the ethanol also reduces the emission of green house gas CO_2 [7]. Ethanol industry has also become an important sector of the U.S. economy. In 2009, ethanol industry contributed $53.3 billion to the nation's Gross Domestic Product (GDP), created nearly 400,000 jobs, and provided $16 billion for American households. This significant economic contribution by ethanol industry will grow as the industry expands and incorporates new production technologies and feedstocks [1].

Currently, the ethanol is mainly made from corn in the U.S. In 2009, 3.8 billion bushels of corn were used for ethanol production [1]. There are two methods for processing corn, wet-milling and dry-milling, and they generate different co-products.

1.1.1 Dry milling process

The dry milling process accounts for current 82% ethanol production and it will account for more because all planned expansions in capacity will also utilize this process

[1]. In dry milling, the whole corn kernel, without any fractionation, is milled by a grinder into a medium-coarse to fine grind meal. This corn meal is then mixed with water to form a slurry and subjected to a cooking procedure. During the cooking process (pH 5-6; temperature 180 -195 ℉), alpha amylase enzyme is added to the slurry to facilitate the hydrolysis of corn starch to dextrose, a simple sugar. With high temperature, the cooking process also reduces the levels of unwanted bacteria before fermentation. The resultant dextrose laden mash is then cooled and sent to fermenters where yeast species, *Saccharomyces cerevisiae*, are added to facilitate the conversion of dextrose to ethanol and carbon dioxide (CO2). When fermentation is complete, the mash (beer), which contains 12-15% ethanol, is transferred into distillation columns to separate the ethanol. The remaining mixture of liquid and solids, referred to as whole stillage (WS), is sent to a centrifuge to separate the coarse solids from the liquid. The liquid, also referred to as thin stillage, is recycled to the beginning of the process or concentrated to about 30% solids in the evaporator which are called Condensed Distillers Solubles (CDS) or "syrup." The coarse solids collected from the centrifuge are wet distillers grains (WDG). The CDS are added to WDG to form wet distillers' grains with solubles (WDGS). Subjected to a further drying procedure, the WDGS forms dried distillers grains with solubles (DDGS) which has a longer shelf life. However, for reducing energy input and transportation costs, there are approximately 20-25% of WDGS sold to local feedlots [1].

DDGS are analyzed to contain about 45% carbohydrates, 29% protein, 10% oil, 9% lignin and 7% of minerals, ash, and others such as vitamins. These high levels of nutrients make DDGS highly valued and nutritious livestock feeds which are widely used in diet for beef (38%), dairy (39%), swine (15%), poultry (7%), and other (1%) [8].

A bushel of corn produces about 2.8 gallons of ethanol and 17-18 pounds of DDGS [1]. In 2009, about 27 million tons of DDGS were produced which increased by 17.3% from previous year and by 900% compared with the year 2000 [1]. With the expansion of ethanol industry, the amount of DDGS will increase as well.

1.1.2 Wet milling process

Wet milling plants are larger and produce more co-products than dry milling plants. The wet milling process is designed to fractionate the corn kernel into its main components for use in various food and industrial products. The corn kernel is comprised of endosperm, germ, aleurone, and a pericap, which hold about 62.0 % starch, 3.8% oil, 7.8% protein, 10.2% fiber, and 15.0% moisture [9]. The endosperm constitutes approximately 82 to 84% of the dry weight of the kernel and contains 86 to 89% of the starch. It also contains 74% of the kernel's protein, 16% of the kernel's lipid. Corn germ makes up 8 to 10% of the dry weight of the kernel and contains 45 to 50% of the kernel's oil. It also contains starch and protein. Pericap and tip cap contain the majority of fiber of the kernel and comprises less than 2% of the dry weight of the kernel [10]. Targeting on the starch, germ, protein, and fiber of the corn kernel, the wet milling can produce corn sweeteners, starch, oil, protein, ethanol, CO_2 and feed co-products, corn gluten feed (CGF) and corn gluten meal (CGM) [9].

In wet milling, the grain is cleaned and steeped in water under controlled conditions of temperature (50 ℃) and sulfur dioxide (SO_2) concentration (2000 ppm) for 24 to 48 hours to soften the kernel texture. This steeping facilitates the separation of the grain into its major component parts. The softened kernel is coarsely ground and the

germs are separated for producing corn oil and germ meal in a two-step operation involving primary and secondary attrition mills and hydroclones. The remaining components are further separated by screening, centrifuging, hydrocloning, and washing to produce starch, fiber, and feed co-products. The starch can be fermented into ethanol and/or processed into modified corn starch and corn syrup. The steeping liquor, also called light steep water (LSW), contains the accumulation of soluble corn matter and 5-10% solids which are 43-45% protein and many micronutrients [9]. It also contains lactic acid and other fermentation products so that it is slightly acidic [9]. Drained from the corn steeping tank, the LSW is concentrated to 40% solids to form heavy steep water. The heavy steep water is then added to the fiber (bran) to form CGF which contains 1/3 steep liquor and 2/3 fiber, accounting for 22–24% of initial corn solids entering the wet mill. The gluten component (protein) is filtered and dried to produce CGM. CGM contains 65–67% protein and low fiber content, accounting for 5% of initial corn solids. A typical wet milling process produces 67.5% starch, 7.5% germ, 5.0% gluten, 11.5% fiber, and 7.6% steep water soluble on a dry-weight basis [9].

The production of CGF and CGM is kind of stable since 2004. There were about 0.6 million metric tons of CGM and 3 million metric tons of CGF produced in 2009 [1].

1.2 Challenges met by the ethanol industry

To meet the request for expanded biofuel use in the Energy Independence and Security Act of 2007, the ethanol industry will keep expanding. Although it is mandated that starting from 2016, the cellulosic ethanol will replace the corn ethanol to meet the

increase in the RFS target [2], at least 15 billion gallons ethanol production from corn are still expected by 2015 [11]. Beyond2015, the corn ethanol will still continue to grow and mature, but with a limited capacity growth.

The corn ethanol industry nowadays faces challenges of economic feasibility and sustainability. Ethanol production has increasingly become a low-profit process in recent years [1,12]. This is mainly caused by the corn price which has increased from previous stable $2 per bushel to about $4 per bushel in 2007, and to $6 per bushel in 2008 [1]. According to USDA, the expenditure on corn feedstock contributes to 58.9% of the corn ethanol operating cost [1,4]. The remainder of the spending by the ethanol industry for ongoing operations include: energy and water (15.4%), industrial chemicals (10%), denaturant (5.6%), plant operations (4.6%), yeast and enzymes (1.9%), maintenance (2.1%), and debt service (10.3%) [4]. The corn price increase is driven by the greater corn demand with the expansion of corn ethanol industry. Currently, the operating costs are almost equal to or higher than the revenue from ethanol. The industry's profit is mainly from the co-products, subsidies and tax waivers [1,12]. Because of the current financial climate, some ethanol plants can't hedge their corn prices anymore. More than 40 ethanol plants have filed for bankruptcy since 2008 [13]. This includes Verasun, the world's largest ethanol producer, which filed for bankruptcy in 2008 [14].

As the corn ethanol has been solidly established as a foundation for the industry and will keep growing, there is need to improve profitability of this industry. For this purpose, one feasible approach is to optimize the use of the co-products produced in the process by increasing the value-gained from corn and produce more value-added by products.

In dry milling process, DDGS is the only co-product. The price of DDGS has been rapidly decreasing, $145/ton in 1980 to $67/ton in 2005 [15]. With the industry's expansion, the DDGS production will increase and its price will fall further. This will jeopardize the industry. DDGS contain all nutritious components from the incoming corn which are not fermentable such as proteins, fiber, fat, etc. Because of the near complete fermentation of starch, these remaining nutrients are supposed to be increased approximately three-fold in concentration compared to levels found in corn kernel [16]. However, these high value nutrients are sold at a discount price with DDGS. If these components could be separated and recovered as value-added co-products, the profitability of the dry-milling industry would be significantly increased. Currently, studies are being carried out to separate zein protein, corn (fiber) oils, and vitamins from the dry-milling process [12,17].

Wet milling produces more co-products than the dry-milling process since the corn kernel is fractioned into its basic components during the process. Even though the major fractions have been separated for products, more value-added products can still be explored, such as minerals, vitamins, phosphorus, etc. and the quality of co-products can be improved.

Considering the facts that the corn for ethanol production accounted for 30% of total corn utilization during 2008/2009 marketing season, and there are 30.5 million metric tons of feed co-products produced [1], producing more value-added products will significantly improve the ethanol industry's economic viability.

1.3 Environmental problems associated with the feed co-products

Although DDGS and CGF have important nutrient contents that add value to animal diets, their phosphorous content is much higher than what is needed in diets. Phosphorous is an essential nutrient for animal growth, accounting for about 22 percent of the mineral ash in an animal's body. It plays a critical role in bone and teeth development, and cellular metabolism. P (% of diet dry matter) is required in amounts ranging from 0.25 to 0.60% in poultry diets [18], from 0.15 to 0.55 % in swine diets [19], and from 0.32 to 0.38% in dairy diets [20]. However, the P levels in DDGS and CGF are 0.9% [21] and 1% [22], respectively. As a result, excess diet P is excreted, resulting in high P manure. A study of 16 Nebraska cattle feeding operations showed these co-products to have P input to output ratios doubled that of those not using such co-products [23]. This means for land application purposes P is more likely to be an environmental problem for animal feeding operations using ethanol co-products as a feedstuff than for those not using the co-products.

Moreover, even though the P levels in DDGS and CGF are high enough for the demand of poultry and swine, inorganic P supplement (such as dicalcium phosphate) is still added in their diets. This is because only 0-50% of the total P in the feeds can be utilized by the animals. This supplemental P is normally overfeed commercially, with excesses of 20 to 100% over published requirements commonly observed, and add more P to the environment [24]. However, in the diets for cattle, there is no supplemental P added because the animals can assimilate the amount of P they need. The reason lies in the fact that most of P (60-70%) in the plant feeds are in form of phytate which can not

be digested by nonruminant animals such as poultry and swine, because these animals lack endogenous enzymes capable of hydrolyzing phytate effectively [24]. The non-utilized phytate P is excreted and degraded by phytase in soil. The released P from phytate, together with the excessive P excreted in the manure, are retained with soil particles and pose potential threats to environment. If the capacity of the soil to retain P is exceeded, the P can go to surface runoff, causing water contamination [26,27,28]. Even worse is that eutrophication may occur as very small amounts of P can raise the concentration above the critical value for eutrophication. McDowell and Sharpley [29] investigated the release of P from soil surface to surface runoff and subsurface drainages. In this study, P concentrations that cause eutrophication was given at 0.01 to 0.03 mg/L. The nonpoint source (NPS) pollution caused by the animal feeding operations and the agricultural activities has been a focused issue for U.S. EPA, USDA, and U.S. agricultural and environmental leaders alike. According to U.S. EPA, NPS is the leading source of water quality impacts to rivers and lakes, the third largest source of impairments to estuaries, and also a major contributor to ground water contamination and wetlands degradation [26].

To reduce the amount of P excreted to the environment, one efficient approach is to increase the bioavailability of phytate P in the animal feeds, avoiding the use of inorganic P supplement, and to remove the excessive P in the animal feeds.

1.4 Phytate and its influence on animal nutrition

Phytate, the salt form of phytic aicd (*myo*-inositol 1,2,3,4,5,6-hexakis dihydrogen phosphate or $InsP_6$), are found in grains and seeds. Phytate serve several physiological functions, especially in seed germination. This organic complex is the main storage form of plant P, accounting for approximately two-thirds of the total P in plants [30]. The structure of phytate, which is based on the structure of phytic acid proposed by Anderson (Fig.1.1) [31], is shown in Fig. 1.2. The structure of phytic acid has been supported by the results of pH-titration and conductivity measurements, chemical hydrolysis, nuclear magnetic resonance, X-ray crystallography and ^{31}P-NMR studies [32]. The phytic acid consists of a ring of six carbon atoms esterified with phosphate groups. It has 12 displaceable protons: six in the strong acid range with a pKa of about 1.5, one in the weak acid range with a pKa of 5.7, two in the weak acid range with a pKa of 6.8-7.6, and three very weak acids with a pKa larger than 10. This suggested that the phytic acid is strongly negatively charged over the entire pH values normally encountered in grains, seeds, and plants. Because of its strong negative charges, phytic acid is a strong chelator, which can have strong ionic interactions with proteins and minerals such as Ca^{2+}, Mg^{2+}, Zn^{2+} and Fe^{2+}. The interaction between phytic acid and minerals can form soluble or insoluble phytate-mineral complexes, depending on pH and involved cations. The complexing is possible within a phosphate group or between two phosphate groups on either the same or different phytic acid molecules. Sodium and potassium phytate are soluble at all encountered pH values. Zinc phytate is insoluble above pH 4.3, and calcium phytate is insoluble above pH 5.5, whereas magnesium is insoluble above 7.2. Ferric

phytate is insoluble at low pH of 1 to 3, but slowly becomes soluble as pH above 4. In contrast, aluminum phytate is soluble at extremes of pH (<2.2 and >5). At a given pH, excess cations existing in the system tend to decrease the solubility of Ca, Mg, Al phytates, etc [24,32].

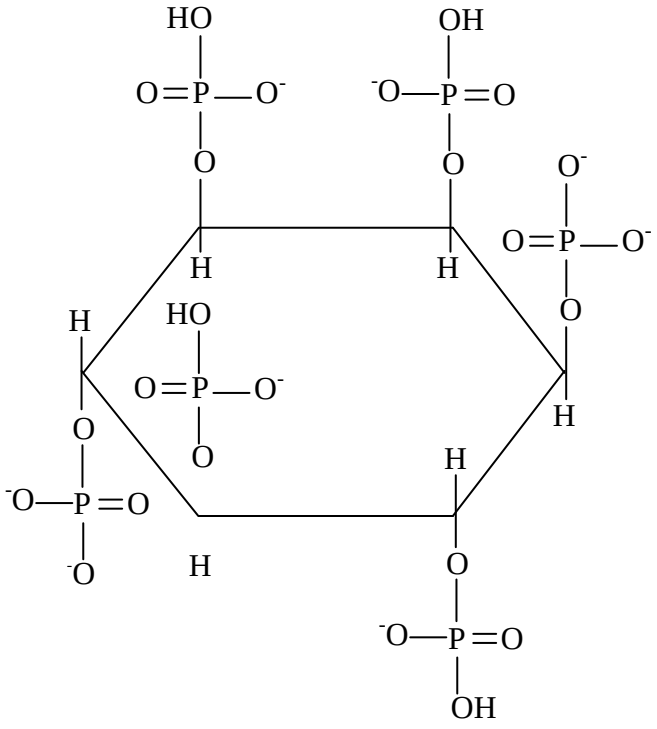

Fig.1.1. Structure of phytic acid [3]

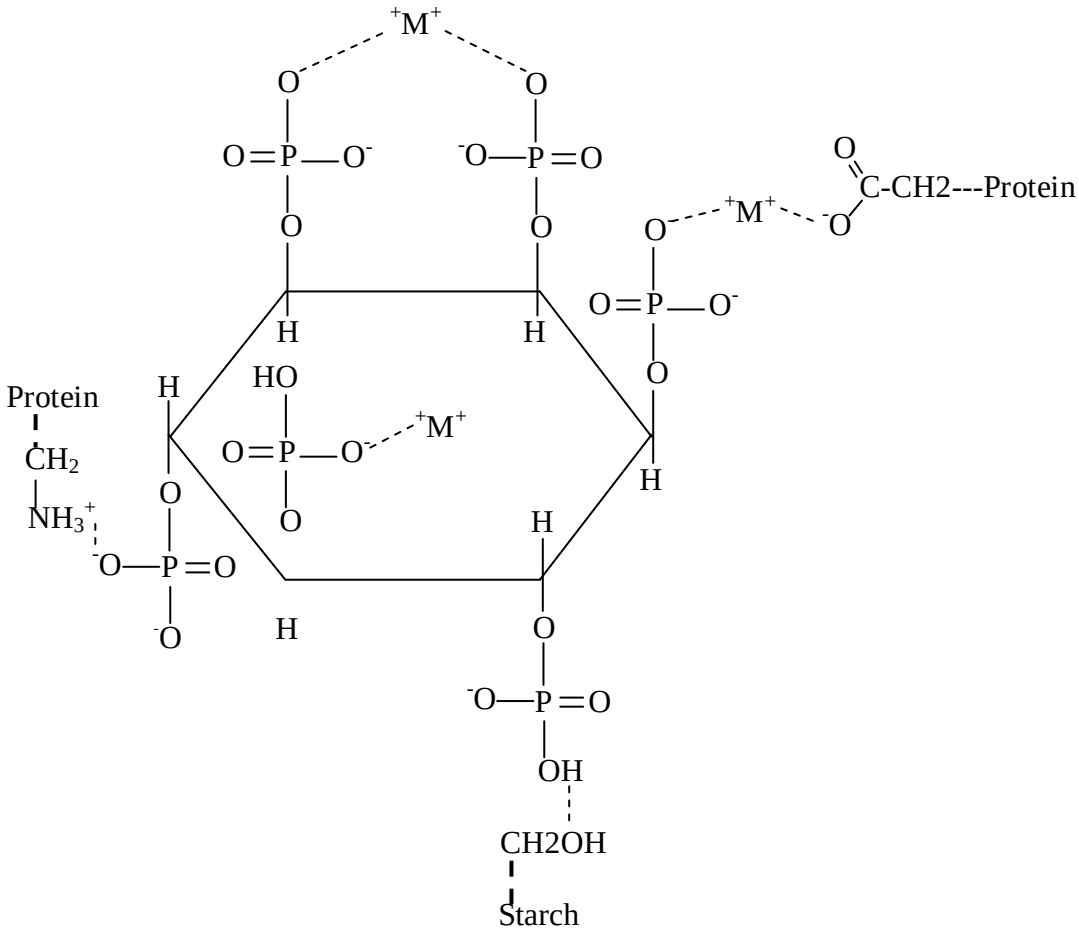

Fig.1.2. Possible structure of phytate

Interactions between phytic acid and protein can form binary phytate-protein or ternary phytate-mineral-protein depending on pH. There are distinct phytic acid and protein interactions in three pH regions: <pH 5, pH 5 to 7, >pH 7. At pH<5 which is below the isoelectric point of proteins, there is strong electrostatic interaction between negatively charged phytic acid and positively charged protein, forming binary phytic aicd-protein complex which only redissolves at pH <3. At pH above 7, multivalent cations can take part in the interaction, forming ternary phytate-minearl-protein complexes, which are completely insoluble. The formations of binary and ternary complexes were displayed in Fig.1.3 [24]. However, for the insoluble phytate precipitates formed at pH 5 to 7, there is a paucity of *in vitro* evidence to support the existence of binary and/or ternary phytic acid-protein complexes. Phytate can also bind with starch either directly by hydrogen bond, or indirectly by proteins associated with starch .Under normal physiological conditions, the minerals, proteins, and starch attached to phytic acid are unavailable for assimilation in nonruminant animals, because the complexes are refractory to pepsin activity. Therefore, phytates have been considered as antinutrients since they diminish the bioavailability of minerals and proteins to animals. In particular, the negative influence of phytate on the availability of Ca and trace minerals, particularly zinc, in human foodstuffs has been extensively investigated [24,32].

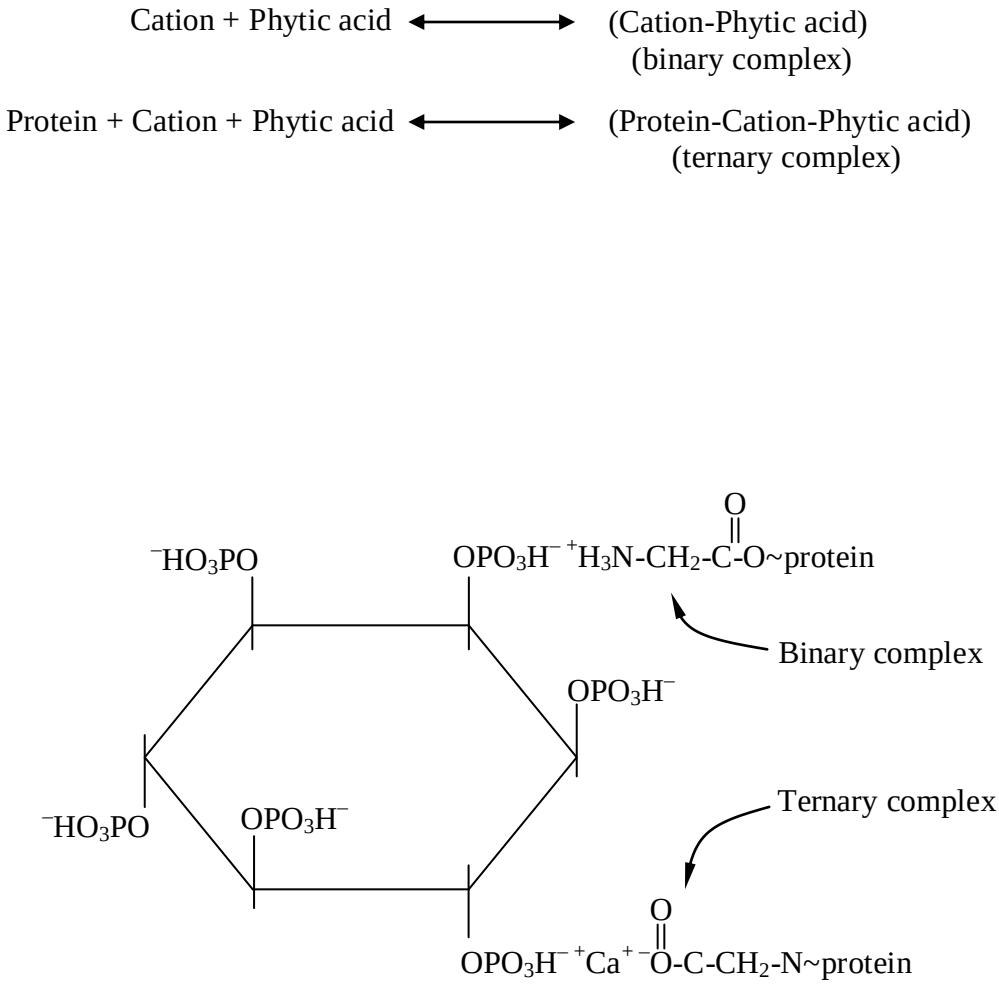

Fig.1.3. Formation of binary and ternary complex of phytate [24,32]

1.5 Benefits associated with phytate removal

Ninety percent of the phytate in corn is found in the germ portion of the kernel which accounts for approximately 50 to 80% of the P in corn [33]. This phytate accumulates in CGF and DDGS during the processes, resulting in high phytate content animal feeds. When animals are fed with these high phytate content diets, both nutritional and environmental problems are likely to occur. The high phytate concentration in DDGS and CGF compromise their quality as animal feeds. To solve these problems, the phytate need to be degraded so that the bonded minerals, proteins, and starch could be released and be available to animals. Meanwhile, part of the phytate P released would potentially satisfy the P requirement of animal diet so that the need for supplemental P in the diet will be eliminated. This will significantly lessen the environmental threats caused by the phytate P and supplemental P. It will also reduce the diet costs for swine and poultry producers, especially considering the fact that the cost of monocalcium phosphate, fed as an inorganic P supplement, has increased from approximtately $200/ton to $900/ton [34]. Another part of phytate P is the excessive P which can be removed from the animal diets and be recovered for fertilizer use. This application could have significant influence on the corn ethanol industry, corn farms, and even the phosphate rock ore storage on the earth. The price of fertilizer has been increasing since 2003. The price of diammonium phosphate (DAP) was $249 per ton in 2003 [35], while it was sold for $1,230 a ton in 2009 [36]. Fertilizer contributes 36% of the costs for corn farmers, which is the largest cost category [4]. Taking into account the fact that the corn feedstock made up 56% of ethanol costs in 2007, then the cost of fertilizer contributed roughly 20% of the cost of

the ethanol [4]. Thus, the excessive P recovered from DDGS and CGF would not only enhance the profitability of the ethanol industry, but also reduce the costs on corn farms, which might further reduce the corn price. Considering the fact that the total amount of P in phytate in all grains and seeds is equal to nearly 65% of the elemental P sold worldwide used in mineral fertilizers [37]. This recycling P will reduce the use of mineral fertilizers, lessen the depletion of mineral P storage on the earth.

Phytate is also a main storage of myo-inositol which can be recovered as a value-added product as well as P. Myo-inositol is a six-carbon, cyclic polyalcohol which was found to be present in mammalian plasma and peripheral nerves [38]. It is a water-soluble member of vitamin B complex and a fat solubilizing agent. Myo-inositol plays an important role as the structural base for a number of secondary messengers in eukaryotic cells which involved in cellular signal transduction [39]. Alterations of myo-inositol content may influence a certain metabolism pathway in living cells. Its deficiency will cause accumulation of triacylglycerols and abnormal fatty acid metabolism [40, 41]. The abnormal metabolism of myo-inositol was found to play a role in the pathogenesis of the polyneuropathies associated with diabetes mellitus and chronic renal failure. Modified amount of dietary myo-inositol was suggested for treating these diseases [42]. Myo-inositol is also considered as an important nutrient for infants since high concentrations of free myo-inositol was found in human milk comparing with that in infant formulae [43]. Myo-inositol has also been found to be promising in the treatment of cancer, depression, obsessive compulsive disorder, panic disorder, etc [44]. Myo-inositol is highly marketed and sold at around $16.95 per 750 mg [45].

With the expansion of corn ethanol industry, their feed co-products, DDGS and CGF, could provide an abundant resource for the production of P and myo-inositol (RFA, 2008). The profit gained from P and myo-inositol will significantly increase the industry's economic viability.

Reference

[1] RFA., 2010. Ethanol industry outlook. Available from: http://www.ethanolrfa.org/page//objects/pdf/outlook/RFAoutlook2010_fin.pdf?nocdn=1

[2] Energy Independence and Security Act of 2007. Available from: http://frwebgate.access.gpo.gov/cgi-bin/getdoc.cgi?dbname=110_cong_public_laws&docid=f:publ140.110.pdf

[3] Dien, B.S., Bothast, R. J., Nichols, N. N., and Cotta, M. A., 2002. The U. S. corn ethanol industry: An overview of current technology and future prospects. Int. Sugar. J. 104(1241), 204-208,210-211.

[4] Curtis, B., 2008. U.S. Ethanol industry: the next inflection point. United States Department of Energy (USDOE), Washington D.C., USA.

[5] National Ethanol Vehicle Coalition., 2010. Available from: http://www.ethanolretailer.com/opportunity-for-profit/

[6] Ward, O.P. and Singh, A., 2002. Bioethanol technology: developments and perspectives. Advances in applied microbiology. 51, 53-80.

[7] Luo, L., van der Voet, E.,and Huppes, G., 2009. Life cycle assessment and life cycle Costing of bioethanol from sugarcane in Brazil. Renewable & Sustainable Energy Reviews. 13(6-7),1613-1619.

[8] RFA., 2010. Industry Resources: Co-products**.** Available from: http://www.ethanolrfa.org/pages/industry-resources-coproducts

[9] Johnson, L. A. and May, J. B., 2003. Corn: Chemistry and Technology, 2nd ed., (White, P. J. and Johnson, L. A., eds.). American Association of Cereal Chemists, St. Paul, MN, pp. 449–494.

[10] Kinsella, J. E., 1995. Advances in food and nutrition.

[11] Korves, R., 2007. The Potential Role of Corn Ethanol in Meeting the Energy Needs of the United States in 2016–2030, prepared for the Illinois Corn Marketing Board, Pro-Exporter Network,Dec.

[12] Kale, A., Zhu, F.Y., and Cheryan, M., 2007. Separation of high-value products from ethanol extracts of corn by chromatography. Ind. Crop. Prod. 26, 44-53.

[13] www.treehugger.com/files/2008/11/40-corn-ethanol-plants-may-go-under-by-early-2009.php

[14] http://gas2.org/2008/11/01/verasun-one-of-usas-largest-ethanol-producers-files-chapter-11/

[15] Brehmer, B., Bals, B., Sanders, J., and Dale, B., 2008. Improving the corn-ethanol industry: studying protein separation techniques to obtain higher value-added product options for distillers grains. Biotechnol. Bioeng. 101(1):49-61.

[16] Kelly S. Davis.,2001. Corn Milling, Processing and Generation of Co-products. Minnesota Nutrition Conference & Minnesota Corn Growers AssociationTechnical Symposium.

[17] Moreau, R.A., Johnston, D. B., and Hicks, K. B., 2007. A comparison of the levels of lutein and zeaxanthin in corn germ oil, corn fiber oil and corn kernel oil. J. Am. Oil. Chem.Soc. 84(11), 1039-1044.

[18] NRC., 1994. Nutrient requirements of poultry. 9th rev. ed. Natl. Acad. Press, Washington, DC.

[19] NRC., 1998. Nutrient requirements of Swine. 10th rev. ed. Natl. Acad. Press, Washington, DC.

[20] NRC., 2001. Nutrient requirements of Diary. 7th rev. ed. Natl. Acad. Press, Washington, DC.

[21] Klopfenstein, T. J., Erickson, G. E., and Bremer, V. R., 2008. Board invited review: use of distillers by-products in the beef cattle feeding industry. J. Anim. Sci. 86:1223-1231.

[22] Myer, B. and Hersom, M. Corn Gluten Feed for Beef Cattle. University of Florida IFAS extension. Available from: http://edis.ifas.ufl.edu/pdffiles/AN/AN20100.pdf.

[23] Koelsch, R., and Lesoing, G., (1999) Nutrient balance on Nebraska livestock confinement systems. J. Anim. Sci. 77, 63-71.

[24] Selle, Peter H., Ravindran, V., 2007. Microbial phytase in poultry nutrition. Anim. Feed.Sci. Tech. 135, 1-41.

[26] EPA., 1998. National water quality inventory: 1996 Report to Congress. EPA841-R-97- 008,Office of Water, Washington, DC. June.

[27] Parry, R., 1998. Agricultural phosphorous and water quality: a US environmental Protection agency perspective. J. Environ. Qual. 27, 258-261.

[28] Sharpley, A., Daniel, T. C., Sims, J. T., Pote, D. H., 1996. Determining Environmentally sound phosphorus levels. J. Soil Water Conserv. 51, 160-166.

[29] McDowell, R.W. and Sharpley, A. N., 2001. Approximating phosphorus release from soils to surface runoff and subsurface drainage. Journal of Environmental Quality. J. Environ.Qual. 30 (2), 508-520.

[30] Reddy, N.R., 2002. Occurrence, distribution, content, and dietary intake of phytate. In: Reddy, N.R. and Sathe, S.K., Editors. Food Phytates, CRC Press, Boca Raton, FL, pp. 25–51.

[31] Anderson, R.J., 1914. A contribution to the chemistry of phytin, J. Biol, Chem. 17,171.

[32] Cheryan, Munir., 1980. Phytic acid interactions in food systems. Crit. Rev. Food. Sci.13, 297-335.

[33] Ravindran, V., Bryden, W. L. and Kornegay, E. T., 1995. Phytates: occurrence, Bioavailability and implications in poultry nutrition.Poult. Avian. Biol. Rev. 6, 125-143.

[34] Augspurger, N.R. and Baker D.H., 2008. The High Cost of Phosphorus for Pigs and Poultry: what are the Options? Available from: http://www.optiphos.net/OptiPhos_White_Paper.pdf.

[35] http://www.agecon.purdue.edu/news/financial/Fertilizer_Market.pdf

[36] http://www.sharecafe.com.au/fnarena_news.asp?a=AV&ai=14271

[37] Lott, J. N. A., I. Ockenden, V. Raboy, and G. D. Batten. 2000. Phytic acid and Phosphorus in crop seeds and fruits: a global estimate. Seed Sci. Res. 10:11–33.

[38] *S.Q. Alam.* The Vitamins: Chemistry, Physiology, Pathology, Methods. New York, Academic Press. (1971), vol. III, pp. 363-367.

[39] A.G. Thorsell, C. Persson, N. Voevodskaya, R. D. Busam, M. Hammarstroem, S. Graeslund, A. Graeslund, B. M. Hallberg. J. Biol. Chem. 283 (2008), 15209-15216.

[40] Eagle, H., Oyama, V. I., Levy, M., Freeman, A. E., 1957. Myo- Inositol as an Essential growth factor for normal and malignant human cells in tissue culture. J. Biol. Chem.226,191-205.

[41] Holub. B. J., 1992. The nutritional importance of inositol and the phosphoinositides. The New England journal of medicine. 326, 1285-1287.

[42] Clements, R.S. and Darnell, B., 1980.Myo-inositol content of common foods: development of a high-myo- inositol diet.The American journal of clinical

nutrition. 33, 1954-1967.

[43] Pereira, G.R., Baker, L., Egler.J., Corcoran. I ., and Chiavacci, R., 1990. Serum Myoinositol concentrations in premature infants fed human milk, formula for infants, and parenteral nutrition. Am. J. Clin. Nutr. 589-593.

[44] Nick, G.L., 2004. Inositol as a treatment for psychiatric disorders: a scientific evaluation of its Clinical effectiveness. In Townsend Letter for Doctors and patients. Available at: findarticles.com/p/articles/mi_m0ISW/is_255/ai_n6211958/

[45] http://www.vitasprings.com/inositol-myoinositol-100-caps-jarrow.html.

Chapter 2

Degradation of phytates in distillers' grains and corn gluten feed by *Aspergillus niger* phytase

2.1 Introduction

In the wet milling process, most of P and phytate P in CGF are attributed to the addition of the light steep water (LSW) which contains the majority of the P entering the plant. LSW is the liquid stream drained from the corn steeping tank. LSW is concentrated and added to the bran to form CGF. Ninety percent of the phytates in corn is found in the germ portion of the kernel which accounts for approximately 50 to 80% of the P in corn [1]. Rausch and coworkers measured the concentration and flow rate of P in three wet milling plants and concluded that 86% of the P entering the steeping process ended up in the LSW [2]. Noureddini and coworkers studied P distribution in corn processing, and found that phytate P accounted for approximately 80% of the total P in the LSW [3].

In the dry grind process, after the separation of ethanol from the beer stream, a slurry stream of all the processing remains called whole stillage (WS) is formed. This stream, which is further processed to form DDGS, contains the whole of the P content of the starting corn.

Since the LSW stream contains most of the P that enters the wet milling process, and the WS stream contains the whole P which is introduced into the dry grind process

from corn, the removal of phytate P from the LSW and WS will significantly reduce its level in CGF and DDGS [1].

Both enzymatic and non-enzymatic hydrolysis have been reported to degrade phytates. Non-enzymatic hydrolysis of phytates normally happens under high-temperature conditions. By autoclaving at 121 ℃ for 1 h, Phillippy et al. [4] studied the hydrolysis of phytic acid ($InsP_6$) and found that at pH 1.0, 2.0, 4.0, 6.0, 8.0, and 10.8, the percentages of $InsP_6$ decomposed were 67.7, 76.8, 89.6, 81.9, 65.8, and 45.1%, respectively. The hydrolysis products were a variety of isomers of $InsP_1$ to $InsP_5$ (Myo-inositol mono-, bis-, tris-, tetrakis-, and pentakis-phosphate) . They also found that in the pH range of 1.0–10.8, the lower the pH, the more even distribution of inositol phosphate isomers. Based on this property, Chen et al. [5] prepared reference standards of myo-inositol phosphates by heating $InsP_6$ solution which contains 2 M HCl at 140 ℃ for 1 h, obtaining a total of 27 peaks representing $InsP_2$–$InsP_6$ isomers. During the process, the decomposition percentage of $InsP_6$ is 95.3%.

The enzymatic hydrolysis, catalyzed by phytases, is more specific than nonenzymatic hydrolysis. Phytases are a special class of phosphatases that catalyze the sequential hydrolysis of phytate to various lower order inositol esters ($InsP_5$-$InsP_1$) and in some cases free inositol, and at the same time release free inorganic phosphates, bound minerals, starch and proteins (Figure 2.1). Phytases are presents in various amounts in plants, microorganisms, and certain animal tissues [7]. Depending on their origin, phytases behave differently in terms of specificity toward the position of hydrolysis on the inositol ring, formation of intermediates and final product , biochemical characteristics (e.g. pH optima and susceptibility to inhibitors and activators), and

biophysical characteristics (e.g. thermostability limits) [7-9].Three distinct classes of phytase, EC 3.1.3.8 (3-phytase), EC 3.1.3.26 (6-phytase), and EC 3.1.3.72 (5-phytase), have been identified, which initiate the dephosphorylation of phytate at the D-3, L-6 or D-4, and D-5 position of the inositol ring, respectively, producing different intermediate myo-inositol phosphate isomers [10,11].

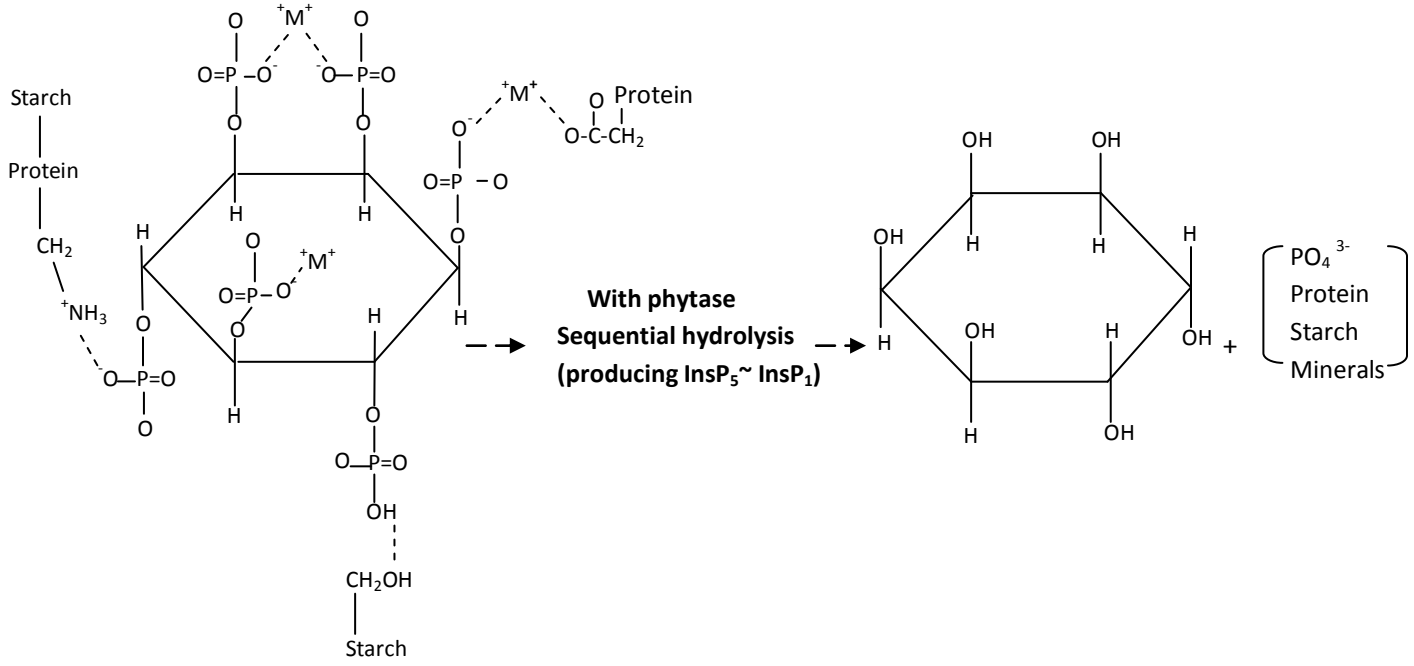

Fig.2.1. Illustration of a complete degradation of phytate

Exogenous microbial phytases (EC 3.1.3.8) have been added to the diets of swine and poultry to improve the utilization of the nutrients and phytate-P. The phytate degradation was assessed indirectly based on weight gain and bone mineralization. The addition of microbial phytases has been proved to improve the weight gain, mineral retention, amino acid digestibility, and bone mineralization [12,13]. The excretion level of phytate-P was also reduced. Nasi et al. observed that by adding 1000 FTU/kg *Aspergillus niger* (*A.niger*) phytase supplements into barley soybean diets, the Phytate-P excretion of pigs was reduced by 32-40%. Camden et al. observed that 500 FTU/kg *A.niger* phytase degraded 29.3% of phytate in a maize-soybean diets [15].

A.niger is one of the microbial phytases which has been most extensively studied because it has shown the highest activity yield when compared to 14 other Aspergillus species in screening for phytase production organisms [16]. *A.niger* derived phytase feed enzyme, with the capacity to liberate phytate-bound P, was commercially produced from 1991 [17]. *A.niger* is a high-molecular-weight (48.5-85 kDa) histidine acid phosphatase. It has a conserved active site motif, RHGXRXP. The other feature of phyA protein is the C-terminal HD motif (His361 and Asp362). The catalytic His (His82) and Asp (Asp362) residues come from very different parts of the protein and are located in close proximity to each other in the active site area of the phytase molecule. The histidine residue (His) has been proposed to serve as a nucleophile in the formation of phosphohistidine intermediate [17, 18]. The phytase optimum temperature was determined to be 55 ℃. Its deactivation occurs at 60 ℃ [18]. *A.niger* is known to produce two phytases, phytase A (PhyA) with an optimal pH at 2.0 and 5.5, and phytase B (PhyB) with an optimal pH at 2.5 [19, 20]. PhyA is the first commercialized phytase (Natuphos^{TM}) and currently holds

a large share of the world market [21]. Its comparatively low price ($1.6~2.4/lb) makes it ideal for industrial applications. The catalytic efficacy of PhyA as an animal feed additive has been testified [22, 23], and thoroughly reviewed by Wodzinski and Ullah [24]. However, the phytate degradation in vivo are not complete due to many factors such as temperature and pH. A better alternative is to provide animals with feeds containing less phytate.

The objective of this study was to explore the feasibility of reducing phytates in CGF and DDGS via hydrolyzing the LSW and WS with PhyA. The extent of hydrolysis was then evaluated by the inorganic phosphates (Pi) released during the process. Influences caused by variables such as enzyme loading and reaction temperature were also investigated. Determination of the distribution and form of P compounds in the corn milling operations and facilitating the degradation of the P in these compounds to Pi form is fundamental to the approaches that need to be taken to properly separate them from these streams and balance the amount of P compounds in the DDGS and CGF coproducts.

2.2 Experimental procedures

2.2.1 Materials

Substrates. LSW samples used in this study were from Cargill, a wet milling corn facility in Blair, Nebraska. WS samples were from Abengoa Bioenergy, a dry grind corn ethanol facility in York, Nebraska. The WS samples were finely grounded for experimental use with a laboratory blender (blender 7010HS, Waring Commercial, Vernon Hills, IL). All samples were kept in a refrigerator (4 ^{o}C) prior to use. When samples contained a mixture of solid and liquid, care was entailed to ensure the homogeneity of the samples taken before experiments.

Enzyme. Natuphos 10,000 liquid enzyme (3-phytase produced from Aspergillus niger) was purchased from BASF (Florham Park, NJ). The nominal activity of this enzyme was 10,000 FTU/g. This enzyme was diluted with DI water into 10, 100, 200 and 400 FTU/mL before use.

***Chemicals*.** Sulfuric acid (95-98%), sodium molybdate dehydrate (99.5%), ascorbic acid, hydrochloric acid (37%), potassium dihydrogen phosphate (1 M), zinc oxide (99.9%), potassium hydroxide, phytic acid (50% w/w), myo-inositol (99%), hydrochloric acid (37%), perchloric acid (70%), iron (III) nitrate nonahydrate (98%) were purchased from Sigma-Aldrich (St. Louis, MO). Deionized (DI) water was further purified by a Simplicity Ultra Pure Water System from Millipore (Billerica, MA). Hydrochloric acid (0.5 M) and a solution of 1 g/L $Fe(NO_3)_3$ in 0.33 M $HClO_4$ were filtered by 0.22 μm membrane filter from Millipore before use.

2.2.2 Enzymatic hydrolysis

Hydrolysis reactions were carried out in capped 125 mL Erlenmeyer flasks. Flasks were initially charged with 100 g of LSW or WS and a pre-specified amount of enzyme. The reaction mixture was incubated in a temperature-controlled incubator (Imperial III, Lab-Line Instruments, Inc., Melrose, IL) in which a shaker (C2 classic platform shaker, New Brunswick Scientific Co., Ltd., Edison, NJ) was placed to mix the reaction flasks at 200 rpm. At 0, 0.5, 1, 2, 4, 6, 8 and 24 h, aliquots of about 10 g each were taken from the reaction mixture. The reaction was terminated by heating the samples in a water bath at 100 °C for 10 min. Precautions were taken to avoid water vapor entering the samples. All hydrolysis experiments were performed in duplicates and the presented data are the mean values for the replicates.

2.2.3 Analysis

2.2.3.1 Enzyme activity

One phytase unit of activity (FTU) is defined as the amount of the enzyme, which, at 37 °C and pH 5.5, liberates 1.00 μmol of inorganic P per minute from 0.0051 mole sodium phytate/L. The analysis was based on the method developed by Engelen and co-workers [25]. In this procedure the phytase source was subjected to incubation with sodium phytate in order to liberate inorganic phosphate from the substrate. Molybdate-vanadate reagent was added to the reaction mixture to stop the reaction. Moreover, this reagent results in the formation of a colored complex with the freed inorganic phosphates. The absorbance of the yellow P complex was measured at a wavelength of 415 nm. A

standard calibration curve which was developed by BASF for the activity of Natuphos 10,000 phytase was used.

2.2.3.2 P analysis

Total phosphorus. The photometric dry-ashing procedure for the analysis of P was based on the standard method as adopted by the Nordic Committee on Food Analysis/AOAC International for determination of P in a variety of food samples [5]. Measurements were based on a colorimetric method where the color of the treated sample reflected the concentration of P. The samples were ashed to remove the organic (C, H, O) materials. Hydrochloric acid was added to the remaining inorganic ash residue to convert the P residues to a dissolved P form. This solution was used for color reaction based on the formation of a blue complex between phosphate and sodium molybdate in the presence of ascorbic acid as the reducing agent. The blue color of the complex was directly proportional to the amount of P.

Phosphorus in phosphate form (Pi). Experiments were carried out to determine the phosphate content in LSW and the liquid fraction of the WS samples during the course of dephosphorylation experiments. These procedures were based on a previous study [3] which recognizes the fact that P in the form of phosphate is totally soluble in water, whereas, P in the form of phytates could be found in both the solid and the liquid fractions of samples. Consequently, the ashing step and the subsequent addition of HCl were eliminated from the color reaction procedure and the rest of the procedure was followed as stated above for the determination of the total phosphorous.

For the determination of P in the liquid fraction of WS, samples were first centrifuged in a centrifuge (8464 Thermo Electron Co., Milford, MA), at 11,000 g for 10 min. The supernatant was then passed through a polytetrafluoroethylene (PTFE) 25 mm, 0.20 µm porosity syringe filter (Agilent Technologies, Wilmington, DE) to ensure the removal of all residual suspended solids. The collected supernatants were then subjected to the drying procedure as mentioned above.

Reagent preparation. All reagents were prepared as described by Pulliainen and Wallin [26] with some modifications. The procedures are as follows: (a) Sodium molybdate solution was prepared by mixing 140 mL of sulfuric acid (18M) with 300 mL DI water and 12.5 g of sodium molybdate in a 500 mL volumetric flask. (b) Ascorbic acid solution was prepared daily by adding 5 g ascorbic acid to DI water in 100 mL volumetric flask. (c) Molybdate-ascorbic acid solution was prepared immediately before use by adding 50 mL molybdate solution and 20 mL ascorbic acid in a 200 mL volumetric flask. (d) A 2 mg P /mL P stock solution was prepared by diluting 8.788 g potassium dihydrogen phosphate (KH_2PO_4) in a 1 L volumetric flask. (e) P working solution was prepared by diluting the P stock solution to0.1 mg P / mL and was used to prepare the calibration curve.

Color reaction. Dried samples (0.5-1.5 g) along were initially ashed with zinc oxide in a muffle furnace (McMaster-Carr 31605k55, Chicago, IL). Sample preparation followed the procedure outlined by Pulliainen and Wallin [26]. A quantity of the P solution so prepared (1.0 -10.0 mL) was taken for the color reaction with molybdate-ascorbic acid solution. Samples were taken in 1 mL cuvettes for analysis. The percent P content of the liquid samples was calculated using the calibration curve.

The experimental procedures for the determination of phosphate content of the supernatant fraction of the samples bypassed the ashing step and the subsequent addition of HCl. The amount of sample taken for these experiments was 1-5 mL in a 200 mL volumetric flask which depended on the expected P concentration. This was then neutralized with 50 % KOH and the rest of the procedure followed Pulliainen and Wallin [26]. All experiments were repeated twice. The mean values for the replicates and the standard deviations are presented in the "results and discussion" section.

Calibration. Quantitative determination of P in the samples was determined based on a calibration curve using different P concentrations. The P working solution was used in the calibration. Known volumes of this solution (1.00, 2.00, 3.00, 4.00, 5.00, and 6.00 mL) were charged into a 50 mL volumetric flask and diluted with DI water to 15 mL. This was followed by addition of 20 mL molybdate-ascorbic acid solution. The rest of the color reaction procedure was followed.

2.2.3.3 Myo-inositol phosphate analysis

The concentration of inositol phosphates in the LSW and WS was analyzed by HPLC equipped with a post column derivatizer. A post column derivatizer provides for the derivatization of the material after they are separated in the column. This is performed in the reactor compartment of this device with an appropriate derivatization reagent.

A UV spectrophotometer (Thermo Electron Co. 335906 GENESYS 10S, Milford, MA) was used to measure the P content by relating the intensity of the blue colored samples to the amount of P in them. The instrument was first zeroed with a blank reference sample. Sample absorbance was measured at 823 nm.

The HPLC system used for the analysis of inositol phosphates (P in phytate form) was a Waters Alliance system (Milford, MA) and consisted of a Separation Module (Waters 2695) and a Dual λ Absorbance Detector (Waters 2487). The HPLC was equipped with a post column derivatization instrument (Pickering Laboratories PCX5200, Mountain View, CA). The analytical column used for the separation was a CarboPac PA-100 and a CarboPac PA-100 guard column manufactured by Dionex (Sunnyvale, CA). The mobile phase was provided by gradient elution of a (0.5 M) HCl (A) and DI water solution (B) at 1.0 mL/min. The following describes the gradient elution profile which was maintained during the run; 0-16 min, 8-20% A, 92-80% B; 16-33 min, 20-37% A, 80-63% B; 33-49 min, 37-100% A, 63-0% B; 49-50 min, 100% A, 0% B; and 50-50.1 min, 100-8% A, 0-92% B. Total run time for this method was 60 min. Samples were filtered with a PTFE 25 mm, 0.20 μm porosity syringe filter (Agilent Technologies, Wilmington, DE) prior to the injection. Samples (25 μL) were injected via an injection port at an initial column temperature of 25 °C. The separated samples were mixed in the post column derivatizer reactor with a mixture of 0.1 % $Fe(NO_3)_3 \cdot 9H_2O$ and 2.0% $HClO_4$ at 0.8 mL /min. The HPLC system pressure range was from 2250 to 2400 psi and post column pressure was held constant at 200 psi. The Dual λ Absorbance Detector was set at 295 nm. Chen et al. [5] have reported the detection of 27 peaks representing IP_2-IP_6 isomers during the acidic hydrolysis (2 M HCl) of commercial phytic acid. This was the basis for identifying the peaks of the phytates in this study.

2.3 Results and discussion

2.3.1 Phosphorus content

Experiments were performed to determine the total P and the Pi content of WS and LSW. The Pi content of the samples established the baseline for the hydrolysis studies. Experimental procedures outlined earlier in the method section were followed. The results are summarized in Table 2.1. The total P and the Pi content for LSW were 5.1 ± 0.04 and 1.2 ± 0.01 mg/g LSW, respectively. The phytate P, quantified by HPLC, was 4.0 ± 0.01 mg/g LSW and was mainly in the form of $InsP_6$, accompanied by small amounts of $InsP_5$. About 0.07 mg/g LSW in Pi was attributed to the phytates which was due to the hydrolysis of $InsP_6$ to $InsP_5$ during the steeping process. The total P content in WS was determined to be 1.3 ± 0.02 mg/g WS. The total P content of the liquid and the solid fractions of the WS were determined to be 1.0 ± 0.06 and 0.3 ± 0.04 mg/g WS, respectively. The Pi in the liquid fraction of the WS was 0.7 ± 0.01 mg/g WS, accounting for 70% of the total P in the liquid fraction or 54% of the total P in WS. The remainder of phosphorous in the liquid fraction of the WS was mainly attributed to phytate P, mostly in form of $InsP_1$ and with trace amounts of $InsP_3$ and $InsP_2$ isomers.

Table 2.1 The distribution of phosphate P and phytate P in the liquid and solid fractions of the LSW and WS samples. All values are based on wet biomass.

Sample Description	Total P [mg P/g sample]	Phytate P [mg P/g sample]	Phosphate P [mg P/g sample]
LSW	5.1 ±0.04	4.0 ±0.01	1.2 ±0.01
WS	1.3 ±0.02	NA	0.7 ±0.01
Liquid fraction of WS	1.0 ±0.06	NA	0.7 ±0.01
Solid fraction of WS	0.3 ±0.04	NA	NA

Abbreviation used: WS, whole stillage; NA, not available. The data are mean value of 2 independent experiments.

2.3.2 Enzymatic hydrolysis of phytates

Hydrolysis experiments were carried out to examine the effect of PhyA enzyme on phytates in LSW as described earlier in the method section. The time dependency of phytate degradation was analyzed by HPLC and the formation of the inositol phosphate isomers was identified based on a reference chromatogram by Chen et al. [5]. The chromatograms for the hydrolysis of phytates in LSW, subjected to 1 FTU/g LSW, 35 ℃ and pH 4.3 is presented in Figure 2.2. As is shown by the chromatogram marked 0 h in this figure, $InsP_6$ was the main component of phytates in LSW, accompanied by a small amount of DL-Ins(1,2,4,5,6)P_5 and trace amount of DL-Ins(1,2,3,4,5)P_5. The analysis of the formed intermediate components in this figure suggests to a stepwise mechanism for the dephosphorylation of the phytates in LSW ($InsP_6$) via the formation of $InsP_5$, $InsP_4$, $InsP_3$ and $InsP_2$. During the first 1 h of the incubation, a marked decrease of $InsP_6$ content of the reaction mixture was observed, with concomitant increases of DL-Ins(1,2,4,5,6)P_5 and DL-Ins(1,2,5,6)P_4 content. Small amounts of DL-Ins(1,2,3,4,5) P_5, DL-Ins(1,3,4,5)P_4, DL-Ins(1,2,4,5)P_4, and trace amount of DL-Ins(2,4,5,6) P_4 were also observed at this time. The formation of DL-Ins(1,2,4,5,6)P_5 as the major $InsP_5$ isomer confirmed that *A.niger* initiates its attack on phytate at the 3 position *(22)*. As the incubation time was increased, the quantities of DL-Ins(1,2,4,5,6)P_5, DL-Ins(1,2,3,4,5) P_5 , DL-Ins(1,2,5,6)P_4 , DL-Ins(1,3,4,5)P_4, DL-Ins(1,2,4,5)P_4 and DL-Ins(2,4,5,6) P_4 decreased and eventually disappeared, while DL-Ins(1,2,6)P_3, DL-Ins(1,4,5)P_3 and DL-Ins(2,4,5)P_3 appeared as the major degradation products in the mixture. After 6 h incubation, $InsP_2$ isomers appeared as the main phytate components. These isomers include DL-Ins(1,2)P_2 , DL-Ins(1,4)P_2, DL-Ins(2,4)P_2, DL-Ins(2,5)P_2 and DL-Ins(4,5)P_2 and are identified by peaks 2-4 in

Figure 2.2. Their further degradation was observed with prolonged incubation. After 8 h incubation, no isomers of phytates were observed in the chromatogram, however, the presence of Ins(2)P_1 is suspect as documented by other researchers [8,10]. InsP_1 isomers were not separated in the analytical procedure which was followed in this study [5].

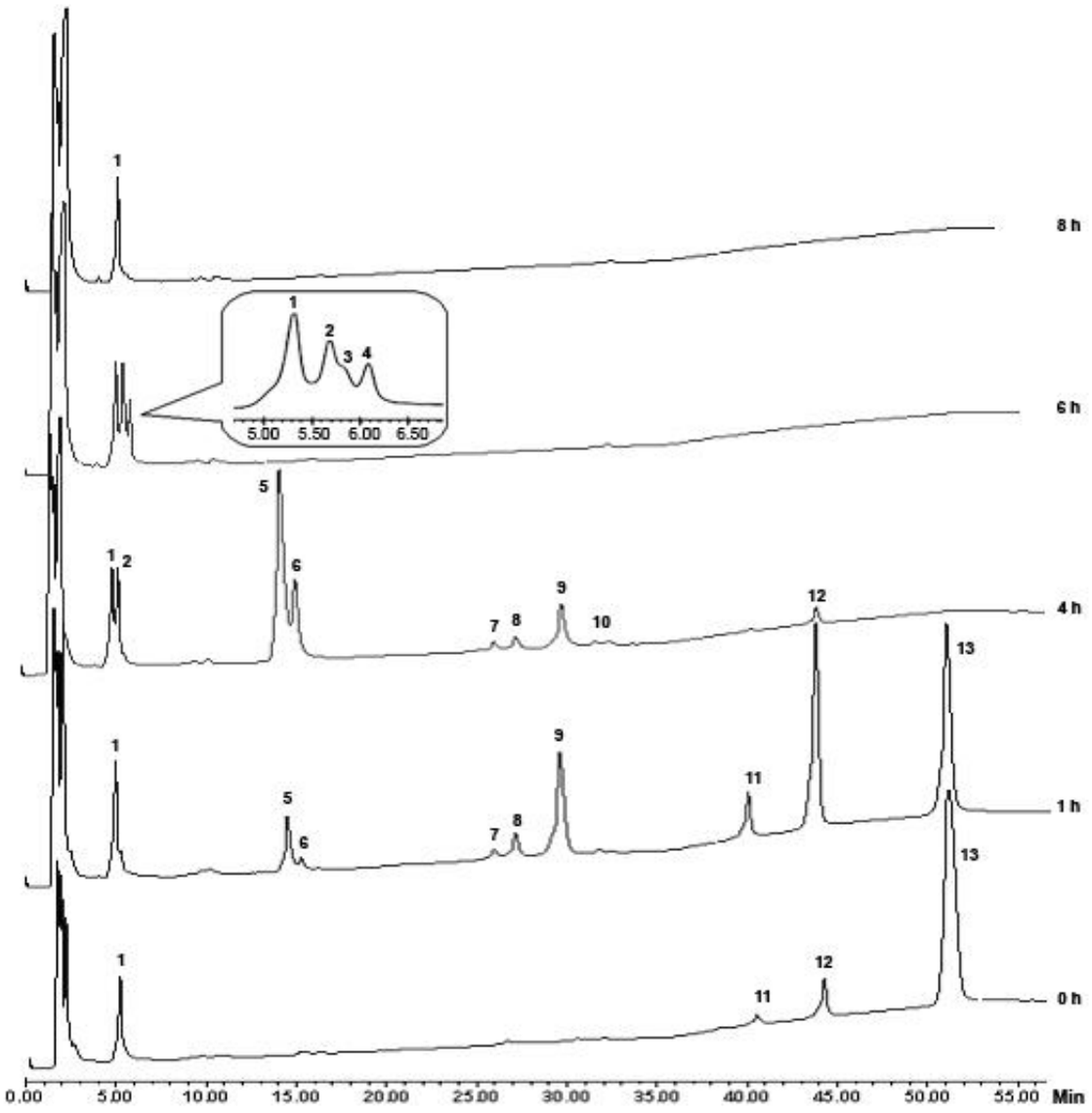

Fig.2.2. Chromatogram of the hydrolysis of phytate in LSW at 35 ℃, pH 4.33 and 200 rpm of shaker speed. Peaks: (1) unknown peak; (2) DL-Ins(1,2)P_2; (3) DL-Ins(2,4)P_2, DL-Ins(1,4)P_2; (4) DL-Ins(2, 5)P_2, DL-Ins(4,5)P_2; (5) DL-Ins(1,2,6)P_3; (6) DL-Ins(1,4,5)P_3, DL-Ins(2,4,5)P_3; (7) DL-Ins(1,2,4,5)P_4; (8) DL-Ins(1,3,4,5)P_4; (9) DL-Ins(1,2,5,6)P_4; (10) DL-Ins(2,4,5,6)P_4; (11) DL-Ins(1,2,3,4,5)P_5; (12) DL-Ins(1,2,4,5,6)P_5; and (13) InsP_6.

2.3.3 Effect of enzyme loading

Experiments were performed to examine the effect of enzyme loading on the hydrolysis of phytates in LSW and WS samples. In these experiments P in the form of phosphates (Pi) was quantified according to the method described earlier in the method section and was recognized as an indicator of the extent of the hydrolysis of phytates [27, 28].

2.3.3.1 LSW hydrolysis

For LSW, the extent of hydrolysis was quantified by the increase in the amount of Pi compared to the initial amount of Pi. The amount of Pi in LSW, which was attributed to slight hydrolysis during the steeping process, was also considered in the determination of the extent of hydrolysis reaction.

Enzyme loadings at 0.1, 1, and 2 FTU/g substrate were investigated for the hydrolysis of phytates in LSW. The experimental results quantifying the amount of released Pi from phytates as a function of time and otherwise identical conditions of 35 ℃, and pH 4.3 are presented in Figure 2.3. Under the performed hydrolysis conditions, a monotonic increase in the amount of released Pi was observed during the first 6 h of incubation. After this initial period, the amount of released Pi leveled off and additional incubation time appeared to have very little effect on the amount of formed Pi. Figure 2.3 reveals for the fastest rate of hydrolysis to correlate with the highest enzyme loading. At 2 FTU/g LSW, the plateau in the formation of Pi was reached after about 4 h, whereas, it

took more than 6 h for this point to be reached at 0.1 FTU/g LSW. The maximum amount of Pi was 4.52 ± 0.03 mg/ g LSW after 8 h incubation. This was reflective of an increase

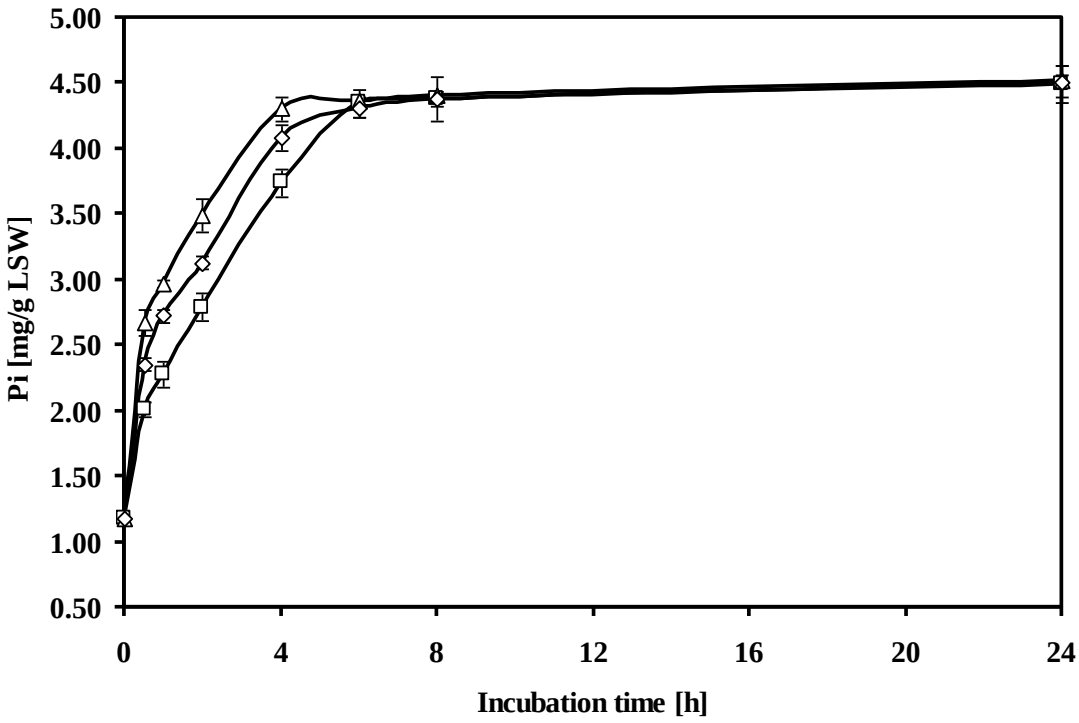

Fig.2.3. The effect of enzyme loading on the extent hydrolysis of LSW at 35 ℃, pH 4.33, 200 rpm of shaker speed (□) 0.1 FTU/g LSW; (◊) 1 FTU/g LSW; (∆) 2FTU/g LSW.

in the amount of Pi from 24 % to 90 wt% based on the total amount of P in the LSW. This level of Pi formation also was indicative of the release of about 83.5% of phytate in Pi form during this process. As was discussed in the previous section, the remaining phytates are believed to be mostly in form of $InsP_1$ [8]. This limitation is suggested to be due to the incapability of the enzyme to degradate $Ins(2)P_1$. $Ins(2)P_1$ as the end product is blamed on the structure of phytic acid. In phytic acid, five of the six phosphate groups are in equatorial position which can be released from the inositol ring easily with the PhyA enzyme, while the 2-phosphate group is in an axial position (Figure 2.4) which is refractory to the hydrolysis with this enzyme [8].

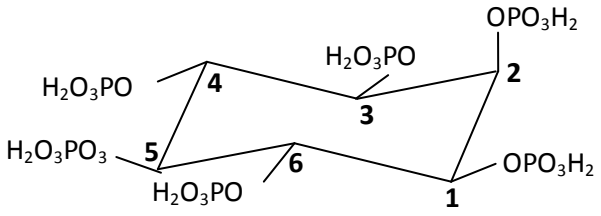

Fig.2.4. Energetically most favorable conformation of phytic acid (myo-inositol hexakisphosphate). The numbering of the carbon atoms is the numbering for the D-configuration

2.3.3.2 WS hydrolysis

Enzyme loadings with activities of 0.1, 1, 2, and 4 FTU/ g WS were investigated for the hydrolysis of phytates in WS. Figure 2.5 summarizes the results which show an increasing trend similar to that of LSW for the formation of Pi from phytates in WS. The most effective period of hydrolysis was during the first 2 h where a monotonic increase in the amount of released Pi was observed. After this initial period, the amount of released Pi leveled off and very little hydrolysis was detected afterward. Under hydrolysis conditions of 35 ℃ and at pH 4.85, the maximum amount of released Pi was detected at 0.86 ±0.01 mg/ g WS, at enzyme loadings of 1, 2 and 4 FTU/g WS. During the process, the Pi in the WS increased from 0.7 ±0.01 mg/ g WS (54% of total P in WS) to 0.86 ± 0.01 mg/ g WS (66% of total P in WS). The amount of Pi released in the hydrolysis mixture with the smallest enzyme loading of 0.1 FTU/ g WS was at 0.81 ±0.02 mg/ g WS.

A comparison between the hydrolysis of phytates in LSW and WS showed a much higher overall conversion of phytates in LSW which is suggestive of a different behavior between the two substrates. The higher conversion of phytates to Pi in LSW may be attributed to the fact that more than 75% of P in this substrate was in the form of soluble phytates (Table 2.1), which were readily available and were hydrolyzed by the PhyA enzyme. The distribution of P in the WS samples was considerably different from LSW. As shown in Table 2.1, more than 75% of the total amount of P was in the liquid fraction of WS substrate with 70% of it in form of Pi. This suggested to an extensive hydrolysis of phytates in this substrate during the course of the corn dry grind process. P

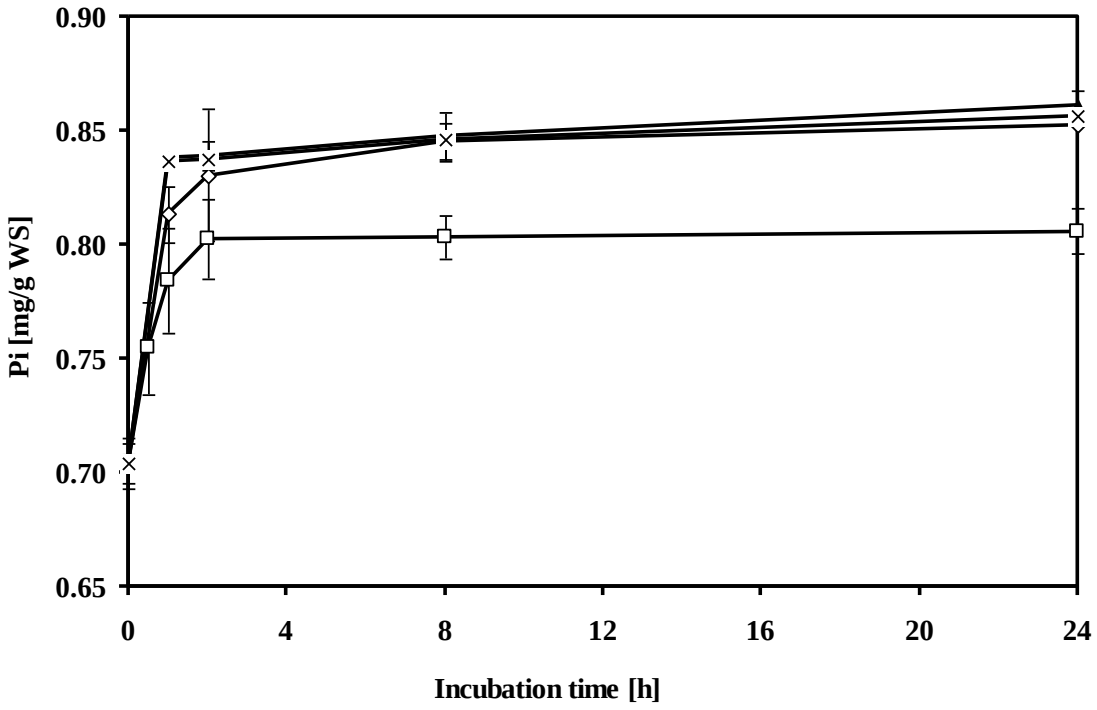

Fig.2.5. The effect of enzyme loading on the extent hydrolysis of WS at 35 ℃; pH 4.85 and 200 rpm of shaker speed. (□) 0.1 FTU/g WS; (◊) 1 FTU/g WS; (∆) 2 FTU/g WS; (×) 4 FTU/g WS.

in the liquid fraction of WS was predominantly in Pi form (70%) with the balance containing mostly $InsP_1$ and traces of $InsP_2$ and $InsP_3$ isomers with no appreciable amount of $InsP_4$ - $InsP_6$ isomers. As the distribution of the Pi released from the liquid and solid fractions of WS indicates (Table 2.2), there was equal contribution from the liquid and solid fractions of the WS to the hydrolysis reaction. This contribution was at about 25% of the unhydrolyzed P in the two fractions after 24 h reaction. The low level of hydrolysis in the liquid fraction is mainly because of the low level of phytates in this stream. As was indicated earlier, most of the P in the liquid fraction was in Pi form and very little of $InsP_2$ and $InsP_3$ were available to be hydrolyzed. The slow rate of hydrolysis of phytates in the solid fraction of the WS may be attributed to the diffusional limitations and lack of their availability to the active sites of the PhyA enzyme. The deactivation of PhyA enzyme due to its adoption to the solid particles may also have played a role in lower conversion of phytates in the WS samples. To investigate potential loss of enzyme activity in the WS samples, fresh enzyme at 0.1 and 1 FTU/g WS were added to WS sample which was initially subjected to hydrolyzed with 0.1 FTU/g WS enzyme for 2 h. As is shown in Figure 2.6, a significant increase in the amount of Pi was observed which was indicative of enzyme deactivation possibly by adsorption to the solid surfaces during the course of the hydrolysis of WS. However, examination of this procedure at higher enzyme loadings did not result in the formation of any additional Pi, which suggests that potential deactivations are compensated for by the higher presence of enzyme at the 1, 2, and 4 FTU/g WS levels of enzyme loadings.

Table 2.2 Time course of phosphate release from liquid and solid fraction of WS

Incubation time [hr]	Pi released from WS [mg/g WS]	Pi released from liquid fraction [mg/g WS]	Pi released from Solid fraction [mg/g WS]
0	0.70 ±0.01	0.70 ±0.01	0.00 ±0.01
0.5	0.80 ±0.01	0.76 ±0.02	0.04 ±0.01
1	0.83 ±0.02	0.75 ±0.03	0.07 ±0.01
2	0.84 ±0.01	0.76 ±0.01	0.08 ±0.01
8	0.85 ±0.02	0.76 ±0.01	0.09 ±0.01
24	0.85 ±0.01	0.78 ±0.01	0.07 ±0.01

Note: Temperature 45 ℃; pH 4.85; enzyme loading: 4FTU/g substrate. The data are mean value of 2 independent experiments

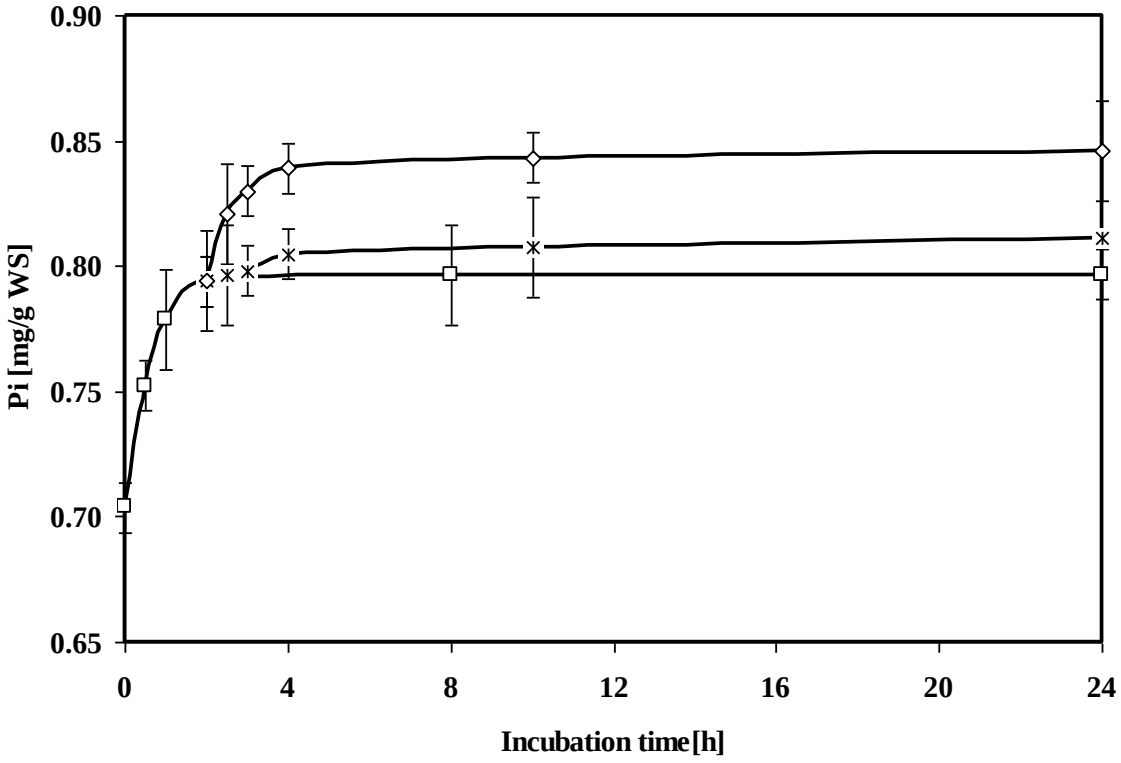

Fig.2.6. Addition of PhyA after 2 h hydrolysis of WS at 35 ℃, pH 4.85 and 200 rpm of shaker speed. (□) 0.1 FTU/g WS; (*) addition of 0.1 FTU/g WS; (◊) addition of 1 FTU/g WS.

2.3.4 Effect of temperature

Experiments were performed to examine the effect of temperature on the extent of the hydrolysis of WS and LSW with PhyA and the formation of Pi. Reactions were carried out at 35 ±1.0 and 45 ±1.0 ℃. As expected and shown in Figs. 2.7 and 2.8, the experimental results confirmed an increasing trend in the formation of Pi as a function of time. The intensity of this trend correlated well with the temperature and enzyme loading. Examination of the results for the hydrolysis of WS (Fig. 2.7) reveals a monotonic increase in the formation of Pi from the inception of the reaction to 2 h into the reaction which then started to slow done and eventually leveled off at longer reaction times. The results show a significant fraction of P in the Pi form at the end of the experiment. For example, at the conclusion of the hydrolysis reaction at 45 ℃ and 4 FTU/g WS of enzyme loading about 66 % of the P was determined to be in the Pi form. Considering the initial form of the Pi in the WS of 54%, there was a 12 % increase in the concentration of Pi. Experimental results for the hydrolysis of LSW revealed a similar trend as for the WS and is presented in Fig. 2.8. Nevertheless, a more significant part of the phytate P was released in the Pi form and a much longer reaction time was required for the reaction to complete. For example, at the conclusion of the hydrolysis of LSW at 45 ℃ and 4 FTU/g LSW of enzyme loading about 90% of the P was determined to be in the Pi form after 8 h reaction. This shows an increase of about 66% due to the hydrolysis reaction. When compared with WS, LSW showed a much higher level of phytate hydrolysis and higher levels of Pi formation which may be attributed to a much larger initial concentration of P in phytate form in LSW compared with the WS stream. The initial form of Pi in the WS was measured at 54% of the total P compared to about 24% for the LSW. Also the

availability of the phytates in the liquid phase in LSW makes their hydrolysis more favorable compared to the WS for which about 20% of the P is in the solid fraction at the beginning of the reaction.

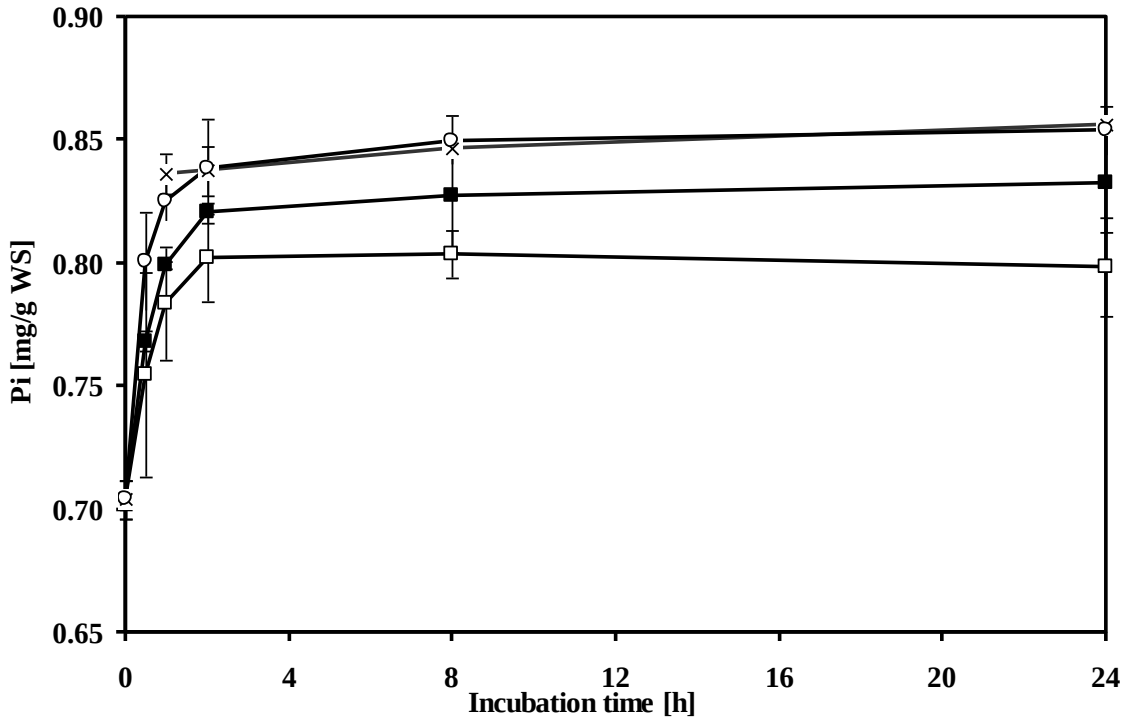

Fig.2.7. The effect of incubation temperature on the extent of hydrolysis of WS at pH 4.85 and 200 rpm of shaker speed. (□) 0.1 FTU/g WS at 35 ºC; (■) 0.1 FTU/g WS at 45 ℃ ; (×) 4 FTU/g WS at 35ºC; (○)4 FTU/g WS at 45ºC .

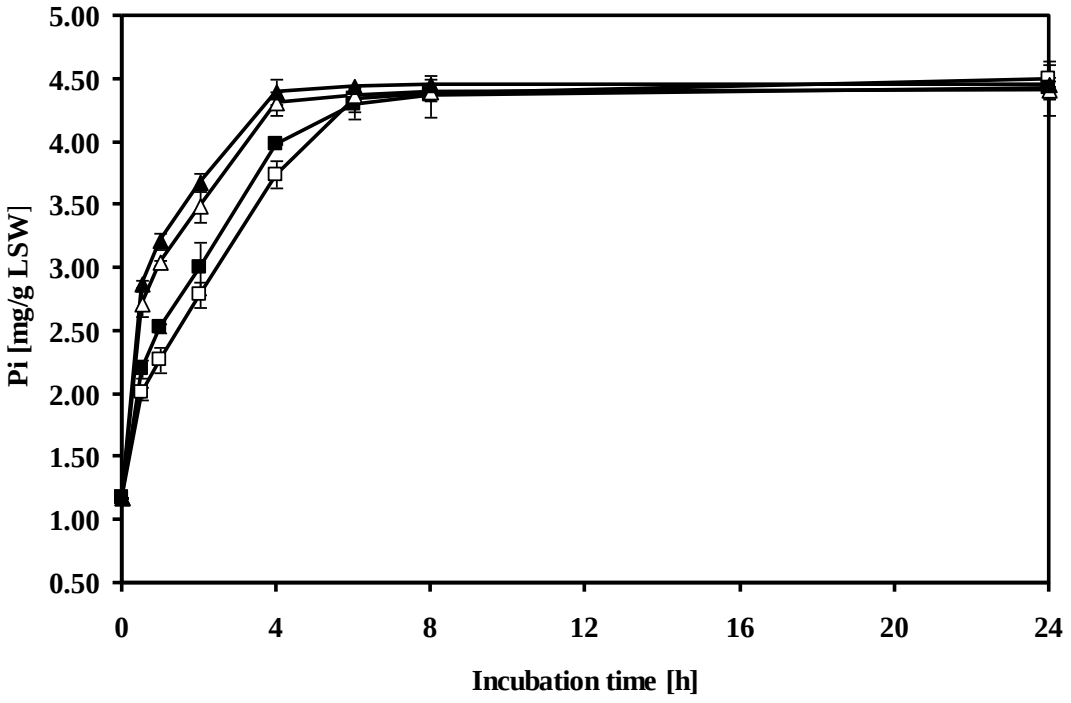

Fig.2.8. The effect of incubation temperature on the extent of hydrolysis of LSW at pH 4.33 and 200 rpm of shaker speed. (□) 0.1 FTU/g LSW at 35 ºC; (■) 0.1 FTU/g LSW at 45 ℃; (∆) 2 FTU/g LSW at 35ºC; (▲) 4FTU/gWS at 45ºC

2.4 Conclusions

The dephosphorylation of phytates in LSW and WS with PhyA from *Aspergillus niger* was investigated, which proceeded via the formation of $InsP_5$, $InsP_4$, $InsP_3$ and $InsP_2$ intermediates with Pi and $InsP_1$ as the end products. During the process, the amount of phosphate P in the substrates was increased from 54 to 66% in the WS, and from 20 to 90% in the LSW, suggesting to a substantial dephosphorylation of the phytates in the LSW and WS via PhyA catalyzed hydrolysis. Furthermore, this finding also suggests that the phytates level in the CGF and DDGS could be largely reduced, since LSW and WS contribute to a significant portion of phytates in these products. The majority of the phytate P in the LSW was in the form of soluble $InsP_6$ and $InsP_5$, which were readily hydrolyzed by the PhyA enzyme. However, the phytate P in the WS exists as both soluble phytates in the liquid fraction (mainly in the form of $InsP_3$ and $InsP_2$) and insoluble phytates in the solid fraction. The phytates in the liquid fraction were readily hydrolyzed by the enzyme, while the phytates in the solid fraction were partly degraded. Diffusional limitations and lack of their availability to the active sites of the PhyA enzyme were blamed for the slow rate of degradation of phytates in the solid fraction of WS.

Variations in enzyme loading and temperature on the hydrolysis rate and extent of the dephosphorylation were also examined. The time dependency of Pi release showed similar trends for both substrates with an increase in the trend of degradation with increases in temperature and enzyme loading. . The most effective period of degradation was during the first 2 h for WS and 6 h for LSW, and further increase of the reaction time

had little or no effect on the total amount of the Pi released. Under the experimental conditions which were investigated, the optimum hydrolysis for both LSW and WS was at 1 FTU/g substrate and at 45 ℃.

Reference

[1] Ravindran, V., Bryden, W. L. and Kornegay, E. T., 1995. Phytates: occurrence, Bioavailability and implications in poultry nutrition.Poult. Avian. Biol. Rev. 6, 125-143.

[2] Rausch, K. D., Raskin , L. M., Belyea ,R. L., Agbisit, R. M., Daugherty, B. J., Clevenger, T. E. and Tumbleson, M.E., 2005. Phosphorus concentrations and flow in Maize wet milling streams. Cereal Chem. 82, 431-435.

[3] Noureddini, H., Malik, M., Byun, J., Ankeny, A. J., 2009. Distribution of phosphorus compounds in corn processing. Bioresource. Technol. 100, 731-736.

[4] Phillippy, B.Q., White, K.D., Johnston, M.R., Tao, S.-H., and Fox, M.R.S., 1987. Preparation of inositol phosphates from sodium phytate by enzymatic and Nonenzymatic hydrolysis. Anal. Biochem. **162.** p. 115.

[5] Chen, Q. C. and Betty, W. L., 2003. Separation of phytic acid and other related inositol phosphates by high-performance ion chromatography and its applications. J.Chromatography A. 1018, 41-52.

[6] Cosgrove, D.J.,1980a. Phytase. In Studies in Organic Chemistry 4, Elsevier Scientific Publishing, Amsterdam, pp 85-98.

[7] Cosgrove, D.J., 1980b. Intermediates in the dephosphorylation of P6-inositols by phytase enzymes. In Studies in Organic Chemistry 4, Elsevier Scientific Publishing, Amsterdam, pp 99-105.

[8] Wyss, M., Pasamontes, L., Friedlein, A., Rémy, R., Tessier, M., Kronenberger, A., Middendorf, A., Lehmann, M., Schnoebelen, L., Röthlisberger, U., Kusznir, E., Wahl, G., Müller, F., Lahm, H. W., Vogel, K. and van Loon, A. P.,1999a. Biochemical characterization of fungal phytases (myo-inositol hexakisphosphate phosphohydrolases): catalytic properties. Appl. Environ. Microbiol. 65, 367-373.

[9] Wyss, M., Pasamontes, L., Friedlein, A., Rémy, R., Tessier, M., Kronenberger, A., Middendorf, A., Lehmann, M., Schnoebelen, L., Röthlisberger, U., Kusznir, E., Wahl, G., Müller, F., Lahm, H. W., Vogel, K. and van Loon, A. P., 1999b. Biophysical characterization of fungal phytases (myo-inositol hexakisphosphate phosphohydrolases):molecular size, glycosylation pattern, and engineering of proteolytic resistance. Appl. Environ. Microbiol. 65, 359 - 366.

[10] Gibson, D. M. and Ullah, A. H.,1988. Purification and characterization of phytase From cotyledons of germinating soybean seeds.Arch. Biochem. Biophys. 260, 503-513.

[11] Barrientos, L., Scott, J. J., and Murthy, P. P.,1994. Specificity of hydrolysis of phytic Acid by alkaline phytase from lily pollen. Plant Physiol. 106, 1489-1495.

[12] Nelson, T.S., Sheih, T. R., Wodzinski, R. J., and Ware, J. H.,1971. Effect of Supplemental phytase on the utilization of phytate phosphorus by chicks. J. Nutr.101, 1289-1294.

[13] Simons, P. C. M., A. Versteegh, H. A. J., Jongbloed, A. W., Kemme, P. A., Slump, P., Bos, K. D., Wolters, M. G. E., Beuteker, R. F., and Verschooor, G. J., 1990. Improvement of phosphons availability by microbial phytase in broilers and pigs. Brit.J. Nutr. 64, 525-540.

[14] Nasi, M., Partanen, K., and Piironen, J., 1999. Comparison of Aspergillus niger phytase and Trichoderma reesei phytase and acid phosphatase on phytate phosphorus availability in pigs fed on maize-soybean meal or barley-soybean meal diets. Arch. Anim. Nutr. 52(1),15-27.

[15] Camden, B. J., Morel, P. C., Thomas, HD. V., Ravindran,V. ,and M. R. Bedford., 2001. Effectiveness of exogenous microbial phytase in improving the bioavailabilities of phosphorus and other nutrients in maize-soybean diets for broilers. Anim. Sci. 73:289–297.

[16] Shieh, T.R. and Ware, J.H., 1968. Survey of Microorganisms for the Production of Extracellular Phytase. Appl. Microbiol. 16, 1348-1351.

[17] Selle, Peter H., Ravindran, V., 2007. Microbial phytase in poultry nutrition. Anim. Feed. Sci. Tech. 135, 1-41.

[18] Rao, D. E. C. S., Rao, K. V., Reddy, T. P., Reddy, V. D., 2009. Molecular characterization, physicochemical properties, known and potential applications of phytases : An overview. Crit. Rev. Biotechnol. 29, 182-198.

[19] Shieh, T.R., Wodzinski,R.J., and Ware, J.H., 1969. Regulation of the Formation of Acid Phosphatases by Inorganic Phosphate in *Aspergillus ficuum.* J. Bacteriol. 100, 1161-1165.

[20] Ullah, A.H. and Sethumadhavan, K., 1998. Differences in the active site environment of *Aspergillus ficuum* phytases.Biochem. Biophys. Res. Commun. 243, 458-462.

[21] Abelson, P.H., 1999. A potential phosphate crisis.Science. 283, 2015.

[22] Kim, T; Mullaney, E. J., Porres, J. M., Roneker, K. R., Crowe, S., Rice, S., Ko, T., Ullah, A.H. J., Daly, C.B., Welch, R., and Lei, X.G., 2006. Shifting the pH Profile of Aspergillus niger PhyA Phytase To Match the Stomach pH Enhances Its

Effectiveness as an Animal Feed Additive. Appl. Environ. Microbiol. 72, 4397-4403.

[23] Cromwell, G. L., Stahly, T. S., Coffey, R. D., Monegue, H. J., Randolph, J. H., 1993. Efficacy of phytase in improving the bioavailability of phosphorus in soybean meal and corn- soybean meal diets for pigs. J. Anim.Sci. 71, 1831-1840.

[24] Wodzinski, R. J. and Ullah, A. H.,1996. Phytase. Adv. Appl. Microbiol. 42, 263-302.

[25] Engelen, A.J., van der Heeft, F.C., Randsdorp P.H.G., and Smit, ELC.,1994. Simple and rapid determination of phytase activity. J. AOAC. Int. 77, 760-764.

[26] Pulliainen, T.K., Wallin, H.C., 1994. Determination of total phosphorus in foods by colorimetric measurement of phosphorus as molybdenum blue after dry-ashing: NMKL interlaboratory study. J. AOAC. Int. 77, 1557-1561.

[27] Angel, R., Tamim, N. M., Applegate, T. J., Ellestad, L. E., and Dhandu, A. S., 2002. Phytic acid chemistry: influence on phytin-phosphorus availability and phytase efficacy. J. Appl. Poult. Res. 11, 471-480.

[28] Xu, P., Price, J. and Aggett, P.J., 1992. Recent advances in methodology for analysis of phytate and inositol phosphates in foods. Prog. Food Nutr. Sci.16, 245-262.

Chapter 3

Phosphorus removal by chemical precipitation

3.1 Introduction

In chapter 2, for reducing phytate P in the CGF and DDGS, PhyA from *Aspergillus niger* was added to the LSW and WS to facilitate the dephosphorylation of phytates. During the process, the amount of phosphate P in the substrates was increased from 20 to 90% in the LSW and from 54 to 66% in the WS. These inorganic phosphorous (Pi) released after phytate degradation need to be removed from LSW and WS.

Technologies for Pi removal could be divided into biological, chemical, and physical methods [1]. Biological methods remove Pi by utilizing biomass to uptake P as their essential nutrient for growth. These include activated sludge method, membrane bioreactors, biological filters, etc. Chemical methods include chemical precipitation (including coagulation/flocculation), crystallization, and ion exchange. Physical methods include membrane filtration and adsorption. In this study, chemical precipitation was chosen as the method to remove Pi in the LSW.

Chemical precipitation for the removal of Pi is perhaps the earliest developed and commonly used method in water and wastewater treatment [1]. In chemical precipitation, Pi is precipitated by forming precipitates of sparingly soluble phosphates with salts of multivalent metal ions. Calcium hydroxide, ferric and aluminum salts are often used for chemical phosphorous removal [2-4]. Calcium hydroxide ($(Ca(OH)_2$) precipitates phosphate as insoluble dicalcium dihydrogen phosphate ($Ca(H_2PO4)_2$), dicalcium

phosphate dehydrate ($Ca(H_2PO_4)_2.2H_2O$), calcium hydrogen phosphate ($CaHPO_4$), calcium hydrogen phosphate dihydrate ($CaHPO_4.2H_2O$), and hydroxyapatite ($Ca_5(PO_4)_3.(OH)$), depending on pH values. Among these products, hydroxyapatite is a relatively stable product. The stated optimum pH for hydroxyapatite formation is in the range of 8 to 9.8 [2].

Ferric and aluminum salts precipitate Pi through a coagulation & flocculation process. Coagulation & flocculation is a physico-chemical process which destabilize dissolved and colloid impurities and producing large floc aggregates which can be removed in subsequent clarification/filtration process. When ferric and aluminum salts are added to water, the metal ions react with the water molecules and form a series of hydrolysis products. These hydrolysis products have large surface area and carry positive charge. For example, when ferric coagulants added to water in the pH range of 6-8, five monomers (Fe^{3+}, $Fe(OH)^{2+}$, $Fe(OH)_2^{+}$, $Fe(OH)_3$ (molecule) and $Fe(OH)_4^{-}$), a dimer and trimer ($Fe_2(OH)_2^{4+}$ and $Fe_3(OH)_4^{5+}$), and a solid precipitate ($Fe(OH)_3$ (s)) are formed. These ferric polymeric species can be represented as $[Fe_m(OH)_x]_n^{(3m-x)n+}$. They precipitate phosphate through charge-neutralization, complexation, and/or adsorption [5-8]:

(1) Charge neutralization

$$Fe(OH)_2^{+} + H_2PO_4^{-} \longrightarrow Fe(OH)_2H_2PO_4$$

(2) Complexation

$$[Fe_m(OH)_x]_n^{(3m-x)n+} + H_2PO_4^{-} \longrightarrow \{[Fe_m(OH)_x]_n\, H_2PO_4\}^{[(3m-x)n-1]+}$$

(3) Adsorption (association without charge neutralization)

$$[Fe_m(OH)_x]_n^{(3m-x)n+} + H_2PO_4^{-} \longrightarrow [Fe_m(OH)_x]_n^{(3m-x)n+}H_2PO_4^{-}$$

Ferric sulphate, ferric chloride, and aluminum sulphate, are the most commonly used coagulants. However, it is found that when added to water/wastewater, these mono-metal salts experience extremely rapid and uncontrolled hydrolysis so that the rate of charge-neutralization, complexation, and adsorption may be much lower than the precipitation rate of their hydroxide products, which compromises their performance as coagulants [5]. To improve the removal efficiency, the aluminum/ferric salts are partially hydrolyzed prior to their addition to the water/wastewater. The subsequent products formed are preformed polymeric aluminum/ferric such as poly-ferric sulphate (PFS) and poly-aluminum sulphates (PAS). These preformed polymers are relatively large and carry a high cationic charge which improve the surface activity and charge neutralizing capacity. They consume less alkalinity than the mono-ferric/aluminum salts does. Furthermore, even with a lower dose, these polymers realize a higher P removal efficiency [5-8].

In some treatments, ferric salts are considered as a better choice than aluminum salts because aluminum will pose substantial risk to health when accumulating in body to a certain level, such as Alzheimer's Syndrome, Osteoporosis, Anemia, and Anorexia [8].

The objective of this chapter was to find the efficiency of chemical precipitation on removing the phosphorous released in LSW after its hydrolysis with 1 FTU A.niger/g LSW at 45 ℃. Both direct chemical precipitation with $Ca(OH)_2$ and coagulation/flocculation with $Al_2(SO_4)_3$, $FeCl_3$, and PFS were tested. LSW (pH 4.3) contains proteins and divalent cations such as Fe^{2+}, Cu^{2+}, Mg^{2+}, Ca^{2+}, Zn^{2+}, etc, which can form insoluble products at elevated pH value, thus, no additional alkaline was added to adjust the pH of the LSW. The pH of the system was only influenced by the chemicals

added for the precipitation. The variations in pH and optimum doses of chemicals for precipitation were investigated. The optimum dose of a coagulant is defined as the value above which there is no significant difference in the increase in removal efficiency with a further addition of coagulant [9].

3.2 Experimental Procedures

3.2.1 Materials

LSW samples used in this study were from Cargill, a wet milling corn facility in Blair, Nebraska. All samples were kept in a refrigerator (4 ^{o}C) prior to use. As samples contained a mixture of solid and liquid, care was entailed to ensure the homogeneity of the samples taken before experiments.

Natuphos 10,000 liquid enzyme (3-phytase produced from *A. niger*) was purchased from BASF (Florham Park, NJ). The nominal activity of this enzyme was 10,000 FTU/g. Aluminum sulphate octadecahydrate (98%), calcium hydroxide (95%), iron (III) chloride (97%), sulfuric acid (95-98%), sodium molybdate dehydrate (99.5%), ascorbic acid were purchased from Sigma-Aldrich (St. Louis, MO). PFS (MW 562, 10-13% Fe concentration) was donated by kemira water solutions Inc. (Bartow, FL). Deionized (DI) water was further purified by a Simplicity Ultra Pure Water System from Millipore (Billerica, MA).

3.2.2 Procedures

3.2.2.1 Enzymatic hydrolysis of LSW

LSW were subjected to 8 h hydrolysis with 1 FTU *A.niger*/g LSW in capped 125 mL Erlenmeyer flasks. The reaction mixture was incubated at 35 ℃ in a temperature-controlled incubator (Imperial III, Lab-Line Instruments, Inc., Melrose, IL) in which a shaker (C2 classic platform shaker, New Brunswick Scientific Co., Ltd., Edison, NJ) was placed to mix the reaction flasks at 200 rpm. After 8 hr, the reaction was terminated by heating the samples in a water bath at 100 °C for 10 min. Precautions were taken to avoid water vapor entering the samples. After hydrolysis, samples were subjected to Pi analysis according to the method described in 2.2.3.

3.2.2.2 Chemical precipitation

A jar test experimental procedure which allowed several tests to be conducted simultaneously was used to evaluate the performance of chemical precipitation. Experiments were carried out at room temperature. HLSW samples were cleared of solid particles in a centrifuge (8464 Thermo Electron Co., Milford, MA), at 11,000 *g* for 10 min, and only the clarified portion of the samples were used for the experiment. 10g clarified HLSW were introduced to each of the jar test beakers. Designed dosages of $Ca(OH)_2$, $FeCl_3$, PFS, and $Al_2(SO4)_3.18H_2O$ were added to each beaker respectively. Immediately after dosing, the jars were stirred at a high RPM (150rpm) for 1 minute for rapid mix. The speed was then reduced to 30 rpm for 30 min to allow the chemical reactions and formation of flocculants. After this, the jars were left to settle. After 60 min settlement, the supernatant was collected and filtered passed through a 0.20 μm porosity cellulose acetate filter (Agilent Technologies, Wilmington, DE) to ensure the removal of all residual suspended solids. The collected supernatants were then subjected to pH measurement with a Oakton Acorn Ion 6 Meter (Coleparmer,Vernon Hills, IL), and Pi

analysis following the procedure described in 2.2.3. The precipitations formed were vacuum filtered, and gently washed twice with DI water to remove any solubles left and dried at 60 ℃ in a 20GC convection oven (Quincy Lab, Inc., Chicago, IL) to constant weight. This weight was then measured and recorded.

All experiments were performed in duplicates and the presented data are the mean values for the replicates.

3.3 Results and discussion

3.3.1 P removal with $Ca(OH)_2$

Experiments were carried out to remove Pi in the hydrolyzed LSW (HLSW) with $Ca(OH)_2$ as described in section 3.2.2.2. The HLSW was prepared according to section 3.2.2.1. After 8 h hydrolysis with 1 FTU *A.niger*/g LSW, the concentration of Pi in the HLSW was 4.6 ± 0.07 mg/g HLSW, accounting for 92% of the total P (TP) which was 5.0 ± 0.04 mg/g HLSW.

Experimental resultsfor the removal efficiency of Pi and TP and pH variation against molar ratio of Ca/P are summarized in Figure 3.1. As shown in the Figure 3.1, the efficiency of Pi removal is related to both the dosage of $Ca(OH)_2$ and pH in the system. While the pH of the system is directly influenced by the amount of $Ca(OH)_2$ added. When pH was below 6.0, which corresponded to a Ca/P ratio of 1.4, some precipitation was observed, but with little removal of Pi. As more $Ca(OH)_2$ was added to the HLSW, the pH was increased and more precipitation was observed. When pH was in the range of 6-7, or molar ratio of Ca/P was in the range of 1.4-1.6, 83-84% of Pi were removed,

accounting for 77-78% of the TP. When the molar ratio of Ca/P was increased to 1.7, or pH above 7.2, a 98% removal of Pi or 91% of TP was observed. When the molar ratio of Ca/P was increased to 2.4, pH of the system reached 8.7 which resulted in 99% of Pi and 92% of TP to be removed from the HLSW.

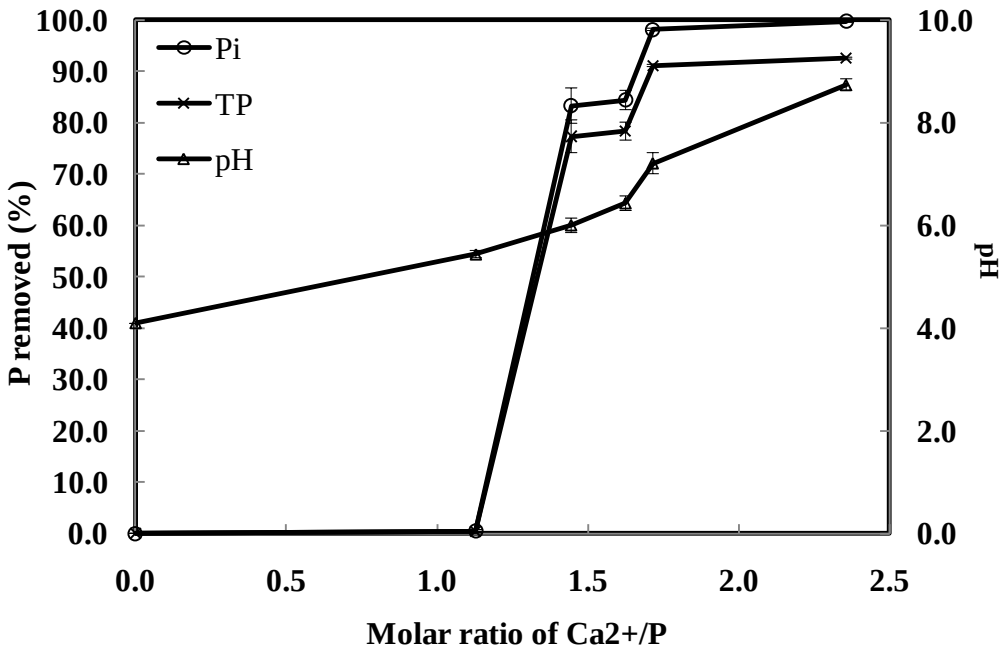

Fig.3.1. Pi removal with $Ca(OH)_2$

The precipitation curves presented in Figure 3.1 is also in line with the pka property of H_3PO_4 which has three pka value: 2.15 ($H_2PO_4^-$), 7.20 (HPO_4^{2-}), and 12.35 (PO_4^{3-}), respectively. Two obvious sections of Pi removal were observed between pH 6-7, and pH 7.2-8.7. When pH is in the range of 6- 7, the dominant precipitation formed of Pi is $Ca(H_2PO_4)_2$ and/or $Ca(H_2PO_4)_2 .2H_2O$. While when pH is between 7.2-8.7, the dominant precipitation is $CaHPO_4$ and/or $CaHPO_4$.H2O. However, from Figure 1, the amount of $Ca(OH)_2$ added to the system are larger than the stoichiometric amount needed of Ca to precipitate the Pi. This might be attributed to the minerals existed in the HLSW, such as Fe^{2+}, Cu^{2+}, Mg^{2+}, Zn^{2+}, etc. which contributed to the additional consumption of $Ca(OH)_2$ and were precipitated as their hydroxide compounds. As the solubility product constants of these minerals are very low, they can be precipitated out at a lower pH. And therefore, the OH^- introduced into the system was consumed partly to increase the pH of the system, and partly to precipitate certain metal ions in the HLSW. This explained the observed precipitation formed when $Ca(OH)_2$ was added to the HLSW (pH 5-6) while little Pi removal was observed. Accordingly, the precipitates formed in the experiments are a mixture of metal hydroxides, $Ca(H_2PO_4)_2$, and/or $CaHPO_4$.

The precipitates formed after adding 19 mg Ca(OH)2 /g HLSW (98% Pi removal) were vacuum filtered and dried and measured as described in section 3.2.2.2. A total of 290.5 mg (dry weight) precipitate was obtained which is more than the stoichiometric amount of 193.8 mg $CaHPO_4$ formed at pH 7.2. This also provided evidence that the metal ions in the HLSW were precipitated as well. Moreover, there are proteins and poly peptides existed in the HLSW. They could be co-precipitated by adsorbing onto the surface area of the precipitates formed.

3.3.2 P removal with coagulation/flocculation

Experiments of coagulation/flocculation were performed to remove Pi in the HLSW. Pre-specified amount of $FeCl_3$, PFS, and $Al_2(SO4)_3.18H_2O$ as the coagulants were added into the jar test beakers following the method described in section 3.2.2.2. Experimental results of different doses of $FeCl_3$, PFS, and $Al_2(SO4)_3.18H_2O$ on the removal of Pi and TP from the HLSW are summarized in Figure 3.2-4, respectively.

Figure 3.2 shows the effects of $FeCl_3$ as the coagulant on removing Pi in the HLSW. With increasing doses of $FeCl_3$, an initial monotonic increase in the Pi removal was observed and reached the maximum of 75% at the molar ratio of 1 (Fe/P). Correspondingly, at this molar ratio of Fe/P, the largest amount of flocs were observed in the system. The flocs formed were a series of hydrolysis products such as $Fe(OH)^{2+}$, $Fe(OH)_2^{+}$, $Fe(OH)_3$ (molecule), etc. After this molar ratio of 1 (Fe/P), the amount of flocs reduced and finally disappeared. Accordingly, the efficiency of Pi removal was reduced and reached 0. In the experiments, the pH of the HLSW reduced gradually due to the consumption of alkalinity by the Fe^{3+}. When the molar ratio of Fe/P was in the range of 0-1and the pH was in the range of 4.2-2.3, a large amount of flocs formed, removing Pi through charge neutralization by ligand competition (e.g. Fe-H_2PO_4), chemical complexation, and adsorption of Pi ions onto the floc surface. However, with further consumption of alkalinity (molar ratio of Fe/P from 1 to 2), no new flocs could be formed, and the formed flocs were dissolved gradually, releasing Pi in the pH range of 2.3-1.3. Therefore the molar ratio of 1 (Fe/P) was determined as the optimum dose of $FeCl_3$ for the removal of Pi in the HLSW. The maximum removal efficiency of Pi was 75%, accounting for 70% of the TP.

Figure 3.3 displays the experimental results of Pi removal with PFS. PFS is a polymeric species with a certain partially hydrolyzed products of ferric which has a larger surface area and a higher cationic charge. Because of the pre-hydrolysis, PFS consume less alkalinity than $FeCl_3$. As shown in Figure 3.3, the pH variation as a function of Fe^{3+}/P molar ratio was not as significant as that of $FeCl_3$ in Figure 3.2. From Figure 3.3, with increases in the amount of PFS from 0 to 42.6 mg/g HLSW, or Fe/P ratio from 0 to 1, the Pi removal increased from 0 to 80 %, accounting for 0-74% of the TP. The pH variation was in the range of 4.21-3.2, accordingly. However, the settling action was too slow to complete due to the formation of large amount of flocs which were predominately higher molecular weight polymers than those formed by $FeCl_3$ [7]. Therefore, no further experiment was carried out to increase the doses of the PFS.

Figure 3.4 shows the Pi removal behavior with $Al_2(SO_4)_3.18H_2O$ as the coagulant. As shown in Figure 3.4, the formation of the flocs required a much larger amount of $Al_2(SO_4)_3.18H_2O$ than that of $FeCl_3$ and PFS. Moreover, the flocs formed were small particles and fewer amounts compared to those formed by $FeCl_3$ and PFS. Accordingly, the Pi removal efficiency was much lower. The maximum removal efficiency was 39% with the coagulant dose of 3.5 g /g HLSW or a molar ratio of Al/P at 69.3 and pH 3. Similar dissolvation of flocs occurred with further increasing dose of $Al_2(SO_4)_3.18H_2O$. The flocs were dissolved completely at the molar ratio of Al/P at 75.3 and pH 2.9. Accordingly, the Pi removal efficiency reduced and reached 0. The lower removal efficiency of $Al_2(SO_4)_3.18H_2O$ could be attributed to the higher solubility product constant of $Al(OH)_3$ than that of $Fe(OH)_3$. Therefore, it can not form as much flocs as ferric salts at a low pH value.

Following the procedure described in section 3.2.2.2, the precipitates formed by $FeCl_3$, PFS, and $Al_2(SO_4)_3.18H_2O$ were dried and weighed and 92.1, 238.4, and 56.2 mg solids were obtained, respectively. Besides Pi, the precipitates might also include the proteins and poly peptides existed in the HLSW which were co-precipitated by adsorbing onto the surface area of the flocs formed.

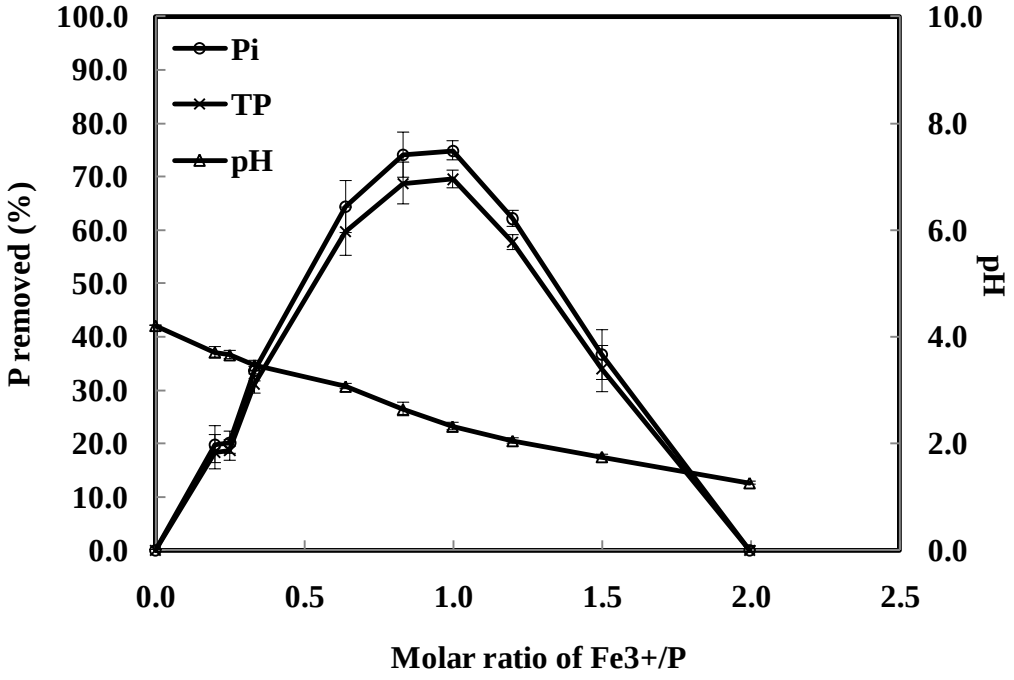

Fig.3.2. Pi removal with $FeCl_3.6H_2O$

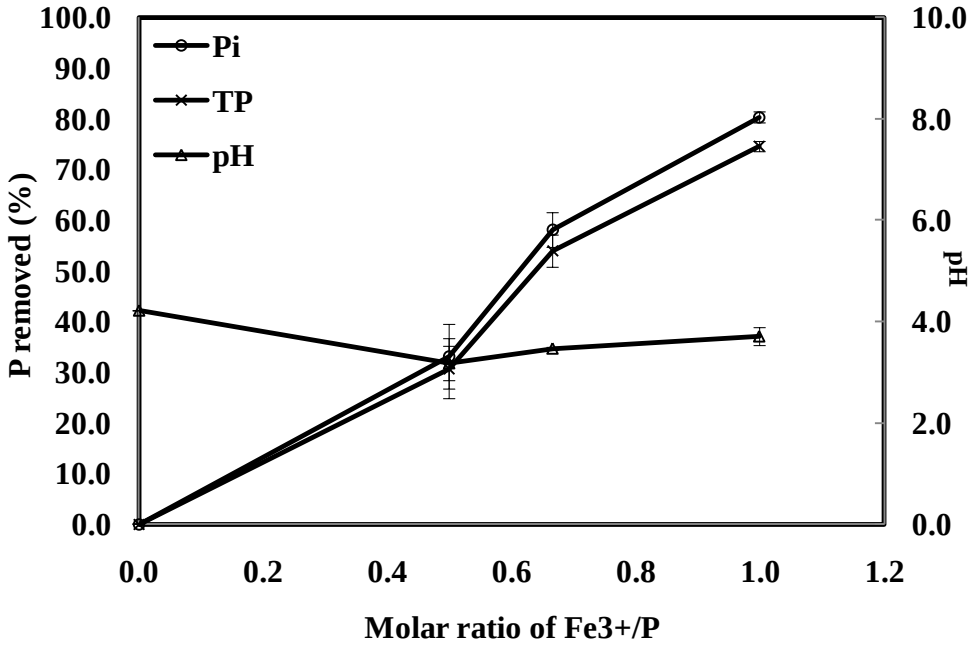

Fig.3.3. Pi removal with PFS

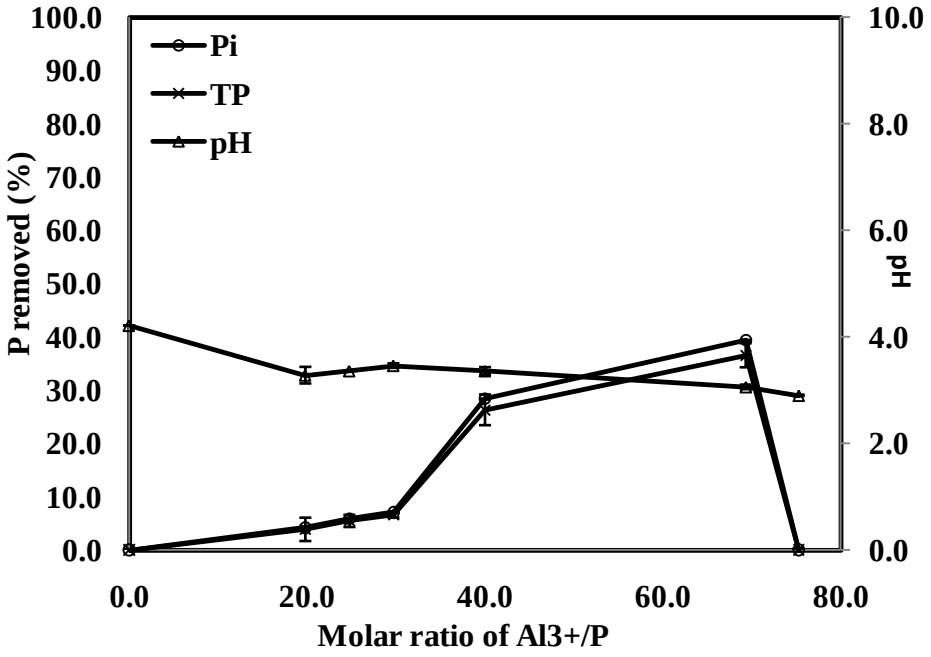

Fig.3.4. Pi removal with $Al_2(SO_4)_3.18H_2O$

3.4 Conclusion

The removal of phosphate in the HLSW by chemical precipitation with $Ca(OH)_2$, coagulation/flocculation with $FeCl_3$, PFS, and $Al_2(SO_4)_3.18H_2O$ were studied. The pHs of the system were influenced by the precipitation chemicals added. At pH 7.2, a 98% removal of Pi or 91% of TP was achieved by adding 19 mg $Ca(OH)_2$ /g HLSW or at the molar ratio of 1.7 (Ca/P). When the molar ratio of Ca/P increased to 2.4, the pH of the system increased to 8.7 and the Pi removal efficiency enhanced a little to 99% or 92% of TP. Heavy metal ions in the HLSW were co-precipitated with $Ca(OH)_2$ as well. In the coagulation/flocculation procedures, the maximum Pi removal efficiency of 75% (70% of the TP) was realized by adding 24.6 mg $FeCl_3$/g HLSW or at the molar ratio of 1 (Fe/P) and pH 2.3. At the same molar ratio of 1 (Fe/P) or 42.6 mg PFS/g HLSW, PFS removed 80 % Pi or 74% of the TP from the HLSW at pH 3.2. PFS formed more flocs than $FeCl_3$ due to the preformed higher molecular weight polymers. Moreover, its pH variation was more stable than that of $FeCl_3$ due to the pre-hydrolysis. However, the settling action of the flocs formed by PFS was incomplete. When $Al_2(SO_4)_3.18H_2O$ was used as the coagulant, a small Pi removal efficiency of 39% was achieved with the coagulant dose of 3.5 g /g HLSW or the molar ratio of Al/P at 69.3 and pH 3.

The high concentration of Pi in the HLSW (4.6 $\pm$0.07 mg/g HLSW) required a large amount of chemicals for its removal. This will not only make the treatment costly, but also result in a large amount of sludge which needs further treatment and investment on its storage. Moreover, the nutritional value of HLSW could be destroyed because of the co-precipitation of minerals, proteins, and poly peptides via direct precipitation and/or adsorption onto the surface area of the flocs. To avoid these problems, there is need to

develop another process which can effectively remove and recover the Pi in the LSW, while at the same time keep the nutritional value of CGF and minimize the wastes produced.

Reference

[1] Morse, G. K., Brett, S. W., Guy, J. A., and Lester, J. N., 1998. Review: phosphorus Removal and recovery technologies. Sci. Total. Environ. 212(1), 69-81.

[2] Yigit, N. O. and Mazlum, S., 2007. Phosphate recovery potential from wastewater by chemical precipitation at batch conditions. Environ. Technol. 28(1), 83-93.

[3] Zouboulis, A. I., Traskas, G., and Ntolia, A., 2007. Comparable evaluation of iron-Based coagulants for the treatment of surface water and of contaminated tap water. Separ. Sci. Technol. 42(4), 803-817.

[4] Omoike, A. I. and Vanloon, G. W., 1999. Removal of phosphorus and organic matter removal by alum during wastewater treatment. Water. Res. 33(17), 3617-3627.

[5] Jiang, J.Q., 2001. Development of coagulation theory and new coagulants for water treatment*:* Its past, current and future trend. Wa. Sci. Technol. 1(4), 57–64.

[6] Jiang, J.Q. and Graham, N.J.D., 1998. Preparation and characterisation of an optimal polyferric sulphate (PFS) as a coagulant for water treatment. J. Chem.Technol.Biot, 73, 351–358.

[7] Jiang, J.Q. and Graham, N. J. D., 2003. Development of optimal poly-alumino–iron-sulphate coagulant. Journal of Environmental Engineering (Reston, VA, United States). 129(8),699-708.

[8] Cheng, W.P. and Chi, F.H., 2002. A study of coagulation mechanisms of polyferric sulfate reacting with humic acid using a fluorescence-quenching method. Water Res. 36(18), 4583- 4591.

[9] Amuda, O.S. and Amoo, I.A., 2007. Coagulation/flocculation process and sludge conditioning in beverage industrial wastewater treatment. J. Hazard.Mater. 141(3), 778-783.

Chapter 4

An integrated approach to the degradation of phytates in the corn wet milling process

4.1 Introduction

Corn wet milling is one of the two main ethanol production processes and accounts for about 18% of the current ethanol production [1]. This process produces several important co-products including CGF, corn gluten meal (CGM), corn germ meal, and corn oil [1]. CGF is commonly used as animal feed for dairy and beef cattle, poultry, swine, and pet food [1. CGF contains important nutrients for animals as well as high levels of phosphorous (P). P in CGF is mainly from the P in corn kernel but is at much higher concentrations. Previous studies have shown that, while the P content of the corn was 2.6±0.2 mg/g corn, it was 11.4±0.2 mg/g CGF [2]. P in corn and CGF is mainly in phytate form. P in phytate form cannot be digested by nonruminant animals such as poultry and swine, leaving significant amounts of phytate P in their excreta. This phytate P-rich manure serves as a source of phosphorous and potentially could cause P pollution in soil and underground water resources [3-5]. Moreover, to guarantee the skeletal integrity and growth performance of swine and poultry, inorganic P supplements are also added into their diets which result in an added P in the animal excrete and further environmental concerns [6].

Most of P and phytate P in CGF are attributed to the addition of the LSW which contains the majority of the P entering the plant. LSW is the liquid stream drained from

the corn steeping tank. LSW is concentrated and added to the bran to form CGF. Ninety percent of the phytates in corn is found in the germ portion of the kernel which accounts for approximately 50 to 80% of the P in corn [7]. Phytate P accounted for approximately 80% of the total P in the LSW, in which inositol hexakisphosphate ($InsP_6$) was the main phytate component, accompanied by a small amount of inositol pentakisphosphate ($InsP_5$). Rausch and coworkers [8], measured the concentration and flow rate of P in three wet milling plants and concluded that 86% of the P entering the steeping process ended up in the LSW.

Phytases (inositol hexaphosphate hydrolase) have been reported to hydrolyze phytate P and when added to feed has shown to result in an increase in the growth performances of animals [6]. Currently, there are two commercially available phytases, *A. niger* phytase (Natuphos^{TM}, BASF, Florham Park, NJ) and *E. coli* phytase (OptiPhos, JBS United Inc., Sheridan, IN). These phytases have been studied extensively, and their catalytic efficacy as animal feed additives have been demonstrated [6, 9]. The properties of *A. niger* phytase have been described in previous chapter. The effectiveness of *A. niger* phytase on the degradation of phytate P in LSW and the hydrolysis pathway have been demonstrated in chapter 2. *E. coli* phytase is a 6- phytase and initiates the dephosphorylation of phytate at the six position of the inositol ring. The molecular weight of *E. coli* phytase ranges from 42 to 46 kDa. *E.coli* phytase is also a member of histidine acid phosphatase family and has the same active site sequence (RHGXRXP), the catalytic dipeptide, and 10 cysteine residues as *A.niger* phytase. Except this, *E.coli* and *A.niger* phytase exhibit no apparent sequence similarity to each other. The catalysis is a two-step process consisting nucleophilic attack on the scissile phosphoester bond by

the histidine residue in the active site motif, followed by hydrolysis of the resulting phospho-histidine intermediate. A conserved aspartic acid residue is the proton donor to the leaving group oxygen [10,11]. *E. coli* phytase has an optimal activation pH and temperature of 4.5 and 55 ℃, respectively. Its deactivation occurs at 60 ℃ [11]. Both *A. niger* and *E. coli* phytases have been reported to degrade phytic acid into myo-inositol 2-monophosphate ($Ins(2)P_1$) as the end product [12].

Upon the phytate degradation with phytases, the phytate P in CGF would potentially satisfy the P requirement of animal diet with no need for supplemental P in the diet. Meanwhile, binded minerals, proteins and starch are released for assimilation during the digestion [13]. Furthermore, the end products of phytate degradation, myo-inositol and P, are of great value and highly marketed products. Based on about 3 million metric tons production in 2009, CGF or more specifically its LSW ingredient could provide an abundant resource for the production of myo-inositol and P [1].

LSW is the liquid drained after corn steeping and contains most of the P that enters the wet milling process. LSW consists of 5~10% solids which contains 45% protein and many micronutrients [14]. The liquid fraction of LSW contains a number of compounds including carbohydrates, amino acids, peptides, organic acids, heavy metals, inorganic ions and myo-inositol phosphates [15]. The pH of LSW is in the range 3.5-4.3, mainly due to the presence of sulfur dioxide and lactic acid and other fermentation product [14]. In this pH range, protein-phytic acid electrostatic interaction occurs, resulting in neutral, insoluble complexes. Moreover, insoluble and/or soluble cation-phytic acid complexes are also likely to form, depending on the cation types existing in the system [13, 16].

Separations of components in the LSW can be done with ion exchange chromatography, based on the differences in electrical charges of the components. Ion exchange chromatography has been widely used as an effective separation method in various fields, e.g. bio-separation, water purification (deionization), waste water treatment, etc [17-19]. By using ion exchange columns, Hull and coworkers [15] separated the components in the LSW into three groups for analysis: anionic fraction (e.g. organic acids), neutral fraction (e.g. carbohydrates), and cationic fraction (e.g. minerals). Anion exchange chromatography was used in the separation of myo-inositol phosphates since they are negatively charged species [20, 21]. On a CarboPac PA-100 (Dionex Corp, Sunnyvale, CA) anion exchange analytical column, Chen and Li [21] separated 27 peaks representing phytic acid, its degraded myo-inositol phosphate (i.e. $InsP_2$ - $InsP_6$) and their isomers. Kney and Zhao [22], successfully removed phosphate from wastewater solutions with polymer ligand ion exchange resins.

The main focus of this chapter was to develop an integrated process to hydrolyze the phytates in LSW to Pi and myo-inositol as end products. Initially, the phytates in LSW were subjected to a controlled hydrolysis with *A.niger* enzyme. The partially hydrolyzed phytates were separated from LSW in an ion exchange column, and were then subjected to complete hydrolysis with *A. niger* and *E. coli* enzymes. The effectiveness of *A. niger* and *E. coli* as well as the effect of the combined use of the two enzymes in the complete hydrolysis of myo-inositol phosphates were investigated. The developed integrated process will provide for a more digestible feed for the nonruminant animals. There is also potential for the production of myo-inositol as a new value-added product from the wet milling process.

4.2. Experimental Procedures

4.2.1 Materials

LSW samples used in this study were from Cargill, a wet milling corn facility in Blair, Nebraska. All samples were kept in a refrigerator (4 ^{o}C) prior to use. As samples contained a mixture of solid and liquid, care was entailed to ensure the homogeneity of the samples taken before experiments.

Natuphos 10,000 liquid enzyme (3-phytase produced from *A. niger*) was purchased from BASF (Florham Park, NJ). OptiPhos 5000 liquid enzyme (*E. coli* AppA2) was generously provided by JBS United Inc. (Sheridan, IN). The nominal activity of this enzyme was 5000 FTU/g.

Myo-inositol standard (99%), sulfuric acid (95-98%), sodium molybdate dehydrate (99.5%), ascorbic acid, hydrochloric acid (37%), potassium dihydrogen phosphate (1 M), zinc oxide (99.9%), potassium hydroxide, phytic acid (50% w/w), perchloric acid (70%), iron (III) nitrate nonahydrate (98%) were purchased from Sigma-Aldrich (St. Louis, MO). DOWEX Marathon MSA anion exchange resin was purchased from Sigma-Aldrich (St. Louis, MO). Deionized (DI) water was further purified by a Simplicity Ultra Pure Water System from Millipore (Billerica, MA). Hydrochloric acid (0.5 M) and a solution of 1 g/L $Fe(NO_3)_3$ in 0.33 M $HClO_4$ were filtered by 0.22 μm membrane filter from Millipore before use.

4.2.2 Procedures

LSW was first subjected to a controlled hydrolysis step where the phytates were partially hydrolyzed to negatively charged phytic acid and its related myo-inositol

phosphates. An anion exchange column was then used to separate the anionic fraction from the neutral and cationic fractions in the system. The anionic fractions were collected and then subjected to complete hydrolysis where myo-inositol phosphates were degraded into P and myo-inositol which could be further separated. The flow diagram of the developed integrated process is presented in Fig. 4.1.

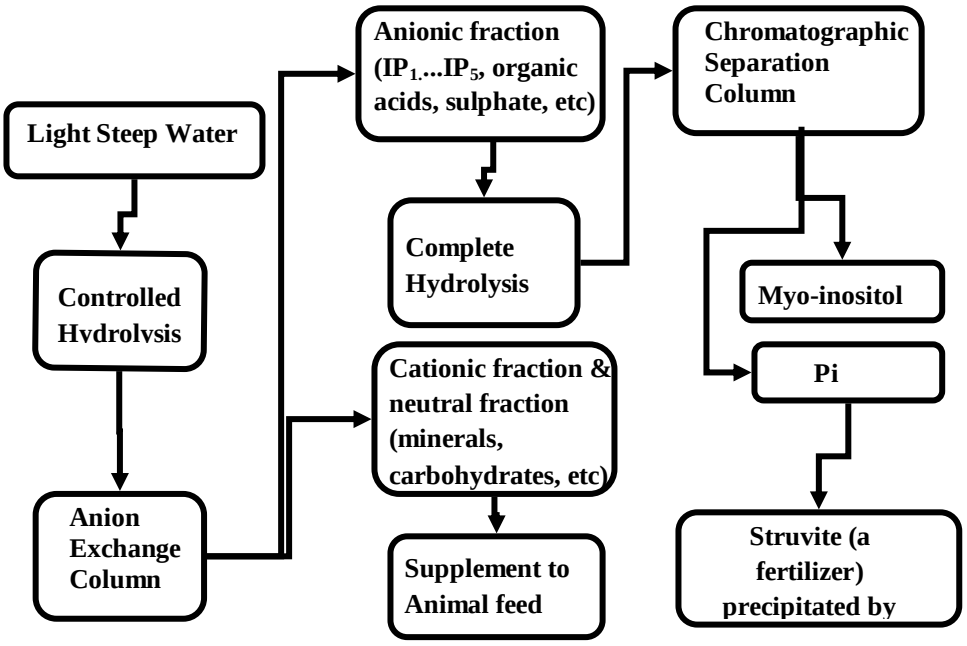

Fig.4.1. The process flow diagram for phytate degradation, and Pi and myo-inositol recovery from LSW.

4.2.2.1 Partial enzymatic hydrolysis

Experiments were performed to partially hydrolyze the phytates in LSW with *A. niger* enzyme. LSW was incubated with 1 FTU *A. niger* /g substrate at 35 ℃. Hydrolysis reactions were carried out in capped 125 mL Erlenmeyer flasks. The reaction mixture was incubated in a temperature-controlled incubator (Imperial III, Lab-Line Instruments, Inc., Melrose, IL) in which a shaker (C2 classic platform shaker, New Brunswick Scientific Co., Ltd., Edison, NJ) was placed to mix the reaction flasks at 200 rpm. At 0, 0.5, 1, 1.5, 2, 4, 6 and 8 h, hydrolyzed LSW aliquots of about 10 mL each were taken from the reaction mixture. The reaction was terminated by heating the samples in a water bath at 100 °C for 10 min. Precautions were taken to avoid water vapor entering the samples. Samples were subjected to phosphate P (Pi) analysis with spectrophotometer and for myo-inositol phosphates analysis with HPLC. All hydrolysis experiments were performed in duplicates and the presented data are the mean values for the replicates.

4.2.2.2 Separation with ion exchange columns

Kontes Flex-Column glass chromatography columns were used (VWR International, Batavia, IL). The columns were 1.0 cm in diameter and 20 cm in length. The DOWEX Marathon MSA anion exchange resin was soaked in distilled water for 2 h to ensure full hydration of the resin. The columns were charged with 10 g of fully hydrated resin. Distilled water was introduced from the base of the column with a peristaltic pump (Cole-Parmer Instrument Co. Chicago, IL) to cover the entire resin volume. This eliminated the air bubbles in the resin bed and potential for channeling. Hydrolyzed LSW samples and regeneration solution were introduced at the top of the column with a peristaltic pump at a flow rate of 1 mL/min and 0.3 mL/min, respectively.

Hydrolyzed LSW samples were cleared of solid particles in a centrifuge (8464 Thermo Electron Co., Milford, MA), at 11,000 *g* for 10 min. and only the clarified portion of the samples were passed over the anion exchange column. The ion-exchange column breakthrough behavior was determined by treating 28 bed volumes of hydrolyzed LSW samples through the column. Samples were taken after every bed volume treatment and were subjected to HPLC analysis for myo-inositol phosphates, and Pi content. The breakthrough curves were used as a reference in the column regeneration experiments. The negatively charged myo-inositol phosphate species which were adsorbed to the anion exchange resin were eluted with 1 M NaCl solution. The regeneration of the column was continued until the analysis of the eluted NaCl solution showed no desorption of myo-inositol phosphates from the column bed resin.

4.2.2.3 Complete enzymatic hydrolysis

Collected elutions from section 2.2.2, containing the myo-inositol phosphate, were incubated with *A. niger phytasee* , *E. coli phytase*, and their equally portioned combination at 45 ℃. Enzyme loadings of 50, 100, and 150 FTU/g NaCl elution were investigated. Reactions were carried out as was described in section 2.2.1. Aliquots of about 2 g each were taken at 0, 0.5, 1, 2, 4, 8, 24, 48, 72, 96, and 120 h. Samples were subjected to total P and Pi analysis with spectrophotometer and also for myo-inositol phosphates analysis with HPLC.

4.2.3 Analysis

4.2.3.1 Enzyme activity

One phytase unit of activity (FTU) is defined as the amount of the enzyme, which, at 37 °C and pH 5.5, liberates 1.00 μmol of inorganic P per minute from 0.0051 mole sodium phytate/L [23]. The analysis was based on the method developed by Engelen and co-workers [24]. In this procedure the phytase source was subjected to incubation with sodium phytate in order to liberate inorganic phosphate from the substrate. Molybdate-vanadate reagent was added to the reaction mixture to stop the reaction. Moreover, the addition of this reagent results in the formation of a colored complex with the freed inorganic phosphates. The absorbance of the yellow P complex was measured at a wavelength of 415 nm.

4.2.3.2 P analysis

4.2.3.2.1 Total P analysis

The photometric dry-ashing procedure for the analysis of total P was based on the standard method as adopted by the Nordic Committee on Food Analysis/AOAC International for determination of P in a variety of food samples [25]. Measurements were based on a colorimetric method where the color of the treated sample reflected the concentration of P. The samples were first ashed to remove the organic (C, H, O) materials. Hydrochloric acid was added to the remaining inorganic ash residue to convert the P residues to a dissolved P form. This solution was used for color reaction based on the formation of a blue complex between phosphate and sodium molybdate in the presence of ascorbic acid as the reducing agent. The blue color of the complex was directly proportional to the amount of P.

4.2.3.2.2 Phosphorus in phosphate form (Pi)

Experiments were carried out to determine the phosphate content in LSW samples during the course of dephosphorylation experiments. These procedures were based on a previous study [2] which recognizes the fact that P in the form of phosphate is totally soluble in water, whereas, P in the form of phytates could be found in both the solid and the liquid fractions of samples. Consequently, the ashing step and the subsequent addition of HCl were eliminated from the color reaction procedure and the rest of the procedure was followed as stated in section 4.2.3.2.1 for the determination of the total phosphorous.

Samples were first centrifuged in a centrifuge (8464 Thermo Electron Co., Milford, MA), at 11,000 *g* for 10 min. The supernatant was then passed through a 0.20 μm porosity cellulose acetate filter (Agilent Technologies, Wilmington, DE) to ensure the removal of all residual suspended solids. The collected supernatants were then subjected to the drying procedure as mentioned in 4.2.3.2.1.

4.2.3.2.3 Reagent preparation

All reagents were prepared as described by Pulliainen and Wallin [25] with some modifications. The procedures were as follows: (a) Sodium molybdate solution was prepared by mixing 140 mL of sulfuric acid (18M) with 300 mL DI water and 12.5 g of sodium molybdate in a 500 mL volumetric flask. (b) Ascorbic acid solution was prepared daily by adding 5 g ascorbic acid to DI water in 100 mL volumetric flask. (c) Molybdate-ascorbic acid solution was prepared immediately before use by adding 50 mL molybdate solution and 20 mL ascorbic acid in a 200 mL volumetric flask. (d) A 2 mg P /mL P stock

solution was prepared by diluting 8.788 g potassium dihydrogen phosphate (KH_2PO_4) in a 1 L volumetric flask. (e) P working solution was prepared by diluting the P stock solution to 0.1 mg P / mL and was used to prepare the calibration curve.

4.2.3.2.4 Color reaction

Dried samples (0.5-1.5 g) were initially ashed with zinc oxide in a muffle furnace (McMaster-Carr 31605k55, Chicago, IL). Sample preparation followed the procedure outlined by Pulliainen and Wallin [25]. A quantity of the P solution so prepared (1.0 - 10.0 mL) was taken for the color reaction with molybdate-ascorbic acid solution. Samples were taken in 1 mL cuvettes for analysis. The percent P content of the liquid samples was calculated using the calibration curve.

The experimental procedures for the determination of phosphate content of the supernatant fraction of the samples bypassed the ashing step and the subsequent addition of HCl. The amount of sample taken for these experiments was 1-5 mL in a 200 mL volumetric flask which depended on the expected P concentration. This was then neutralized with 50 % KOH and the rest of the procedure followed Pulliainen and Wallin [25]. All experiments were repeated twice. The mean values for the replicates and the standard deviations are presented in the results section.

4.2.3.2.5 Calibration

Quantitative determination of P in the samples was determined based on a calibration curve using different P concentrations. The P working solution was used in the calibration. Known volumes of this solution (1.0, 2.0, 3.0, 4.0, 5.0, and 6.0 mL) were charged into a 50 mL volumetric flask and diluted with DI water to 15 mL. This was

followed by addition of 20 mL molybdate-ascorbic acid solution. The rest of the color reaction procedure was followed.

4.2.3.3 Analysis of myo-inositol phosphates

A UV spectrophotometer (Thermo Electron Co. 335906 GENESYS 10S, Milford, MA) was used to measure the P content by relating the intensity of the blue colored samples to the amount of P in them. The instrument was first zeroed with a blank reference sample. Sample absorbance was measured at 823 nm.

The concentration of myo-inositol phosphates in LSW was analyzed by a HPLC equipped with a post column derivatizer. The HPLC system used for the analysis of inositol phosphates was a Waters Alliance system (Milford, MA) and consisted of a Separation Module (Waters 2695) and a Dual λ Absorbance Detector (Waters 2487). The HPLC was equipped with a post column derivatization instrument (Pickering Laboratories PCX5200, Mountain View, CA). The analytical column used for the separation was a CarboPac PA-100 and a CarboPac PA-100 guard column manufactured by Dionex (Sunnyvale, CA). The mobile phase was provided by gradient elution of a (0.5 M) HCl (A) and DI water solution (B) at 1.0 mL/min. The following describes the gradient elution profile which was maintained during the run; 0-16 min, 8-20% A, 92-80% B; 16-33 min, 20-37% A, 80-63% B; 33-49 min, 37-100% A, 63-0% B; 49-50 min, 100% A, 0% B; and 50-50.1 min, 100-8% A, 0-92% B. Total run time for this method was 60 min. Samples were filtered with 0.20 μm porosity cellulose acetate filters (Agilent Technologies, Wilmington, DE) prior to the injection. Samples (25 μL) were injected via an injection port at an initial column temperature of 25 °C. The separated samples were

mixed in the post column derivatizer reactor with a mixture of 0.1 % $Fe(NO_3)_3 \cdot 9H_2O$ and 2.0% $HClO_4$ at 0.8 mL /min. The HPLC system pressure range was from 2250 to 2400 psi and post column pressure was held constant at 200 psi. The Dual λ Absorbance Detector was set at 295 nm. Chen et al. [21] have reported the detection of 27 peaks representing $InsP_2$- $InsP_6$ isomers during the acidic hydrolysis (2 M HCl) of commercial phytic acid. This was the basis for identifying the peaks of the phytates in this study.

4.2.3.4 Analysis of myo-inositol

The HPLC system used for the analysis was the same as the module which was described in section 2.3.3. The separation was performed by an isocratic elution program on a Bio-Rad Micro-Guard Cation H Refill Cartridges (30 x 4.6 mm), a Fermentation Monitoring column (150 x 7.8 m) and a Aminex® HPX-87H column (300 x 8.7 mm) in series (Bio- Rad Laboratories, Hercules, CA). A Waters 2414 RI detector was used for the detection. The column temperature was maintained at 65 ℃ inside a Waters column heater module and the RI detector was held at 30 ℃. Sulfuric acid (0.5 mM) was used as the mobile phase at a flow rate of 0.4 mL/min. Total run time for this method was 60 min. The elution time for myo-inositol was about 22 min. The injection volume of standards and sample solutions were 20 µL. Prior to the chromatographic analysis, aliquots of hydrolysis solutions were deionized with AG 501-X8 Resins (Bio- Rad Laboratories, Hercules, CA) and filtered through 0.20 µm porosity cellulose acetate filters (Agilent Technologies, Wilmington, DE). Myo-inositol content of samples was quantified based on a calibration curve which was prepared using standards solutions.

4.3 Results and discussion

4.3.1 P analysis of LSW

A complete assessment of the P content and distribution in the LSW samples was carried out to establish the baseline for this work. In this assessment, the total P, phytate P, and Pi content of LSW were determined. Experiments were performed to quantify total P and Pi, following the experimental procedures outlined earlier in section 4.2.3. The amount of Phytate P was quantified by taking the difference between total P and Pi. The results are summarized in Table 4.1. The total P, phytate P, and Pi content for LSW were 4.1 $\pm$0.03, 3.4 $\pm$0.03, and 0.8 $\pm$0.04 mg/g LSW, respectively. HPLC analysis showed that the phytate P was mainly in the form of $InsP_6$, accompanied by small amounts of $InsP_5$. The total P content of the liquid and the solid fractions of the LSW were determined to be 3.8 $\pm$0.06 and 0.3 $\pm$0.02 mg/g LSW, respectively. The total P in the liquid fraction accounted for 93% of the total P in LSW. The phytate P in the liquid fraction of the LSW was 3.0 $\pm$0.05 mg/g LSW, accounting for 79% of the total P in the liquid fraction or 73% of the total P in LSW. Data in Table 4.1 also indicate that the P in the solid fraction of the LSW was mainly in form of phytate P.

Table 4.1 The distribution of P in the liquid and solid fractions of the light steep water samples

Sample description	Total P (mg P/g sample)	Phytate P (mg P/g sample)	Phosphate P (mg P/g sample)
Light steep water	4.1 ±0.03	3.4 ±0.03	0.8 ±0.04
Liquid fraction	3.8 ±0.06	3.0 ±0.05	0.8 ±0.04
Solid fraction	0.3 ±0.02	NA	0

Abbreviation used: NA, not available.

4.3.2 Partial hydrolysis

Partial hydrolysis of LSW was carried out to transform insoluble and soluble phytates in this substrate to negatively charged myo-inositol phosphates. This transformation allowed for the separation of negatively charged species from the neutral species (e.g. carbohydrates) and the positively charged species (e.g. proteins & minerals) in LSW. Experiments, as described in section 4.2.2.1, were performed to determine the optimum reaction time for the partial hydrolysis. Reaction temperature of 35 ℃ and enzyme loading of 1FTU *A. niger*/g substrate were adopted. Two criterions were followed during the course of the hydrolysis. The first criterion was to ensure that the insoluble phytates were degraded into soluble myo-inositol phosphates. This was achieved by extending the hydrolysis to a point where the difference between the Pi in the hydrolyzed LSW and the Pi in the hydrolyzed LSW's supernatant (without the insoluble components) reached a constant value. It was also critical for the partial hydrolysis to be stopped short of the formation of $InsP_1$ species.

Pi was quantified according to the method described earlier in section 4.2.3.2 and was recognized as an indicator of the extent of the hydrolysis of phytates. The experimental results quantifying the differences between the Pi released from the hydrolysis of LSW and the hydrolysis of LSW's supernatant as a function of time are presented in Fig. 4.2. As is shown in this figure and under the performed hydrolysis conditions, a monotonic increase in the amount of released Pi from LSW into LSW's supernatant was observed during the first 2 h of incubation. After this initial period, the amount of released Pi leveled off and additional incubation time appeared to have very little effect on the amount of the differences of Pi. The amount of Pi released from LSW

into LSW's supernatant was 0.15 ± 0.01 mg/g LSW after 2 h incubation. As was described earlier, the phytates in the LSW could exist as insoluble protein-phytic acid

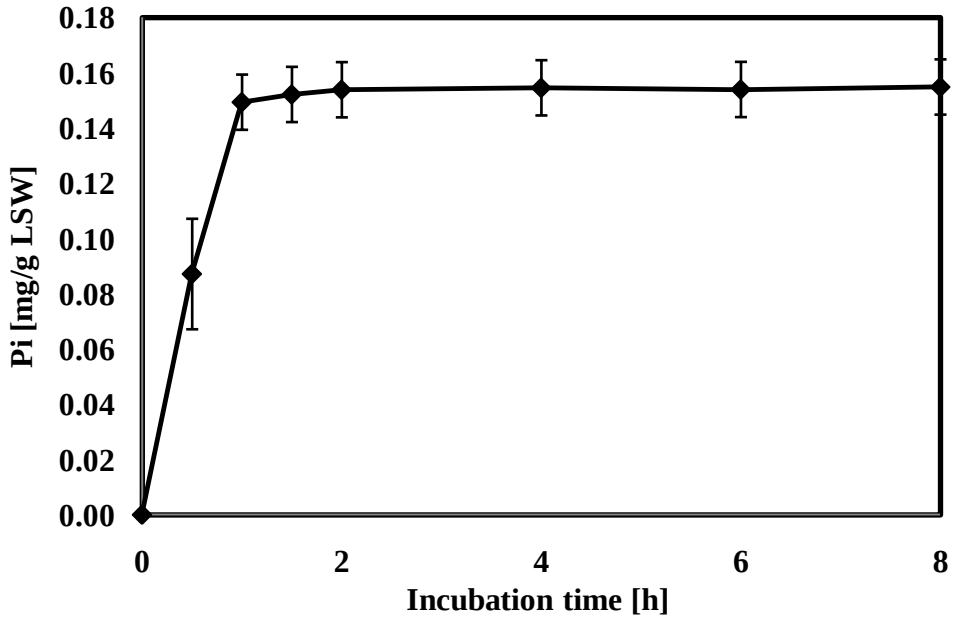

Fig.4.2. Time course of the differences in Pi released from the hydrolysis of LSW and LSW supernatant subject to 1 FTU A. niger /g susbstrate at 45 ℃, pH 4.33, and 200 rpm of shaker speed.

complexes and cation-phytic acid complexes. The data presented in Fig. 4.2 is indicative of the insoluble phytic acid complexes in LSW. The first 2 h was the effective period for the degradation of insoluble phytates in LSW where about 50% of the insoluble phytate P from the solid fraction of LSW were released into the liquid fraction.

The pathway of phytate degradation by *A. niger phytase* was presented in section 2.3.2, chapter 2. The myo-inositol phosphates formed during the hydrolysis were analyzed by HPLC and the degradation products were identified based on a reference chromatogram by Chen et al. [21]. This is corroborated with the chromatogram shown in Fig. 4.3 which confirms a stepwise mechanism for the dephosphorylation of the phytates in LSW ($InsP_6$) via the formation of $InsP_5$, $InsP_4$, $InsP_3$ and $InsP_2$. After 2 h hydrolysis, $InsP_5$, $InsP_4$, and $InsP_3$ were the main components in the LSW, accompanied by a small amount of $InsP_2$, which assured that $InsP_1$ were not produced at this time. After 4 h incubation, $InsP_5$ and $InsP_4$ disappeared, and $InsP_3$ and $InsP_2$ became the dominant components in the system. Further incubation resulted in a decrease in the amount of $InsP_3$ and $InsP_2$. Based on the results of this study, 2 h was chosen as the optimum reaction time for partial hydrolysis of LSW. The partial hydrolysis step resulted in a significant increase in the Pi content of the LSW supernatant from the initial 0.8 ± 0.04 mg/g LSW (19% of total P in LSW) to 2.5 ± 0.03 mg/g LSW (60% of total P in LSW).

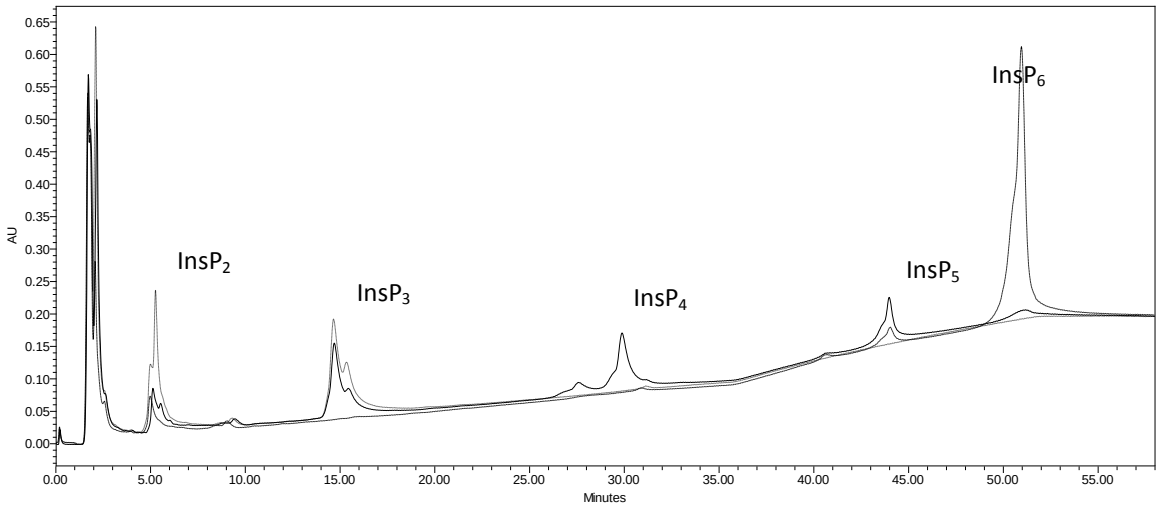

Fig.4.3. Chromatogram of the hydrolysis of phytate in LSW at 35 ℃, pH 4.33 and 200 rpm of shaker speed. ····· 0 h; ——2 h; - - - - - 4 h.

4.3.3 Separation by ion exchange chromatography

Experiments were carried out to determine the breakthrough behaviors for the adsorption of myo-inositol phosphates to the DOWEX Marathon MSA anion exchange resin packed column. The resin used in this study was a strong base anion resin which had an operating pH range of 0-14. No adjustment was made to the pH of the hydrolyzed LSW before use. The hydrolyzed LSW was passed through the column as described in section 4.2.2.2. The breakthrough profiles for the adsorption of myo-inositol phosphates and phosphate are presented in Fig.4.4. The breakthrough curves revealed the order of affinity of these species to the column as: $InsP_5$> $InsP_4$> $InsP_3$> $InsP_2$ > phosphate, which correlated well with the number of the negative charges on the species. Phosphate broke through the column shortly after the LSW was supplied, due to its low affinity for the resin in the presence of other stronger poly-anions in the system, and its high concentration in the feed. Phosphate normalized concentration (C/C_0) reached a constant value of 1 after approximately 5.5 bed volumes passed through the column, suggesting that phosphate was not taken up by the column resin. The onset of $InsP_2$ through the column appeared after approximately 4 bed volumes, followed by $InsP_3$ at 6 bed volumes, $InsP_4$ at 12 bed volumes, and $InsP_5$ at 20 bed volumes. The complete breakthrough for $InsP_2$, $InsP_3$, $InsP_4$, and $InsP_5$ occurred after 11.5, 19.5, 26, and 28 bed volumes, respectively. The normalized concentration of $InsP_2$, $InsP_3$, and $InsP_4$ increased above unity and then tapered off to 1. This is believed to be due to an initial adsorption of the species to the resin and eventual displacement from resin by anions with stronger

affinities for the resin. The pH of the effluent from the column-loading test did not change significantly compared with that of the LSW fed to the column.

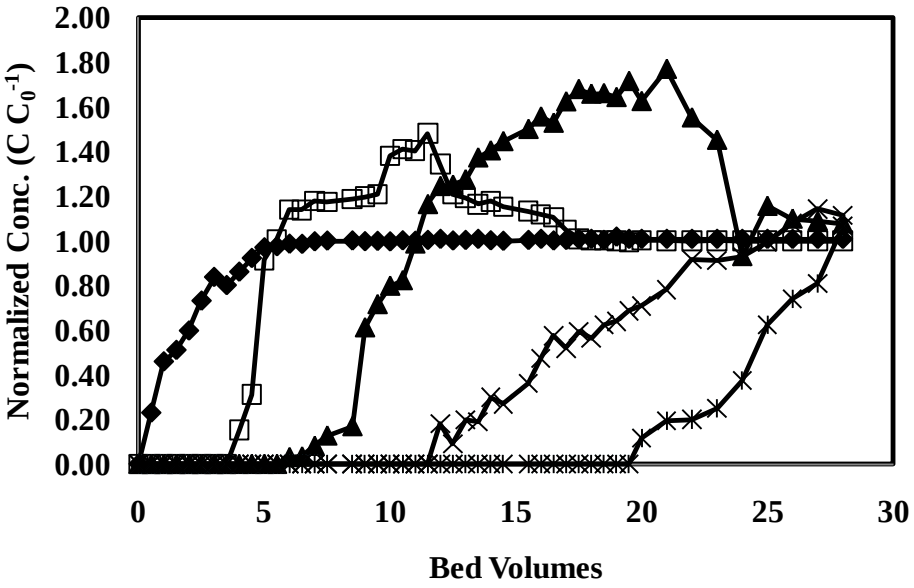

Fig.4.4. Myo-inositol phosphates and phosphate breakthrough curves in a fixed column exhaustion run using DOWEX Marathon MSA anion exchange resin. pH 4.10. (■) Pi; (□) $InsP_2$; (▲)$InsP_3$; (×) $InsP_4$; (*) $InsP_5$.

Based on the breakthrough curves of Fig.4.4, the resin retained the entire myo-inositol phosphates species after processing 4 bed volume of LSW with a slight loss of $InsP_2$ after the processing of 5 bed volumes. Desorption of the negatively charged myo-inositol phosphates from the resin was carried out with 1 M NaCl and after 5 bed volumes of LSW were processed through the column. Experiments were carried out as was described in section4.2.2.2. HPLC results showed that after the processing of 4 bed volumes of 1 M NaCl solution through the column, no myo-inositol phosphates were detected in the eluded material. As expected, the sequence of desorption of the myo-inositol phosphates was: $InsP_2$> $InsP_3$> $InsP_4$> $InsP_5$.

Furthermore, other anionic ions such as organic acids might be also replaced by the more negatively charged myo-inositol phosphates so that the ion exchange column only contained the myo-inositol phosphate isomers and a small amount of Pi. This was proved by the coupled Fermentation Monitoring column (150 x 7.8 m) and a Aminex® HPX-87H column (300 x 8.7 mm) which can also be used to separate organic acids such as lactic acids.

4.3.4 Complete hydrolysis

The NaCl elution of section 4.3.3, containing the negatively charged myo-inositol phosphates were collected and subjected to complete hydrolysis with *A. niger* and *E. coli* phytases and their respective combination. Enzyme loadings of 50, 100, and 150 FTU/g NaCl elution were examined. The time course of the hydrolysis as described in section 4.2.2.3 was determined. The NaCl elution had a pH range of 4.8-5.0, which was near the optimum pH activity for *A. niger* and *E. coli* phytases which are 5.0 and 4.5, respectively.

Previous research is conclusive in that the end-product of phytate degradation, catalyzed by *A.niger and*/or *E.coli* phytases was Ins(2)P_2 [12, 26, 27]. However, in these studies much smaller enzyme loadings, in the range of 0.1- 4 FTU/g substrate were used. Much higher enzyme loadings in the range of 50-150 FTU/g substrate were used in this study to facilitate complete hydrolysis and the formation of myo-inositol as the end product. In these experiments, myo-inositol and Pi were quantified according to the methods described in section 4.2.3.2 and 4.2.3.4, respectively. Fig.4.5 presents several chromatograms for the stream which was eluded from the ion exchange column by 1 M NaCl solution (as was described earlier in section 4.3.3) and was subjected to total hydrolysis with 100 FTU *E.Coli*/g LSW, 45 ℃ and pH 5.0 for 8 h. As is shown in this figure, E.*coli* phytase at 100 FTU/g substrate degraded myo-inositol phosphates into myo-inositol and Pi as the end products. The myo-inositol eluted out of the HPLC column at around 22 min and its amount was increased in time. The degradation of phytates to myo-inositol, was also observed in the complete hydrolysis of the LSW with *A.niger* phytase and with the combination of *A.niger* and *E.coli* phytases.

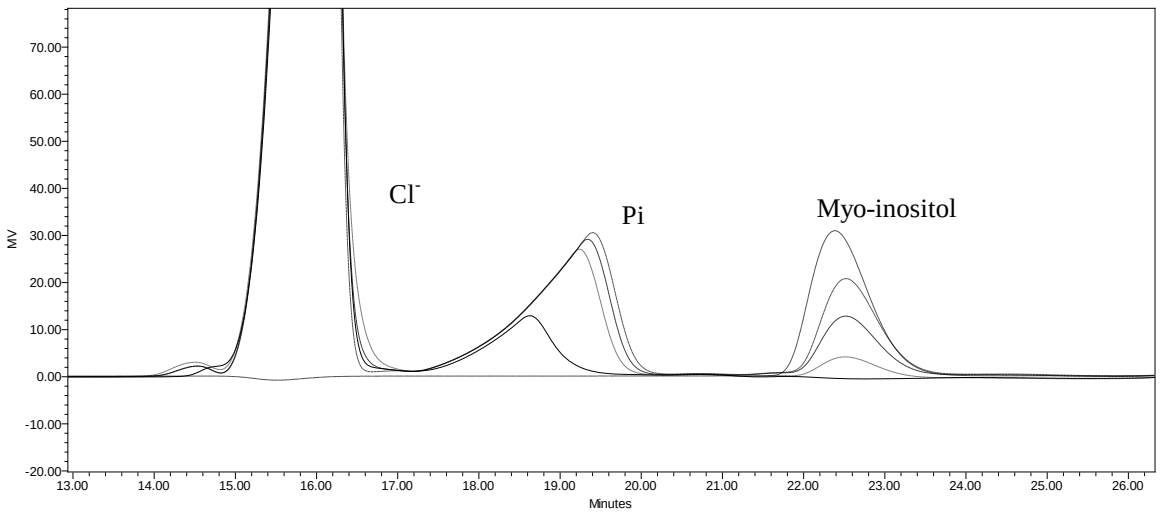

Fig.4.5. Chromatogram of the complete hydrolysis of myo-inositol phosphates at 100 FTU E.Coli/g LSW, 45 ℃ and pH 5.0. —— 0 h; ····· 0.5 h; - - - - - 2 h; – · – 8 h; - · - · - Myo-inositol standard (5 mg/ml).

The experimental results quantifying the amount of myo-inositol as a function of time at 45 ℃, and pH 5.0 are presented in Figs. 4.6.1 – 4.6.3. As shown in these figures, in all investigated cases the amount of myo-inositol increased monotonically during the first 8 h of hydrolysis and then gradually leveled off. Figs. 4.6.1 – 4.6.3 also revealed that *E. coli* phytase resulted in the highest rate of formation of myo-inositol, suggesting to the strongest catalytic activity of this enzyme, while *A.niger* phytase resulted in the lowest rate of formation of myo-inositol. No apparent synergism was observed when *A. niger* and *E .coli* phytases were combined. As shown in Figs.4.6.1 – 4.6.3, the rate of hydrolysis correlated well with the enzyme loading and the fastest reaction was catalyzed by150 FTU/g NaCl elution, followed by 100 FTU, and then 50 FTU. The maximum amount of myo-inositol was 3.73 ± 0.03 mg/g NaCl elution which was detected after 48 h reactions catalyzed by 100 FTU *E. coli*, 150 FTU *E.coli*, and 150 FTU of the combination of *A. niger* and *E. coli* phytases. In these reactions, the time course of the released Pi showed a similar trend to that of myo-inositol and the released Pi reached a maximum amount of 3.30 ± 0.05 mg/g NaCl elution after 48 h incubation at the enzyme loadings for which the maximum concentration of myo-inositol were reached.

To examine the extent of the total hydrolysis reaction and the correlation between the formation of myo-inositol and Pi, the time course of the formation of these compounds were experimentally determined and compared with their corresponding theoretical yields. The theoretical yields were based on 218.5 g hydrolyzed LSW processed through the anion exchange column which resulted in 179.5 g of NaCl elution. Based on the amount of $InsP_6$ in the liquid fraction of the LSW, the theoretical yield for myo-inostol was 3.76 mg/g NaCl elution. The theoretical yield for the Pi in the NaCl

elution was 3.33 mg P/g NaCl elution. The yield for Pi was based on the $InsP_2$-$InsP_5$ which were collected in the NaCl elution. The experimental results

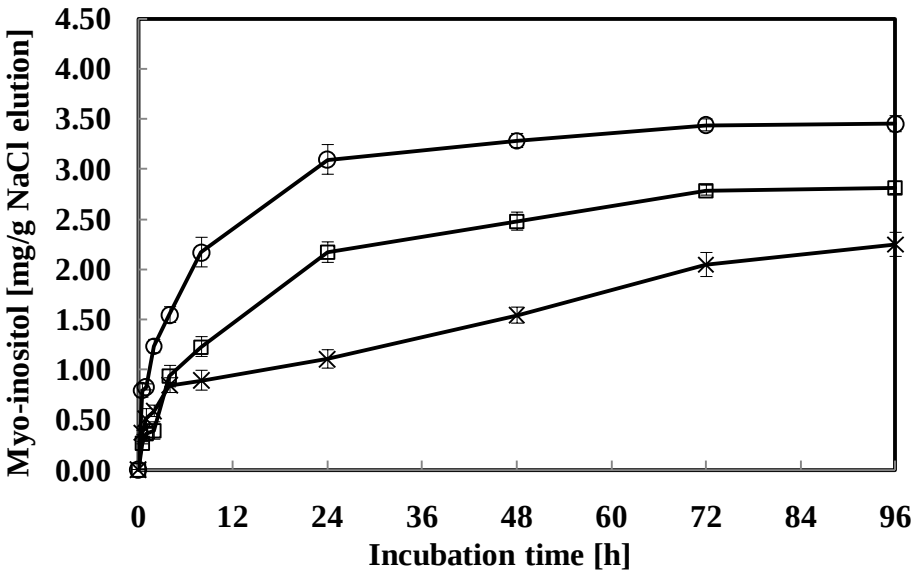

Fig.4.6.1. Complete hydrolysis of myo-inositol phosphates subject to 50 FTU enzyme/g NaCl elution, 45 ℃, pH 5.0, and 200 rpm of shaker speed. (×) *A.niger*; (□) *A.niger* and *E.Coli*; (○) *E. Coli.*

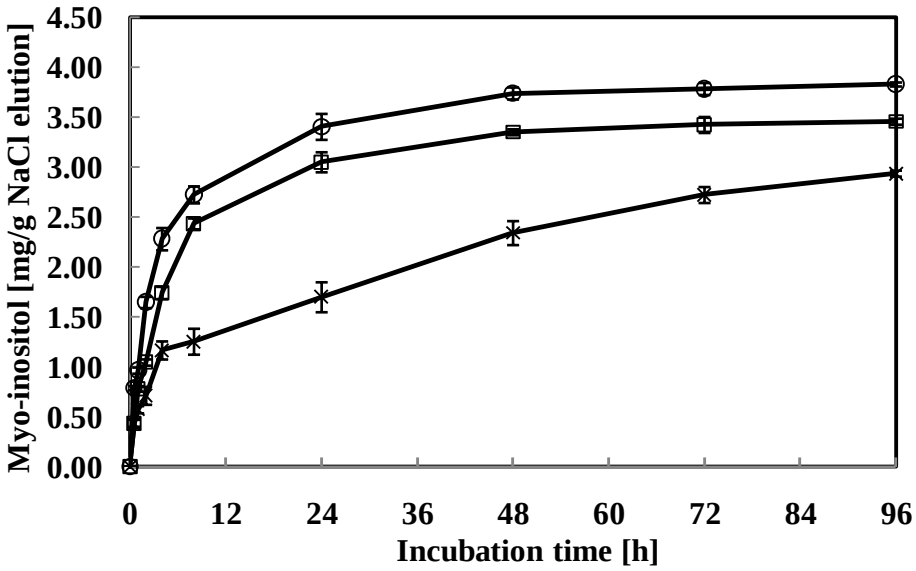

Fig.4.6.2. Complete hydrolysis of myo-inositol phosphates subject to 100 FTU enzyme/g NaCl elution, 45 ℃, pH 5.0, and 200 rpm of shaker speed. (×) *A.niger*; (□) *A.niger* and *E.Coli*; (○) *E.Coli*.

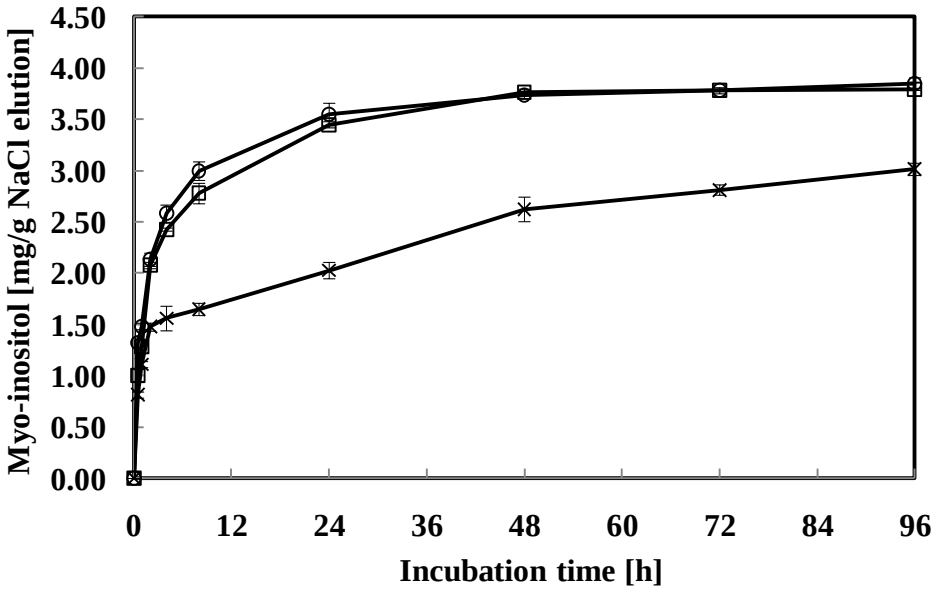

Fig.4.6.3 . Complete hydrolysis of myo-inositol phosphates subject to 150 FTU enzyme/g NaCl elution, 45 ℃, pH 5.0, and 200 rpm of shaker speed. (×) *A.niger*; (□) *A.niger* and *E.Coli*; (○) *E.coli*.

for the measured amounts of myo-inositol and Pi are summarized in Table 4.2. As is shown in this table, *E. coli* phytase was consistently more effective than *A. niger* phytase at all enzyme loading levels. This was consistent with the findings by Wyss et al. [12]. The formation of myo-inositol increases as the enzyme loading was increased from 50 – 150 FTU/g NaCl elution. The highest production of myo-inositol was at 99.8% of the theoretical yield which was observed at the enzyme loading of 100 FTU *E.coli*/g NaCl elution. At the enzyme loading of 150 FTU/g NaCl elution, near complete hydrolysis was also observed in reactions catalyzed by *E.coli,* and the combination of *A. niger* and *E. coli* phytases. At the lowest enzyme loading of 50 FTU *A. niger* /g NaCl elution, the formation of myo-inositol reached 41% of the theoretical yield while the formation of Pi was at 65% of the theoretical yield. This trend was also observed at 100 FTU *A. niger*/g NaCl elution enzyme loading while an opposite trend was observed with *E. coli* phytase where close to equal percentage of the theoretical yield was observed for both the myo-inositol and Pi. This phenomena may be attributed to a different hydrolysis mechanism for the two enzymes.

The overall hydrolysis efficiency was based on the initial amount of phytate P in LSW. The initial amount of phytate P in LSW was the sum of phytate P in the liquid and the solid fractions (3.4 ± 0.03 mg/g LSW). The highest overall efficiency was observed at the enzyme loading of 100 FTU *E.coli*/g NaCl elution, where 3.00 ± 0.05 mg Pi/g LSW were resulted from the hydrolysis of the phytates in the liquid fraction and 0.15 ± 0.01 mg Pi/g LSW were resulted from the hydrolysis of phytates in the solid fraction. As was discussed earlier in Section 4.3.2, while the hydrolysis resulted in near complete conversion of phytates in the liquid fraction, the conversion of phtates in the solid

fraction was only 50%. This is mostly attributed to the mass transfer limitations and the inaccessibility of the phytate sites to the enzyme.

Table 4.2 Formation of Pi and myo-inositol resulting from the complete hydrolysis of myo-inositol phosphates

Enzyme loading (FTU)	Enzyme	Myo-inositol (mg/g NaCl elution)	P (mg/g NaCl elution)
50	*A.niger*	1.54 ±0.02	2.16 ±0.02
	A. niger and E. coli	2.48 ±0.06	2.48 ±0.01
	E.coli	3.28 ±0.07	2.69 ±0.01
100	*A.niger*	2.34 ±0.03	2.44 ±0.04
	A. niger and E. coli	3.35 ±0.03	3.04 ±0.02
	E.coli	3.74 ±0.02	3.32 ±0.02
150	*A.niger*	2.62 ±0.03	2.78 ±0.03
	A. niger and E. coli	3.76 ±0.01	3.23 ±0.04
	E.coli	3.73 ±0.03	3.30 ±0.05
Theoretical maximum		3.76	3.33

The presented data in Table 4.2 suggest to the fact that at a higher enzyme loading and longer incubation time, *A. niger* and *E. coli* enzymes are capable of completely hydrolyzing myo-inositol phosphates to myo-inositol and Pi. This may be attributed to a relatively high enzyme loading used in the experiments which provided abundant binding opportunities for the myo-inositol phosphates. The increased binding of myo-inositol phosphates may result in an increased catalytic activity of the enzyme by creating substrate-induced conformational change in Glu 219 of *E.coli* phytase which promotes proton transfer to the leaving phosphate group [9], 2000). The complete hydrolysis could also be attributed to the presence of sodium and chloride ions in the NaCl elution substrate. In a study by Ullah et al. [28], sodium chloride enhanced the catalytic activity of *A. niger* phytase in the pH range of 1.5 - 5.0, while it suppressed the activity of *E. coli* phytase at above pH 3. Findings of this study suggest that, the effects due to the presence of NaCl may have been compensated for by the much higher activity of this *E. coli* phytase and the overall activity of this enzyme was higher than that of *A. niger* phytase. This was consistent with the findings by Wyss et al. [12] which suggested to an eight-fold higher specific activity of *E. coli* phytase in the hydrolysis of phytic acid compared with *A. niger* phytase.

4.4 Conclusions

An integrated process was developed to hydrolyze the myo-inositol phytates in LSW and to simultaneously isolate Pi and myo-inositol products. This process comprised of partial and total hydrolysis of LSW and intermediate anion exchange separation technique.

The maximum amount of myo-inositol and the corresponding Pi reached the theoretical yield for myo-inostol and Pi of 3.76 and 3.33 mg /g NaCl elution, respectively. The proposed integrated process will be helpful in resolving the environmental and nutritional concerns in the use of CGF in the animal diets. Moreover, CGF and more specifically its LSW ingredient could provide an abundant resource for the production of Pi and myo-inositol.

Reference

[1] RFA (2008), Ethanol industry outlook. Available from: www.ethanolrfa.org/industry/ resources/coproducts.

[2] Noureddini, H., Malik, M., Byun, J., Ankeny, A. J., 2009. Distribution of phosphorus compounds in corn processing. Bioresource. Technol. 100, 731-736.

[3] EPA., 1998. National water quality inventory: 1996 Report to Congress. EPA841-R-97- 008, Office of Water, Washington, DC. June.

[4] Parry, R., 1998. Agricultural phosphorous and water quality: a US environmental Protection agency perspective. J. Environ. Qual. 27, 258-261.

[5] Sharpley, A., Daniel, T. C., Sims, J. T., Pote, D. H., 1996. Determining Environmentally sound phosphorus levels. J. Soil Water Conserv. 51, 160-166.

[6] Selle, Peter H., Ravindran, V., 2007. Microbial phytase in poultry nutrition. Anim. Feed. Sci.Tech. 135, 1-41.

[7] Ravindran, V., Bryden, W. L. and Kornegay, E. T., 1995. Phytates: occurrence, bioavailability and implications in poultry nutrition.Poult. Avian. Biol. Rev. 6, 125-143.

[8] Rausch, K. D., Raskin , L. M., Belyea ,R. L., Agbisit, R. M., Daugherty, B. J., Clevenger, T. E. and Tumbleson, M.E., 2005. Phosphorus concentrations and flow in maize wet milling streams. Cereal Chem. 82, 431-435.

[9] Nyannor, E. K. D. Williams, P., Bedford, M. R., Adeola, O., 2007. Corn expressing An Escherichia coli -derived phytase gene: a proof-of-concept nutritional study in pigs. J. Anim.Sci. 85, 946-1952.

[9] Lim, D., Golovan, S., Forsberg, C. W., Jia, Z., 2000. Crystal structures of Escherichia coli phytase and its complex with phytate. Nat. Struct. Biol.7, 108-113.

[10] Rao, D. E. C. S., Rao, K. V., Reddy, T. P., Reddy, V. D., 2009. Molecular characterization, physicochemical properties, known and potential applications of phytases: An overview. Crit. Rev. Biotechnol. 29, 182-198.

[12] Wyss, M., Pasamontes, L., Friedlein, A., Rémy, R., Tessier, M., Kronenberger, A., Middendorf, A., Lehmann, M., Schnoebelen, L., Röthlisberger, U., Kusznir, E., Wahl, G., Müller, F., Lahm, H. W., Vogel, K., van Loon, A. P., 1999. Biochemical characterization of fungal phytases (myo-inositol hexakisphosphate phosphohydrolases): catalytic properties. Appl. Environ. Microbiol. 65, 367 - 373.

[13] Selle, P. H., Ravindran, V., Caldwell, A., Bryden, W. L., 2000. Phytate and phytase: Consequences for protein utilisation. Nutr. Res. Rev.13, 255-278.

[14] Johnson, L. A. and May, J. B., 2003. Corn: Chemistry and Technology, 2nd ed., (White, P. J. and Johnson, L. A., eds.). American Association of Cereal Chemists, St. Paul, MN, pp. 449–494.

[15] Hull, S. R., Yang, B. Y., Venzke, D., Kulhavy, K., Montgomery, R., 1996. Composition of Corn Steep Water during Steeping. J. Agr.Food.Chem, 44, 1857-1863.

[16] Cheryan, Munir., 1980. Phytic acid interactions in food systems. Crit. Rev. Food. Sci.13, 297-335.

[17] Ackermann, G. R., Waitz, W. H., Jr., 1976. Pollution abatement through the treatment of industrial waste water with ion exchange resins. Proceedings - Institute of Environmental Sciences. 22, 491-495.

[18] Flook, K., Woodruff, A., Saini, C., Rao, S., Thayer, J., Rey, M., Agroskin, Y., Pohl, C., 2008. Multidimensional Bioseparations Using Ion-Exchange and Reversed-Phase Monolith Columns. Dionex Corporation, Sunnyvale, CA USA 2008 presentation. Available at: www.dionex.com/en-us/webdocs/66092-IE_RP_Monolith%20Columns_LPN%202025-01.pdf.

[19] Paul, D.H., 2000. An overview of deionization technologies. Ultrapure Water. 17, 72-74.

[20] Skoglund, E., Carlsson,N.G., Sandberg, A.S., 1998. High-Performance Chromatographic Separation of Inositol Phosphate Isomers on Strong Anion Exchange Columns. J. Agric. Food. Chem 46, 1877-1882.

[21] Chen, Q. C. and Li, B. W., 2003. Separation of phytic acid and other related inositol phosphates by high-performance ion chromatography and its applications. J.Chromatography A. 1018, 41-52.

[22] Kney, A. D., Zhao, D., 2004. A pilot study on phosphate and nitrate removal from secondary wastewater effluent using a selective ion exchange process. Environ. Technol. 25, 533-542.

[23] International union of biochemistry. 1979. Enzyme nomenclature: recommendation of the nomenclature committee of the international union of biochemistry. Academic press, New York, NY.

[24] Engelen, A.J., van der Heeft, F.C., Randsdorp P.H.G., and Smit, ELC., 1994. Simple And rapid determination of phytase Activity. J. AOAC. Int. 77, 760-764.

[25] Pulliainen, T.K., Wallin, H.C., 1994. Determination of total phosphorus in foods by colorimetric measurement of phosphorus as molybdenum blue after dry-ashing: NMKL interlaboratory study. J. AOAC. Int. 77, 1557-1561.

[26] Kemme, P. A., Lommen. A., De Jonge, L. H., Van der Klis, J. D., Jongbloed, A.W., Mroz, Z., Beynen, A. C., 1999. Quantification of inositol phosphates using (31) P Nuclear magnetic resonance spectroscopy in animal nutrition. J. Agr.Food.Chem. 47, 5116-5121.

[27] Noureddini, H., Dang, J., 2009b. Degradation of phytates in distillers' grains and Corn gluten feed by Aspergillus niger phytase. Appl. Biochem. Biotech. 159, 11-23.

[28] Ullah, A. H. J., Sethumadhavan, K., Mullaney, E. J., 2008. Salt effect on the pH profile and kinetic parameters of microbial phytases. J. Agr. Food. Chem. 56, 3398-3402.

Chapter 5

HPLC method development for myo-inositol and Pi analysis

5.1. Introduction

In chapter 4, an integrated process was developed for the enzymatic hydrolysis of phytates in light steep water (LSW) to myo-inositol and inorganic phosphate (Pi) with phytase enzymes. The proposed integrated process will be helpful in resolving the environmental and nutritional concerns in the use of corn gluten feed (CGF) in the animal diets. As the developed process included an intermediate anion exchange separation step where NaCl solution was used as the elutant, the final product consisted of myo-inositol, NaCl, and Pi. To evaluate the extent of hydrolysis and recovery of the myo-inositol and Pi products, a simple and non-destructive method was developed which was used for the routine analysis of myo-inositol and Pi.

Determination methods for myo-inositol in biological samples have been extensively investigated. Enzymatic analytical methods by means of NADH cycling have been described in several studies [9-13]. In one approach, myo-inositol was first oxidized by NAD^+ dependent myo-inositol 2-dehydrogenase. The resultant NADH was reoxidized with oxalacetate and malate dehydrogenasehere where the produced malate was measured fluorimetrically [9,10]. Alternatively, the oxidized NADH was reoxidized by iodonitrotetrazolium chloride and diaphorase, and the formed formazan was measured spectrophotometrically [11]. The myo-inostol may also be oxidized by the coenzyme

which is comprised of both thio-NAD^+ and NAD^+ and the resultant was quantified by measuring the increases in absorbance caused by thio-NADH at 405 nm and 37 ℃ [12]. The photon emission of NADH with bioluminescence assay has also been used to determine the concentration of myo-inositol [13].

Gas chromatography (GC) methods with flame ionization detection and ion trap mass spectrometry (MS) are available for myo-inositol analysis. In these methods, myo-inositol is silylated and measured as hexa-O-trimethylsilyl ethers or tri-fluoroacetyl derivative [14-16]. HPLC methods coupled with various modes of detection, such as UV-VIS, diode-array detector, and MS, are also available. As myo-inositol lacks chromophoric properties, pre-column derivatizations are normally required for spectrophotometeric detections [17-19].

Capillary electrophoresis (CE) combined with electrochemical detection has been reported for the analysis of myo-inositol. The myo-inositol was determined by detecting the electricity produced from the oxidation of myo-inositol at Cu electrodes in strongly alkaline conditions [20, 21].

Concentrations of myo-inositol in biological samples are normally very low and in the range of nanogram quantities [2-13]. With the growing interest in quantifying the concentration of myo-inositol in food and other nutrient resources, where its concentration is at much higher levels than in the biological samples, a fast, non-destructive and convenient method of analysis is highly desirable [18]. HPLC and CE methods have been reported for the analysis of myo-inositol in food samples, however, CE methods have not been fully explored yet and the HPLC methods normally require pre-column derivatization, which are time consuming and also destructive to parent

analyte [20]. Some HPLC methods replaced the pre-column derivatization step with more elaborate detection methods, such as mass spectrometer which can provide reliable and sensitive results [19].

As mentioned earlier, Pi is the co-product of the enzymatic hydrolysis of phytates and it is highly desirable to be qualified, preferably along with the myo-inositol. Pi plays important roles in plant growth and animal metabolism. For Pi analysis, the most widely used method is the colorimetric method developed by Pulliainen and Wallin[22]. This method utilizes a blue complex formed via the reduction of phospho-molybdate complex ($(NH_4)_3PO_4 \cdot 12MoO_4$) by ascorbic acid. However, the procedure consists of several tedious and relatively time consuming step.

In this chapter, a quick and simple isocratic HPLC method for the analysis of myo-inositol and Pi in the hydrolysate of LSW was developed. The devised HPLC method was capable of quantifying myo-inositol and Pi simultaneously with no interference from the coexistence of NaCl in the samples.

5.2. Experimental procedures

5.2.1 Chemicals

Hydrochloric acid (37%), myo-inositol standard (99%), sodium sulphate (99%), and sulfuric acid (95-98%) were purchased from Sigma-Aldrich (St. Louis, MO). Sodium chloride (99.6%) was purchased from Mallinckrodt (St. Louis, MO). Potassium Phosphate Monobasic (KH_2PO_4)(99+%) was purchased from Fisher Scientific (Pittsburgh, PA). Deionized (DI) water was further purified by a Simplicity Ultra Pure Water System from Millipore (Billerica, MA).

5.2.2 Apparatus

The HPLC system used for the analysis was a Waters Alliance system (Milford, MA) and consisted of a Separation Module (Waters 2695) and a RI detector (Waters 2414). The separation was performed on a coupled Bio-Rad Fermentation Monitoring column (150 x 7.8 m) and an Aminex® HPX-87H column (300 x 8.7 mm), in series, with a Bio-Rad Micro-Guard Cation H Refill Cartridges (30 x 4.6 mm) (Bio- Rad Laboratories, Hercules, CA) guard column. The column temperature was maintained at 65 ℃ inside a waters column heater module. The RI detector was held at 30 ℃. The mobile phase was a 0.5 mM sulfuric acid solution. Analysis was performed isocratically by delivering the mobile phase at a flow rate of 0.4 mL/min. Total run time for this method was 60 min. The elution time for myo-inositol was about 22 min. The injection volume of standards and sample solutions were 20 µl.

5.2.3 Sample and standards preparation

Myo-inositol standard solutions were prepared in purified DI water as described in section 2.1. Myo-inositol was prepared at 20 mg/ml concentration which was then serially diluted at 1:2 ratios to 9.8 µg/ml concentration. The concentration of myo-inositol ranged from 9.8 µg/ml to 20 mg/ml. Pi standard solutions were prepared in DI water with KH_2PO_4. KH_2PO_4 was dried in a convection oven (20GC Quincy Lab, Inc., Chicago, IL) at 101 ℃ for 2 hr before use. The dried KH_2PO_4 was then used to prepare standard solutions of 0.1, 1, 2, 4, 6, 8, 10 mg Pi/ml for calibration.

Two types of samples, one of known composition and one from the hydrolysate of LSW were prepared. Sample with known composition was comprised of 4.3 mg/ml myo-inositol, 0.1 M NaCl, and 1.8 mg/ml Pi. The hydrolysate samples were collected from the

complete hydrolysis of myo-inositol phosphates in the LSW [1]. These samples were prepared by first subjecting LSW to a 2 h hydrolysis with 1 FTU *A.niger* phytase/g LSW at 35 ℃, where the phytates in the LSW were partially hydrolyzed to negatively charged myo-inositol phosphates. An anion exchange column was then used to separate the myo-inositol phosphates from the neutral and cationic fractions in the system. The myo-inositol phosphates adsorbed onto the ion exchange column were eluted with 1 M NaCl and then subjected to complete hydrolysis with 100 FTU *E.coli* phytase/g NaCl solution at 45 ℃. Samples were taken at 0, 0.5, 2, 4, 8, 24 and 48 h. The details of this procedure is presented elsewhere [1]. All standards and samples were prepared freshly before use, and filtered through 0.20 μm porosity cellulose acetate filters (Agilent Technologies, Wilmington, DE) prior to the chromatographic analysis.

5.3 Results and discussion

5.3.1 Detection and chromatography

As the sample solution contain abundant negatively charged Cl^- and Pi, HPLC columns in which the stationary phase could form precipitation with these ions should be avoided. To prevent the formation of precipitation in the column, a column with H^+ bonded stationary phase where the acidic mobile phase could be used with no potential for precipitation was deemed appropriate for the analysis. Therefore, a Fermentation Monitoring column coupled with an Aminex® HPX-87H column was used for the analysis.

Fig.5.1. shows the chromatograms obtained under the described isocratic conditions for a blank reagent containing myo-inositol (4.3 mg/ml), NaCl (0.1M), and Pi

(1.8 mg/ml), and for a sample collected from a 4 h hydrolysis of myo-inositol phosphates at 45 ℃ and pH 5.0 with 100 FTU *E.coli* phytase /g of eluded sample with NaCl solution. Based on individual standard samples of myo-inositol, Pi, NaCl, Na_2SO_4, and HCl, the three peaks on the chromatogram of Fig. 5.1 were labeled accordingly. The chromatogram presented in Fig. 5.1 shows that the developed system of analysis is capable of separating myo-inositol, Cl^-, and Pi in the samples. Cl^- eluted first followed by Pi and myo-insositol. The retention time for Cl^-, Pi, and myo-inositol were 15, 17, and 22 min, respectively.

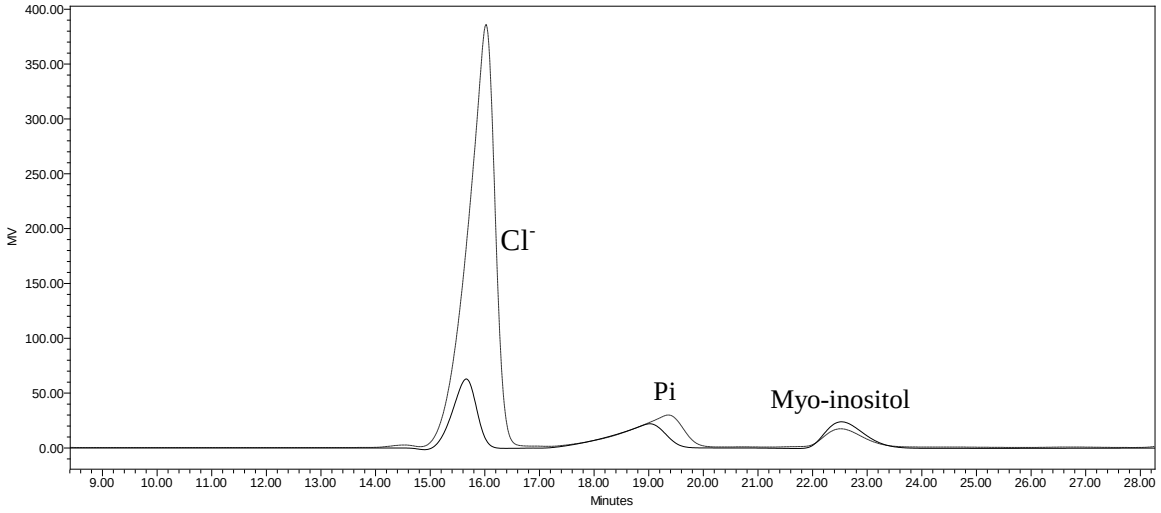

Fig.5.1. Isocratic HPLC chromatograms for: ----- Reagent blank containing: myo-inositol (4.3 mg/ml), NaCl (0.1M), and Pi (1.8 mg/ml); —— Sample collected from a 4 h hydrolysis of myo-inositol phosphate at 45 ℃ and pH 5.0 with 100 FTU *E.coli* phytase/g of eluded sample with NaCl solution.

5.3.2 Method validation

The linearity of the detector for myo-inositol was examined by injecting standard samples containing myo-inositol at 9.8 µg/ml to 20 mg/ml concentrations and the corresponding peak areas were plotted against concentration (Fig.5.2.). Five replicates of each standard were made. The standard solutions show good linearity (R^2=1) within the concentration range of 19.5 µg/ml to 20 mg/ml LSW. At the concentration level of 9.8 µg/ml myo-inositol was not detectable. The statistical analysis of the calibration curves are summarized in Tables 5.2.1 and 5.2.2. As is shown in Table 5.3.1, the relative standard deviations for all peak areas were low in the range of 0.14-5.46%. The limit of detection (LOD) and the limit of quantification (LOQ) were calculated according to a method described by International Conference on Harmonization [23], 3.3 and 10 times of standard deviation of the response divided by the slope of the calibration curve, respectively. After calculation, the LOD was 0.01 mg/ml, while the LOQ was 0.04 mg/ml.

The HPLC method developed in this study was also found to be an easy and fast method for the quantification of Pi. A calibration curve (Fig.5.3) was constructed with 0.1, 1, 2, 4, 6, 8, 10 mg Pi/ml standard solutions which covered the range required for the analysis of all the samples collected from the hydrolysis of LSW. As shown in Fig. 3, a good linearity (R^2 = 0.9996) was observed for all the Pi concentrations under investigation. The calibration curve was then used to quantify the amount of Pi in the collected samples. Similarly, table 5.3.1 and 5.3.2 summarizes the statistical analysis of the calibration curves of Pi. The relative standard deviations for all peak areas were in the

range of 0.15-0.80% (table 5.3.1). The LOD and LOQ for Pi analysis were 0.05 and 0.17 mg/ml, respectively. The linear range was 0-10 mg/ml.

To validate this method for the analysis of Pi, this method was compared with the colorimetric method by Pulliainen and Wallin in the analysis of Pi for the samples of LSW before hydrolysis, and the LSW which was hydrolyzed for 2 h and was then subjected to NaCl elution from the anionic exchange column as was explained in section 5.2.3. Results summarized in table 5.4 show a good agreement between the developed HPLC method and the colorimetric method on Pi quantification, supporting the validation of this method. Also shown in this table is a much lower standard deviation for the HPLC method.

Table 5.2.1 Statistical analysis of the data obtained from calibration curve of analysis of myo-inositol standards (1).

Myo-inositol concentration [mg/ml]	Mean peak area (mV*s)	Standard deviation	Relative standard deviation (%)
0.0098	NA	NA	NA
0.0195	7,405.11	329.97	4.46
0.0391	15,407.60	840.51	5.46
0.0781	30,741.52	1,650.37	5.33
0.1563	62,087.40	2,966.38	4.78
0.3125	123,338.94	4,548.69	3.69
0.6250	248,122.54	4,920.68	1.98
1.25	492,205.54	5,432.66	1.10
2.5	986,324.74	6,227.32	0.63
5	1,974,082.71	9,670.13	0.49
10	3,936,986.25	8,801.84	0.22
20	7,868,463.59	11,283.42	0.14

Table 5.2.2 Statistical analysis of the data obtained from calibration curve of myo-inositol standards (2).

Calibration line	
Slope ± Stdev.	393557 ± 600.62
Intercept ± Stdev.	0 ± 0.00
R^2	1
Residual stdev.	693.54
Linear range (mg/ml)	0-20
LOD (mg/ml)	0.01
LOQ (mg/ml)	0.04

Note: LOD = 3.3* б/S
LOQ=10* б/S
Where б is the standard deviation of the response, and S is the slope of the calibration curve.

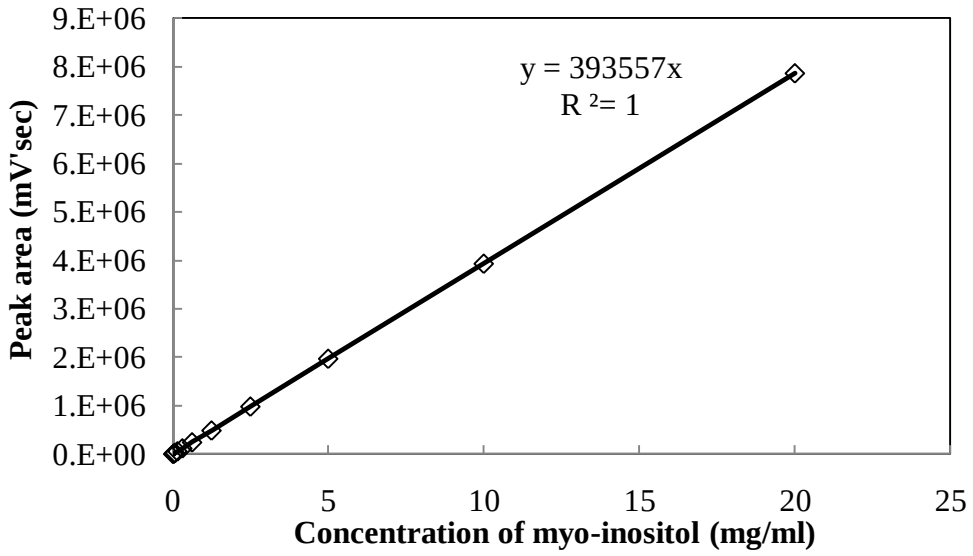

Fig.5.2. Calibration curve for myo-inositol standards. Isocratic elution (0.5mM H_2SO_4) at 0.4 ml/min, 60 ℃. Detector: RI. Injection volume, 20 µl.

Table 5.3.1 Statistical analysis of the data obtained from calibration curve of analysis of Pi standards (1).

P concentration [mg/ml]	Mean peak area (mV*s)	Standard deviation	Relative standard deviation (%)
0.01	9500.9196	42.01	0.44
1	968310.26	1633.06	0.17
2	1887670.7	6732.11	0.36
4	3742056	29967.14	0.80
6	5537703.2	11597.95	0.21
8	7343803.3	10823.79	0.15
10	9027082.1	31699.06	0.35

Table 5.3.2 Statistical analysis of the data obtained from calibration curve of Pi standards (2).

Calibration line	
Slope ± Stdev.	911720 ± 2605.135
Intercept ± Stdev.	0 ± 0.00
R^2	0.9996
Residual stdev	3008.2
Linear range (mg/ml)	0-10
LOD (mg/ml)	0.05
LOQ (mg/ml)	0.17

Note: LOD = 3.3* б/S
LOQ=10* б/S
Where б is the standard deviation of the response, and S is the slope of the calibration curve.

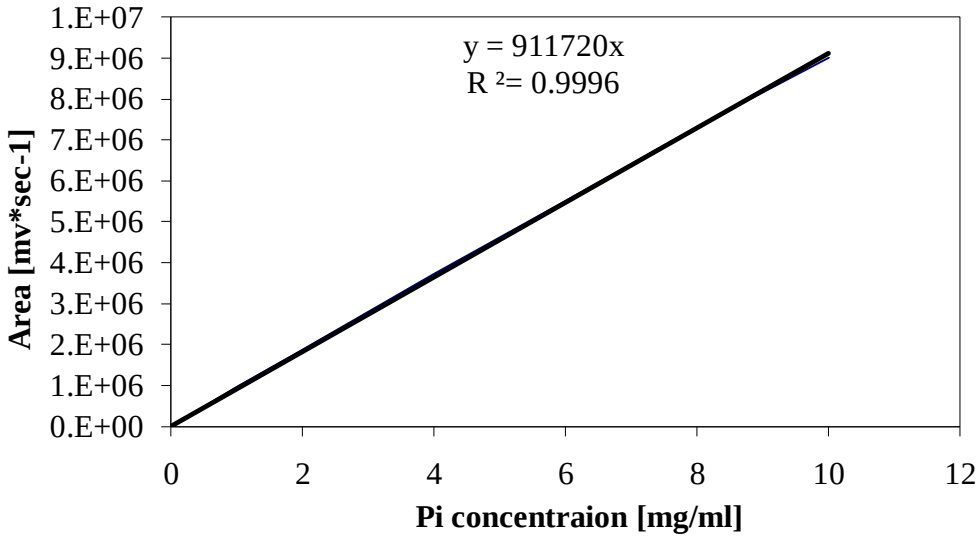

Fig.5.3. Calibration curve for phosphate standards. Isocratic elution (0.5mM H_2SO_4) at 0.4 ml/min, 60 ℃. Detector: RI. Injection volume, 20 µl.

.

Table 5.4 Pi analysis applying two different analytical methods.

Sample	Pi [mg/g LSW]	
	HPLC method	Colorimetric method
LSW	1.29 ±0.02	1.17 ±0.16
2hr hydrolyzed LSW	2.54 ±0.02	2.47 ±0.08
NaCl elution	1.22 ±0.02	1.15 ±0.15

5.3.3 Recovery of myo-inositol and Pi from the hydrolysis of phytates in the LSW

To evaluate the extent of the hydrolysis of phytates in the LSW and the degree of the efficiency of the recovery of myo-inositol and Pi, the developed method was used to determine the myo-inositol and Pi produced in the process as described in section 5.2.3. Analysis was made for samples from LSW, partially hydrolysis of LSW after 2 h, and the hydrolyzed samples subjected to NaCl elution. The total P, phytate P, and Pi content for LSW were determined to be 4.1 $\pm$ 0.03, 3.4 $\pm$0.03, and 0.8 $\pm$0.04 mg/g LSW, respectively. After 2 h partial hydrolysis with 1 FTU *A.niger* phytase/g LSW, the Pi content of the LSW supernatant increased from the initial 0.8 $\pm$0.04 mg/g LSW (19% of total P in LSW) to 2.5 $\pm$ 0.03 mg/g LSW (60% of total P in LSW) which was mainly contributed to th degradation of phytate P. The hydrolyzed LSW was then passed through an anionic exchange column onto which the negatively charged myo-inositol phosphates were adsorbed. A 1 M solution of NaCl was used to elute out the adsorbed components. The analysis of the eluded solution showed 1.22 mg Pi/g LSW and as expected detectable levels of myo-inositol. The collected myo-inositol phosphate containing NaCl elution was subjected to a complete hydrolysis with 100 FTU *E.coli* phytase/g NaCl elution at 45 ℃ and pH 5.0. Samples were taken and analyzed at 0, 0.5, 2, 4, 8, 24 and 48 h. The resulting chromatograms for 0.5, 2, and 8 h samples are summarized in Fig.5.4. The chromatograms in this figure show an increasing trend in the formation of myo-inositol and Pi as a function of time. After 48 h hydrolysis, both myo-inositol and Pi reached their maximum values of 3.06 $\pm$ 0.02 and 2.71 $\pm$ 0.02 mg/g LSW, respectively. Based on the amount of phytate in the liquid fraction of the LSW, the theoretical yield for myo-inostol and Pi in the NaCl elution were determined to be 3.11 and 2.73 mg/g LSW, respectively.

The recovery of myo-inositol and Pi on the HPLC column was 98.4% and 99.3%, respectively. Furthermore, the HPLC quantification also showed that, during this developed integrated process, about 3.15 ±0.04 mg/g LSW Phytate P was converted into Pi, accounting for 92.6% degradation of the phytate P in the LSW. In all experiment, the measured concentrations of myo-inositol and Pi fell into their linear range of detection.

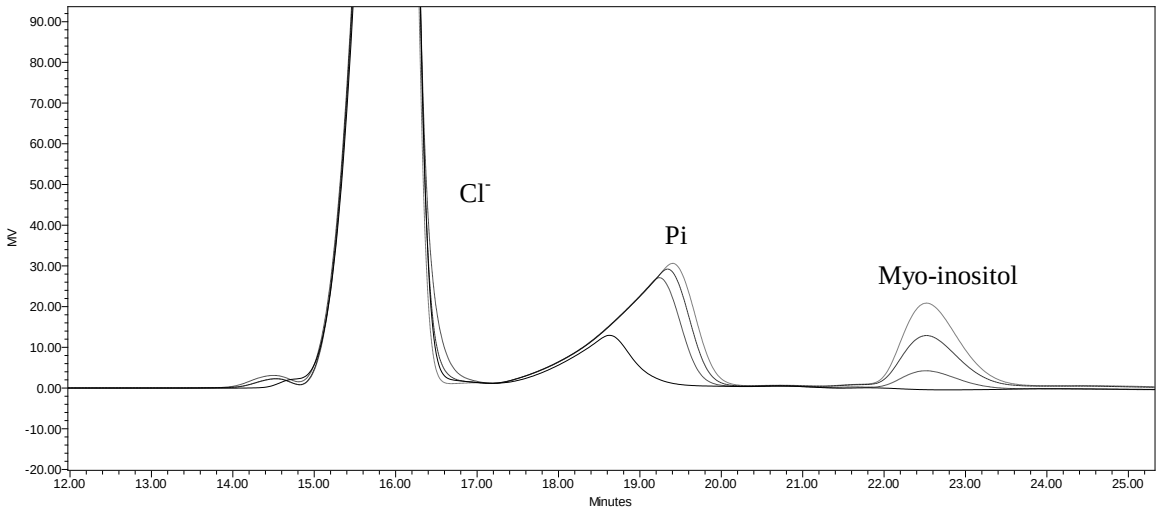

Fig. 5.4. Chromatograms of hydrolysis of myo-inositol phosphate containing NaCl elution with 100 FTU *E.coli* / g NaCl elution. 45 ℃, pH 5.0. —— 0 hr; -·-·- 0.5 hr; ·····2 hr;- - - - - 8 hr.

5.4 Conclusion

An isocratic HPLC method was demonstrated for the separation, detection and quantification of Cl^-, myo-inositol, and Pi samples collected from the hydrolysis of LSW. All three components eluted in one column volume. The retention time for Cl^-, Pi, and myo-inositol is 15, 17, and 22 min, respectively. The concentrations of myo-inositol and Pi produced from the hydrolysis of phytate in the LSW are within the linear range of the detector. Therefore, this method is a fast and reliable method for myo-inositol and Pi analysis in samples where their concentrations are larger than those in the biological samples. The linear range of this method for myo-inositol was 0-20 mg/ml. The quantification of myo-inositol was validated in the concentration range of 19.5 µg/ml to 20 mg/ml standard solution, the limit of detection was 0.01 mg/ml, and the limit of quantification was 0.04 mg/ml. The developed HPLC method provides for simultaneous determination of Pi. The LOD and LOQ for Pi analysis were 0.05 and 0.17 mg/ml, respectively. The linear range was 0-10 mg/ml.

Reference

[1] Noureddini, H., Dang, J., 2010. An integrated approach to the degradation of phytates in the corn wet milling process. Bioresour. Technol. 101, 9106-9113.

[2] Alam, S.Q., 1971. The Vitamins: Chemistry, Physiology, Pathology, Methods. New York, Academic Press. vol. III, pp. 363-367.

[3] Thorsell, A.G., Persson, C., Voevodskaya, N., Busam, R. D., Hammarstroem, M., Graeslund, S., Graeslund, A., Hallberg, B. M., 2008. Structural and biophysical characterization of human myo-inositol oxygenase. J. Biol. Chem. 283, 15209-15216.

[4] Eagle, H., Oyama, V. I., Levy, M., Freeman, A. E., 1957. myo- Inositol as an Essential growth factor for normal and malignant human cells in tissue culture. J. Biol. Chem. 226,191-205.

[5] Holub. B. J., 1992. The nutritional importance of inositol and the phosphoinositides. The New England journal of medicine. 326, 1285-1287.

[6] Clements, R.S., Darnell, B., 1980. Myo-inositol content of common foods: development of a high-myo- inositol diet. The American journal of clinical nutrition. 33, 1954-1967.

[7] Pereira, G.R., Baker, L., Egler.J., Corcoran. I ., Chiavacci, R., 1990. Serum myoinositol concentrations in premature infants fed human milk, formula for infants, and parenteral nutrition. Am. J. Clin. Nutr. 589-593.

[8] Nick, G.L. In Townsend Letter for Doctors and Patients. (2004), available at: findarticles.com/p/articles/mi_m0ISW/is_255/ai_n6211958/

[9] MacGregor, L.C. and Matschinsky., F.M., 1984. Serum myoinositol concentrations in premature infants fed human milk, formula for infants, and parenteral nutrition.Anal. Biochem. 141, 382-389.

[10] Loewus, F.A.,1994. Enzymic determination of inositol and inositol phosphates. Methods in Carbohydrate Chemistry. 10, 63-68.

[11] Ashizawa, N., Yoshida, M., and Aotsuka, T., 2000. An enzymatic assay for myo-inositol in tissue samples. J. Biochem. Bioph. Meth. 44, 89-94.

[12] Kouzuma,T., Takahashi, M., Endoh,T., Kaneko, R., Ura, N., Shimamoto, K., and Watanabe, N., 2001. An enzymatic cycling method for the measurement of myo-inositol in Biological samples. Clinica. Chimica. Acta. 312, 143-151.

[13] Gudermann,T.W. and Cooper, T.G., 1986. A sensitive bioluminescence assay for myo-inositolAnal. Biochem. 158, 59-63.

[14] de Koning, A. J., 1994. Determination of myo-inositol and phytic acid by gas chromatography using scyllitol as internal standard. Analyst (Cambridge, United Kingdom).119, 1319-23.

[15] Troyano, E., Villamiel, M., Olano, A., Sanz, J., and Martinez-Castro, I., 1996. Monosaccharides and *myo*-Inositol in Commercial Milks. J. Agr.Food.Chem. 44, 815-817.

[16] March, J. G., Forteza, R., and Grases, F., 1996. Determination of inositol isomers and arabitol in human urine by gas chromatography mass spectrometry Chromatographia. 42, 329-331.

[17] Lauro, P.N., Craven, P.A., and DeRubertis, F.R., 1989. Micro-quantitation of lens Myo-inositol by anion exchange chromatography. Anal. Biochem. 178, 331-335.

[18] Indyk, H.E. and Woollard, D.C., 1994. Determination of free myo-inositol in milk and infant formula by high-performance liquid chromatography. Analyst (Cambridge, United Kingdom). 119, 397-402.

[19] Perello, J., Isern, B., Costa-Bauza, A., and Grases, F., 2004. Determination of myo-inositol in biological samples by liquid chromatography–mass spectrometry.J. Chromatogr. B. 802, 367-370.

[20] Soga, T. and Heiger, D.N., 1998. Simultaneous Determination of Monosaccharides in Glycoproteins by Capillary Electrophoresis Anal. Biochem. 261, 73-78.

[21] Kong, L.Y., Wang, Y., and Cao, Y.H., 2008. Determination of *Myo*-inositol and d-*chiro*-inositol in black rice bran by capillary electrophoresis with electrochemical detection. J. Food. Compos. Anal. 21(6), 501-504.

[22] Pulliainen, T.K., Wallin, H.C., 1994. Determination of total phosphorus in foods by colorimetric measurement of phosphorus as molybdenum blue after dry-ashing: NMKL interlaboratory study. J. AOAC. Int. 77, 1557-1561.

[23] Guideline on the Validation of Analytical Procedures: Methology Q2B from International Conference on Harmonization, 1996.

Chapter 6

A SEC approach for myo-inositol and phosphate recovery

6.1 Introduction

An integrated process was developed to completely degrade the phytates in LSW into myo-inositol and inorganic phosphate (Pi) with *E.coli* (AppA2) phytase. This process was presented in chapter 4 of this dissertation. As this process included an intermediate anion exchange separation step where NaCl solution was used as the eluent, the final products consisted of *E.coli* phytase, myo-inositol, NaCl, and Pi. If separated, the myo-inositol and Pi are highly desirable and have potential to be marketed. Since there is a large difference in molecular weights of *E.coli* phytase (~46 kDa) and other components: myo-inositol (~180 Da), NaCl (~58.44 Da), and Pi (~98 Da), size exclusion chromatography (SEC) was selected and studied for this separation.

SEC has been widely used in the separation and characterization of biopolymers (peptides, proteins, polysaccharides etc.), carbohydrates, cellulosics, fats, humic acids and related compounds, inorganic compounds and colloids, etc [1]. SEC (or gel-filtration chromatography) is a technique for separating components on the basis of molecular size. In SEC, molecules larger than the pore size of the stationary phase elute in the void volume, whereas those entering the pores are eluted in order of decreasing molecular size. However, owing to specific solute-matrix interactions, non-size-exclusion effects are also observed in SEC columns, for both organic and inorganic supports. These include: ion exclusion and ion exchange, hydrophobic interaction and hydrogen bonding

[1-4]. Fig.6.1. gives examples of non-size-exclusion effects on two SEC columns, silica-based and polysaccharide-based, respectively.

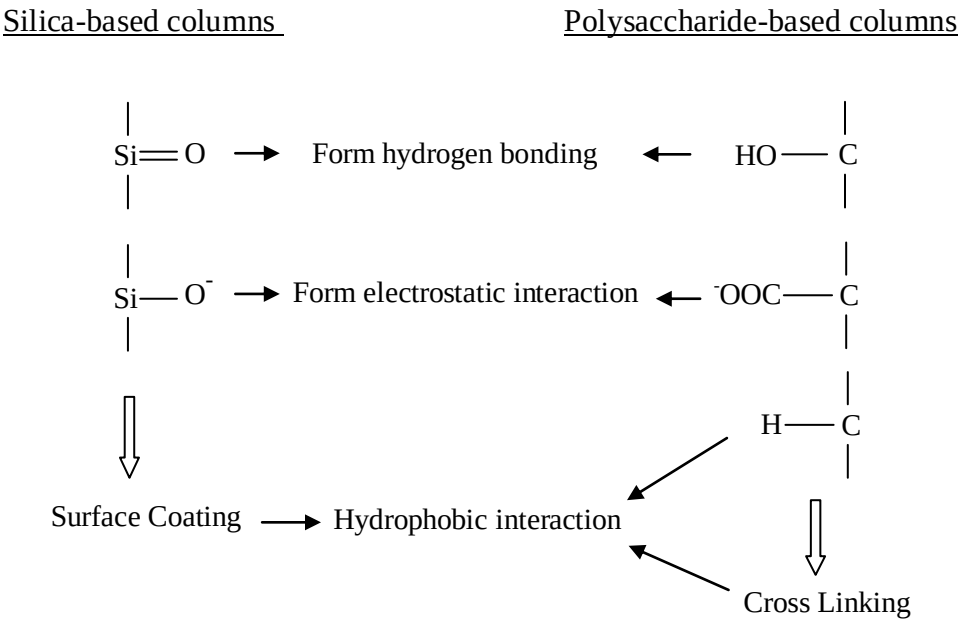

Fig.6.1. Chemical groups present on the surfaces of resins that are responsible for non-size-exclusion effects [6]

Non-size-exclusion effects cause the elution of most polyions and biopolymers deviating from a pure size-exclusion mechanism. By using mathematical modeling, Garcia et al. (1995) investigated the separation profiles of polyanions which were influenced by electrostatic and hydrophobic interactions in a silica-based SEC column [2]. Rao et al. reported a deviation behavior of tryptofan on a Toyopearl HW-40S column which was mainly caused by the hydrophobic interaction between the solute and the matrices [5]. Specht and Frimmel (2000) studied the specific interactions of several organic substances on a Toyopearl TSK HW 50S column. Elution profiles of buffered and non-buffered samples were investigated and compared. Ion-exclusion interactions with the matrix were observed for monocarboxylic acids which carry negative charges. With a buffered solution, the repulsive interactions between capronic acid and the gel were reduced, resulting retardation of this component. They also investigated the chromatograms of several alcohols and found that the hydrophobic interaction dominates the specific interactions between the solute and the packings, while there is little influence caused by ionic strength variation. The hydrophobic interaction gets stronger as the number of carbon atoms increases [3].

In general it is desirable to minimize the non-size-effects, particularly for characterization purposes, so that a better resolution and sharp peaks can be obtained [1]. For example, in determining proteins and humic substances in natural organic matter, a solution of strong ionic strength, normally a NaCl or phosphate buffer, is needed to reduce interactions between the stationary phase and solutes [1, 4, 6]. However, in some instances, the non-size-effects are also exploited to improve the separation of macromolecules of similar hydrodynamic volume. For example, based on the ionic

exchange interactions, Sullivan and Weber (2006) separated hydrophilic neutrals (carbonyls, polyols, and saccharides) from bases on a Superdex^{TM}-30 column [4]. Moreover, by utilizing the gel chromatographic effects caused by differences in ionic strength between sample and eluent, Specht and Frimmel (2000) concluded that more structural information of natural organic matter could be obtained [3].

The purpose of this work was to explore the possibility to isolate *E.coli* phytase, myo-inositol, NaCl, and Pi with a SEC based approach, by utilizing both size-exlusion and non-size exclusion effects. The effects between solute and the stationary phase of SEC was utilized for the separation of myo-inositol, NaCl, and Pi, since these components are different in their structures and electrical charges carrying on.

The well known TSK-Toyopearl HW gels were selected as the packings. The gels were comprised of hydrophilic matrices prepared from a copolymerization of ethylene glycol and methacrylate. This group of resins is slightly negatively charged. Toyopearl resins are mechanically stable and can be used under high pressure conditions [7].

6.2 Experimental procedures

6.2.1 Materials

LSW samples used in this study were from Cargill, a wet milling corn facility in Blair, Nebraska. All samples were kept in a refrigerator (4 ^{o}C) prior to use. As samples contained a mixture of solid and liquid, care was entailed to ensure the homogeneity of the samples taken before experiments.

Natuphos 10,000 liquid enzyme (3-phytase produced from *A. niger*) was purchased from BASF (Florham Park, NJ). OptiPhos 5000 liquid enzyme (*E. coli* AppA2) was generously provided by JBS United Inc. (Sheridan, IN). The nominal activity of this enzyme was 5000 FTU/g. Optiphos enzyme was purified with a fisherbrand dialysis tubing (Nominal MWCO: 6,000-8,000 Da) (Fisher Scientific, Pittsburgh, PA) before experiments.

Myo-inositol standard (99%), sulfuric acid (95-98%), sodium molybdate dehydrate (99.5%), ascorbic acid, hydrochloric acid (37%), potassium dihydrogen phosphate (1 M), zinc oxide (99.9%), and potassium hydroxide were purchased from Sigma-Aldrich (St. Louis, MO). Potassium Phosphate Monobasic (KH_2PO_4)(99+%) was purchased from Fisher Scientific (Pittsburgh, PA). DOWEX Marathon MSA anion exchange resin was purchased from Sigma-Aldrich (St. Louis, MO). Toyopearl HW-40S resin was kindly provided by Tosoh Bioscience LLC (Grove City, OH). Deionized (DI) water was further purified by a Simplicity Ultra Pure Water System from Millipore (Billerica, MA).

6.2.2 Sample preparation

LSW was subjected to a 2 hr hydrolysis with 1 FTU *A.niger* phytase/g LSW at 35 ℃, where the phytates in the LSW were partially hydrolyzed to negatively charged myo-inositol phosphates. The reaction mixture was incubated in a temperature-controlled incubator (Imperial III, Lab-Line Instruments, Inc., Melrose, IL) in which a shaker (C2 classic platform shaker, New Brunswick Scientific Co., Ltd., Edison, NJ) was placed to mix the reaction flasks at 200 rpm. The reaction was terminated after 2 hr by

heating the samples in a water bath at 100 °C for 10 min. Precautions were taken to avoid water vapor entering the samples.

Hydrolyzed LSW samples were cleared of solid particles in a centrifuge (8464 Thermo Electron Co., Milford, MA), at 11,000 *g* for 10 min. 10 g fully hydrated DOWEX Marathon MSA anion exchange resins were packed into a Kontes Flex-Column glass chromatography column (VWR International, Batavia, IL) which is 1.0 cm in diameter and 20 cm in length. 5 bed volumes of the clarified portion of the samples were passed over the anion exchange column to separate the myo-inositol phosphates from the neutral and cationic fractions in the system.

The negatively charged myo-inositol phosphate species adsorbed to the anion exchange resin were eluted with 1 M NaCl solution. The NaCl elution was then subjected to a complete hydrolysis with 100 FTU *E.coli* phytase/g NaCl solution, 45 ℃ and pH 5.0. After 48hr, the reaction was terminated by heating the samples in a water bath at 100 °C for 10 min.

6.2.3 SEC Chromatography

Low pressure SECs were performed on a Kontes Flex-Column glass chromatography column (VWR International, Batavia, IL)., 1.0 cm ID x 20 cm length, and two stainless steel columns: 0.75 cm ID x 72 cm length and 0.75 cm ID x 150 cm length, respectively. Columns were hand-packed with Toyopearl HW-40S resin according to the manufacturer's instructions. The resin has exclusion limits up to 10,000 Da. The mobile phase used was deionized (DI) water purified by a Simplicity Ultra Pure

Water System from Millipore (Billerica, MA). The three new columns were flushed with 1 column volume of water each, and then equilibrated with 5-10 column volumes of water (flow rate 0.2 ml/min.)

1 mL sample prepared as described in section 2.2 was manually injected by means of a superloop of 3 ml volume. The mobile phase was pumped into the columns using a peristaltic pump at room temperature and a flow rate of 0.16 mL/min. Samples were manually collected every 5 min for 1.5 column volume elution. Samples were analyzed for the myo-inositol and Pi content with the HPLC method developed in chapter 5.

To investigate the non-size-exclusion effects, another experiment was carried out on the 0.75 cm ID x 150 cm length stainless steel column, with 0.1 M NaCl buffer as the mobile phase. The column was equilibrated with 0.1 M NaCl for 12 hr before experiments. Experiment conditions and sample collections were the same as presented above.

6.2.4 Analysis

The HPLC system used for the analysis was a Waters Alliance system (Milford, MA) and consisted of a Separation Module (Waters 2695) and a RI detector (Waters 2414). The separation was performed on a coupled Bio-Rad Fermentation Monitoring column (150 x 7.8 m) and an Aminex® HPX-87H column (300 x 8.7 mm), in series, with a Bio-Rad Micro-Guard Cation H Refill Cartridges (30 x 4.6 mm) (Bio- Rad Laboratories, Hercules, CA) guard column. The column temperature was maintained at 65 ℃ inside a waters column heater module. The RI detector was held at 30 ℃. The mobile phase was a 0.5 mM sulfuric acid solution. Analysis was performed isocratically by delivering the mobile phase at a flow rate of 0.4 mL/min. Total run time for this

method was 60 min. Peaks were identified by injecting standards of NaCl, Na_2SO_4, HCl, KH_2PO_4, and myo-inositol into the system. The injection volume of sample solutions were 50 µl. The elution time for Cl^-, Pi and myo-inositol was about 15 min, 17 min, and 22 min, respectively.

Pi and Myo-inositol content of samples were quantified based on calibration curves using standards solutions. Pi standard solutions were prepared in DI water with KH_2PO_4. KH_2PO_4 was firstly dried in a 20GC convection oven (Quincy Lab, Inc., Chicago, IL) at 101 ℃ for 2 hr. The dried KH_2PO_4 was then used to prepare 0.1, 1, 2, 4, 6, 8, 10 mg Pi/ml standard solutions for calibration. Myo-inositol standard solutions were prepared in DI water. 20 mg/ml myo-inositol was initially prepared and 1:2 serial dilutions were made until the concentration reached 9.8 µg/ml. The concentration of myo-inositol is ranged from 9.8 µg/ml to 20 mg/ml.

6.3 Results and discussion

6.3.1 The amount of myo-inositol and Pi for recovery

Samples were prepared following the process outlined earlier in section 6.2.2. Myo-inositol and Pi produced were quantified as described in section 6.2.4. The myo-inositol and Pi produced in the process are 3.74 ± 0.02 and 3.32 ± 0.02 mg/g NaCl solution, respectively. The concentration of Cl^- was determined to be 26.57 mg/g NaCl solution.This is the baseline for determining the recovery efficiency of myo-inositol and Pi on the SEC columns in this work.

6.3.2 SEC separation

The separation of *E.coli* phytase, myo-inositol, NaCl, and Pi were performed on SEC columns packed with Toyopearl HW-40S resins. The upper exclusion limit of this resin is 10,000 Da. Since the *E.coli* phytase used in this study has a molecular weight of 46 kDa which is larger than the exclusion limit, it eluted in the void volume. To prevent the introduction of unwanted ions into the system, DI water was used as the mobile phase. Experiments were performed as described in section 6.2.3. Samples were collected and analyzed by a HPLC column according to section 6.2.4. The peaks appeared were identified as Cl^-, Pi and myo-inositol which eluted at 15.7, 18, and 22 min, respectively. Data obtained from the HPLC system are summarized and presented in Fig.6.2-4.

Fig.6.2 presents the elution profile of myo-inositol, Cl^-, and Pi on a 1.1 cm ID x 20 cm length column. As shown in Fig.6.2, the peaks of myo-inositol, Cl^-, and Pi significantly overlapped with each other. However, a small portion of Pi and myo-inositol was still separated.

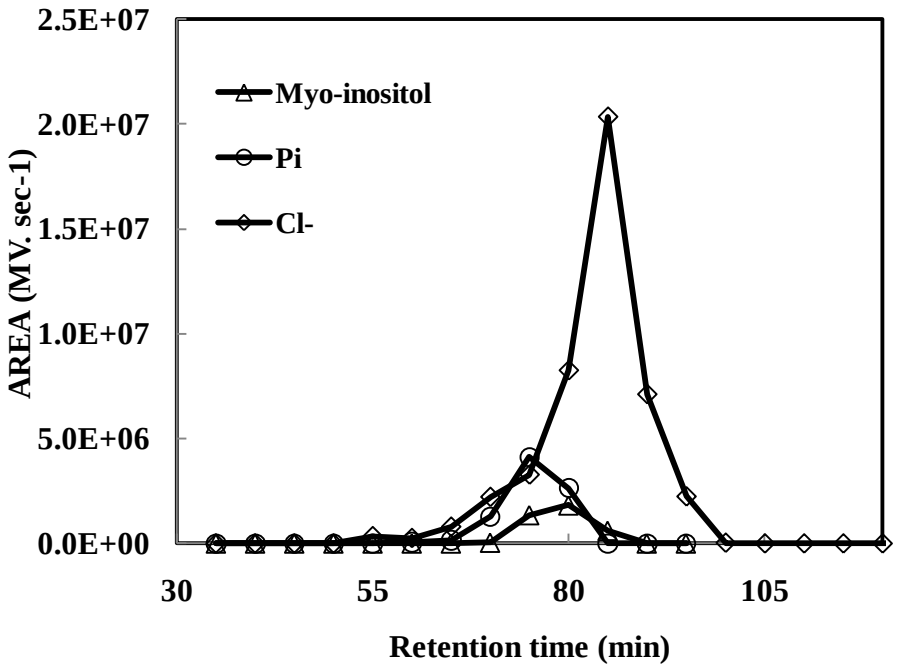

Fig.6.2. Separation profile of Pi, myo-inositol, and Cl^- on a 1.1 cm ID x 20 cm length column packed with Toyopearl HW-40S resins. Eluent was DI water at room temperature and a flow rate of 0.16 ml/min. Sample injection volume was 1 mL.

on the column. After quantification, there were about 15.9% myo-inositol (of total myo-inositol) and 18% Pi (of total Pi) separated from each other. From Fig.6.2, Pi eluted before myo-inositol, indicating the existence of non-size-exclusion effects between the solute and the Toyopearl HW-40S resins. In the absence of non- size-exclusion effects in the system, myo-inositol would have been expected to elute ahead of Pi. Thus, this SEC approach might be able to separate myo-inositol from Pi. To verify this, a 0.75 cm ID x 72 cm length column, which has a higher number of plates, was used.

The separation profile on a 0.75 cm ID x 72 cm length column is presented in Fig.6.3. From Fig.6.3, myo-inositol, Pi, and Cl^- were separated a little further. Pi eluted first followed by myo-insositol and finally Cl^-. However, as shown in Fig.6.3, there were still large areas of overlap. On this 0.75 cm ID x 72 cm length column, based on the calibration curve calculation, 35.3% myo-inositol and 37.7% Pi were separated from each other and 50% Cl^- was obtained as pure product, while the rest of Cl^- was mixed with myo-inositol and Pi. This indicated that a better separation might be achieved on a longer column. Thus, a 0.75 cm ID x 150 cm length column was used and studied for the separation of myo-inositol, Cl^- and Pi.

Fig.6.4 presented the separation of myo-inositol, Cl^-, and Pi on a 0.75 cm ID x 150 cm length column. From Fig.6.4, clear resolutions were observed with these three components. There were about 69.8% myo-inositol and 69.8% Pi separated from each other. If taking 1% contamination into account, the production of myo-inositol and Pi was 94.1% and 87.8 % respectively. Meanwhile, about 93% of total Cl^- was completely separated from myo-inositol and Pi. The rest of Cl^-, about 7%, was mixed with myo-

inositol. With the inclusion of Cl^-, the pure product of myo-inositol on this column was about 53%.

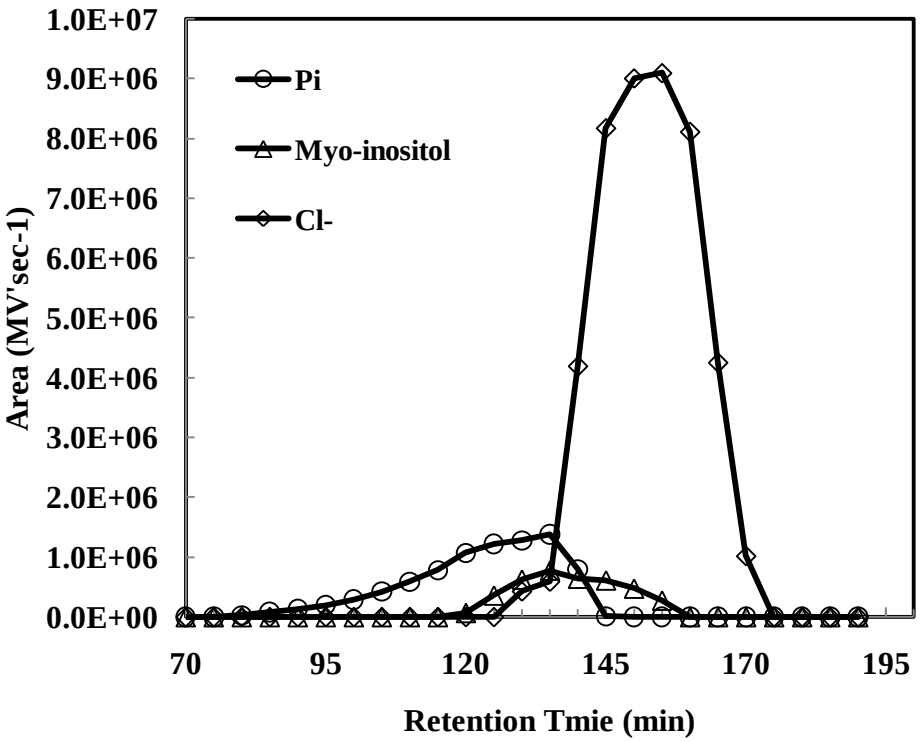

Fig.6.3. Separation profile of Pi, myo-inositol, and Cl^- on a 0.75 cm ID x 72 cm length column packed with Toyopearl HW-40S resins. Eluent was DI water at room temperature and a flow rate of 0.16 ml/min. Sample injection volume was 1 mL.

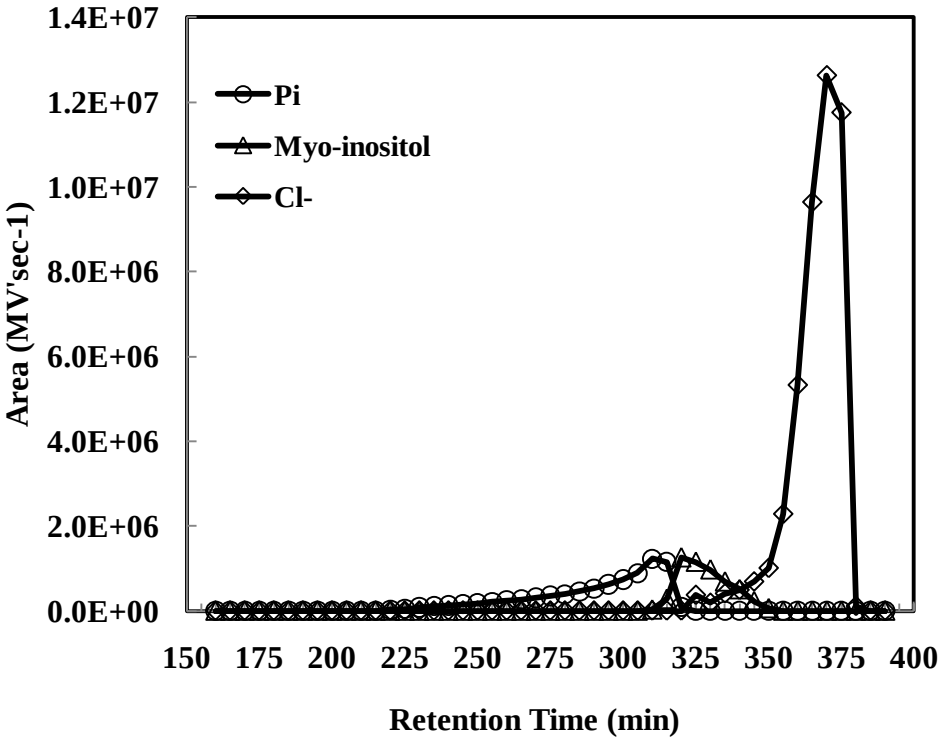

Fig.6.4. Separation profiles of Pi, myo-inositol, and Cl^- on a 0.75 cm ID x 150 cm length column packed with Toyopearl HW-40S resins. Eluent was DI water at room temperature and a flow rate of 0.16 ml/min. Sample injection volume was 1 mL.

From the results presented, non-size-exclusion-effects were involved in the separation of myo-inositol, Cl^-, and Pi. If there were only size-exclusion-effects in the system, the elution sequence on the columns should be myo-inositol, Pi, and Cl^-, which is from larger molecules to smaller molecules. However, the elution sequence of Pi, myo-inositol, and Cl^- on the columns indicated the existence of non-size-exclusion-effects. The elution of Pi before myo-inositol might be attributed to the dominancy of ion-exclusion effects between Pi and the slightly negatively charged stationary phase over the size-exclusion-effects. The separation of myo-inositol might be dominated by the hydrophobic interactions among the carbon atoms [3]. However, for Cl^- which had ion-exclusion effects with the stationary phase, the results showed that the size-exclusion-effects dominated in its separation, since it is eluded last.

The bed volumes of these three columns were 15.7, 30.91, and 66.2 ml, respectively. From Fig.6.2-4, all components were excluded in one bed volume of elution. Mass balance calculations indicated that there was no irreversible adsorption of the solutes on the column, every component eluted completely. The separation efficiency on these three columns were calculated and summarized in table 6.1. The results showed that *E.coli* phytase, myo-inositol, Cl^-, and Pi were able to be separated on Toyopearl HW-40S resins by utilizing both size-exclusion-effects and non-size-exclusion-effects.

Table 6.1 Separation efficiency of Pi, myo-inositol, and Cl^- on SEC columns

Column	Column Volume (ml)	Mobile phase	myo-inositol (% of Total myo-inositol)	Pi (% of Total Pi)	Cl^- (% of Total Cl^-)
1.0 cm ID x 20 cm L	15.70	water	15.9	18.0	20.9
0.75 cm ID x 72 cm L	30.91	water	35.5	37.7	50.0
0.75 cm ID x 150 cm L	66.23	water	69.8	69.8	93.0
0.75 cm ID x 150 cm L	66.23	0.1 M NaCl	41.2	48.5	N/A

Note: NA, not available. The data are mean value of 2 independent experiments.

6.3.3 Investigation of non-size-exclusion effects

Experiments were performed according to section 6.2.3 to further investigate the existence of non-size-exclusion effects. In the experiment, samples were separated on the 0.75 cm ID x 150 cm length stainless steel column, with 0.1 M NaCl buffer as the mobile phase. Samples were collected and analyzed according to section 6.2.4. Results are summarized in Fig. 6.5 and table 6.1.

From Fig.6.5, the separation efficiency of myo-inositol and Pi decreased, compared with the one with DI water as the mobile phase. There were about 41.2% myo-inositol and 48.5% Pi separated from each other. Results showed that Pi was strongly influenced by the ionic strength of the mobile phase. With 0.1 M NaCl buffer as the mobile phase, the elution volume of Pi increased and the peak was narrower and sharper. This indicated the decrease of repulsive interactions between Pi and the column, owing to the increase of ionic strength in the mobile phase. Therefore, the 0.1 M NaCl buffer has a charge shielding effect on Pi. As a result, Pi elution was retarded. The sharper peak obtained on the column could be attributed to both the ion-exclusion effect and the size-exclusion-effects. However, the elution profile of myo-inositol was almost not affected by the ionic strength differences of the mobile phase, as the interaction between myo-inositol and the column was mainly hydrophobic interaction.

This experiment showed that non-size-exclusion effects were involved in the separation of components in the samples.

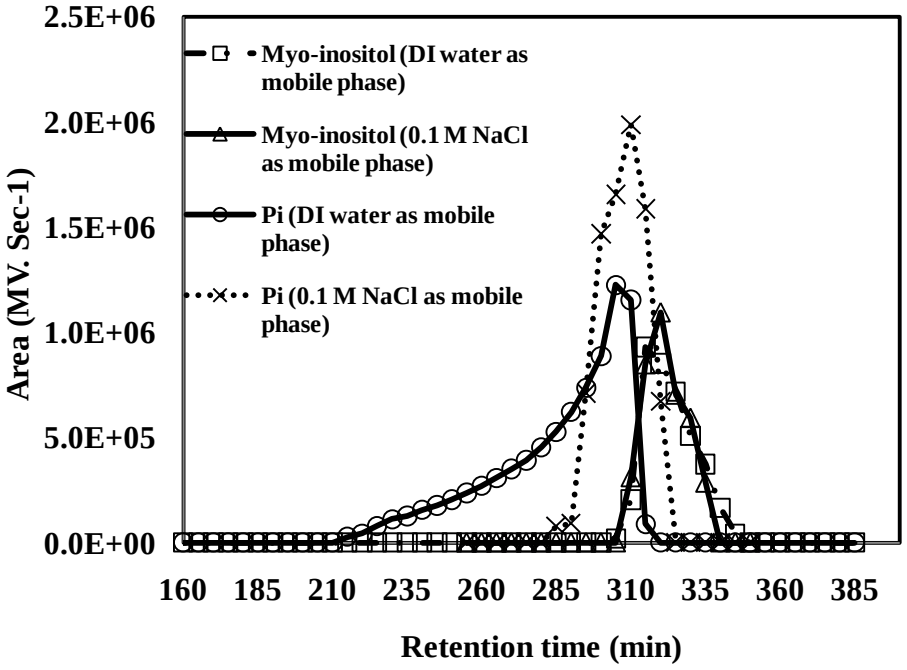

Fig.6.5. Separation profiles of Pi and myo-inositol, and Cl^- on a 0.75 cm ID x 150 cm length column packed with Toyopearl HW-40S resins. Eluent was 0.1 M NaCl buffer at room temperature and a flow rate of 0.16 ml/min. Sample injection volume was 1 mL.

6.4 Conclusion

Size-exclusion chromatography packed with Toyopearl HW-40S resins can be used to isolate and purify myo-inositol and Pi from their mixture with *E.coli* phytase and Cl^-. *E.coli* phytase was separated from the system by size-exclusion-effects. Whereas myo-inositol, Cl^-, and Pi were separated by both size-exclusion and non-size-exclusion-effects, depending on which effect dominates. For the three different length columns investigated in this study, 1.1 cm ID x 20 cm length, 0.75 cm ID x 72 cm length, and 0.75 cm ID x 150 cm length column, respectively, the separation efficiency increased with the increase in column length or number of plates. On the 0.75 cm ID x 150 cm length column, 53% myo-inositol (of the total myo-inositol) and 69.8% Pi (of the total Pi) were recovered as pure products. A complete separation of myo-inositol and Pi might be achieved with a longer column or with a high pressure SEC approach.

Reference

[1] Barth, Howard G., Boyes, Barry E., and Jackson, Christian., 1998. Size exclusion chromatography and related separation techniques. Analytical Chemistry, 70(12), 251R-278R.

[2] Garcia, Rosa., Porcar, Iolanda., Figueruelo, Juan E., Soria, Vicente., and Campos, Agustin., 1996 Solution properties of polyelectrolytes. XII. Semi-quantitative approach to mixed electrostatic and hydrophobic polymer -gel interactions. Journal of Chromatography, A.721(2), 203-12.

[3] Specht, Christian H. and Frimmel, Fritz H., 2000. Specific interactions of organic substances in size - exclusion chromatography. Environmental Science and Technology. 34(11), 2361- 2366.

[4] Sullivan, Amy P. and Weber, Rodney J.,2006. Chemical characterization of the Ambient organic aerosol soluble in water : 2. Isolation of acid, neutral, and basic fractions by modified size-exclusion chromatography. Journal of Geophysical Research, [Atmospheres]. 111(D5).

[5] Rao, Pingfan., Liu, Shutao., Zhang, Rongzhen., Chen, Gongrui., and Zheng, Yuqiang., 1997. Deviation of size - exclusion chromatographic behavior of tryptophan on Toyopearl HW- 40S column. Fuzhou Daxue Xuebao, Ziran Kexueban. 25(2),116-119.

[6] Arakawa, Tsutomu., Ejima, Daisuke., Li, Tiansheng., and Philo, John S., 2010. The critical role of mobile phase composition in size exclusion chromatography of protein pharmaceuticals. Journal of Pharmaceutical Sciences. 99(4),1674-1692.

[7]http://www.separations.us.tosohbioscience.com/Products/ProcessMedia/ByMode/SEC/Toyop earlHW40.htm

Chapter 7

Discussion of possible scale-up for the developed integrated progress

A mid-size wet milling process produces around 1,403 ton light steep water per day [1]. Depending on the market demand of myo-inositol, part (or all) of the light steep water would be subjected to the treatment of the developed integrated process, as described in chapter 4. A process flow diagram was created for a possible scale-up of this process (Fig 7.1.) Light steep water from the steeping tank was subjected to a partial hydrolysis catalyzed with *A.niger* phytase. The temperature during the steeping is in the range 45 to 55 ℃ [2], thus the light steep water from the steeping tank could be directed to the reactor for partial hydrolysis without heating. Flow reactors, *continuous stirred-tank reactor* (*CSTR*) or piston flow reactor (PFR), could be chosen for the partial hydrolysis. Flow reactors can produce high-volume chemicals, involving considerations such as heat and mass transfer, ease of scale up, and the logistics of materials handling. In CSTRs, reactants and products are at steady state with continuous flow. The components throughout the entire reactor assumes a uniform composition, exit stream has the same composition as in the reactor. CSTRs have good temperature control and low operating cost. They are easy to construct and clean. However, the conversion per unit volume in this reactor is low. For comparison, PFRs have higher conversion per unit volume and good heat transfer. However, in PFRs, undesired thermal gradients may exist. Temperature control in the PRFs is also poor and shutdown and cleaning may be expensive [3].

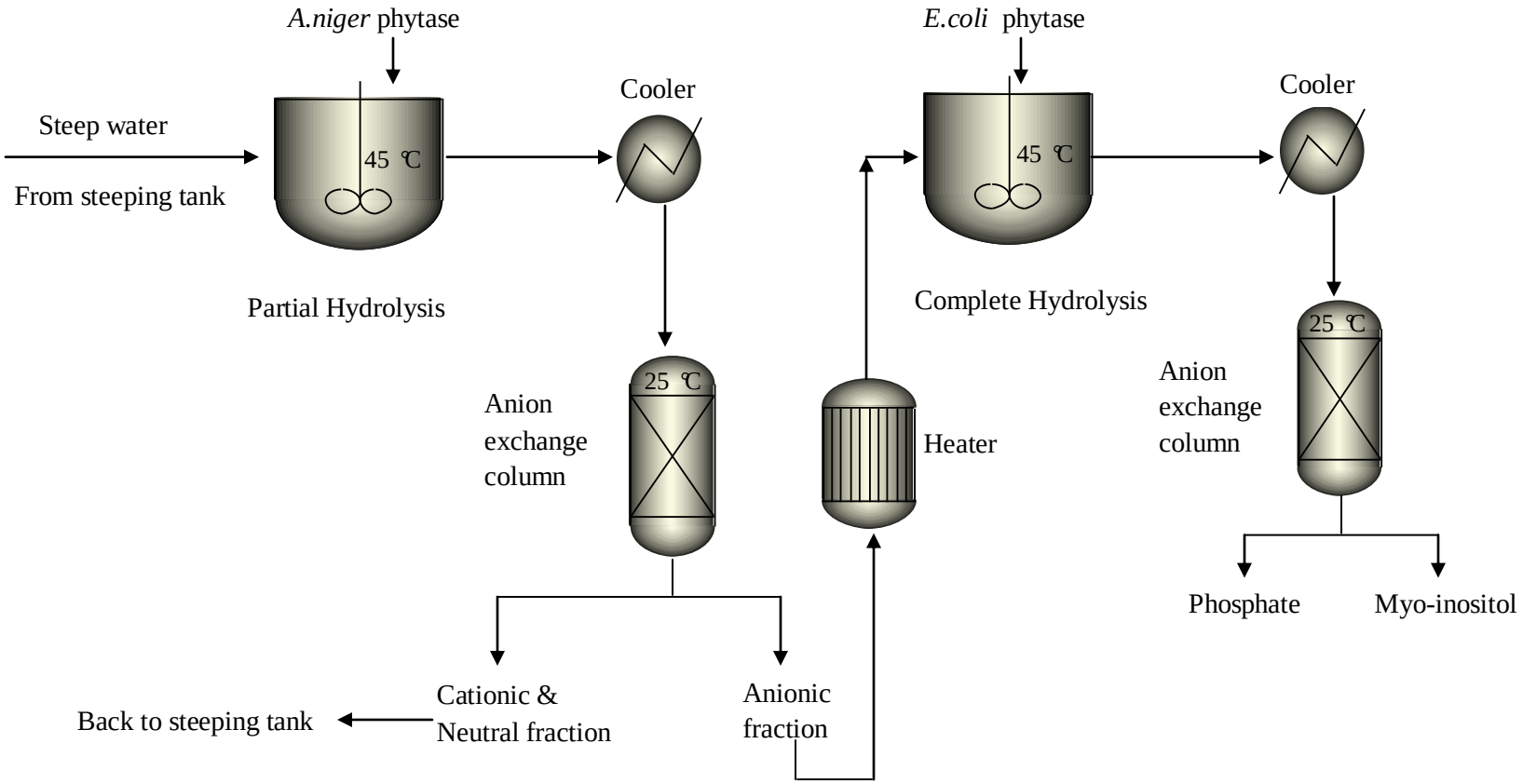

Fig.7.1. Process Flow Chart of scale up process

After partial hydrolysis, the light steep water was subjected to an anion exchange treatment. Before supplied to the column, it should be cooled down to room temperature. For the scale up of anion exchange column, resins of long lifetime, lot-to-lot consistency, and long-term availability should be used. During the scale up, the column volume should be increased by keeping the height of the resin bed constant and increasing the column diameter. The total load of substrate per unit of resin should keep the same and the linear flow rate should be identical [4].

The anionic fraction collected from the anion exchange column was then heated up to around 45 ℃ and subjected to complete hydrolysis. The reactors for the complete hydrolysis could also be CSTRs or PFRs. After complete hydrolysis, the separation of myo-inositol and phosphate will be carried out with chromatography. Size exclusion chromatography or gel filtration separates components based on size exclusion and non-size exclusion effects. However, because this method is slow, its application to pilot scale is often limited. Considering the charge differences between myo-inositol and phosphate, an anion exchange chromatography might be used instead. This requires E.coli phytase to be separated in previous step. To facilitate their separation from the main stream, phytases could be immobilized onto solid supports. The immobilized phytases can also be recovered and reused in the reactions.

Besides above mentioned, for scale-up, it is also important to maintain the same physical and chemical conditions as in lab scale.

Reference

[1] Rausch, K. D., Raskin , L. M., Belyea ,R. L., Agbisit, R. M., Daugherty, B. J., Clevenger, T. E. and Tumbleson, M.E., 2005. Phosphorus concentrations and flow in Maize wet milling streams. Cereal Chem. 82, 431-435.

[2] Johnson, L. A. and May, J. B., 2003. Corn: Chemistry and Technology, 2nd ed., (White, P. J. and Johnson, L. A., eds.). American Association of Cereal Chemists, St. Paul, MN, pp. 449–494.

[3] Nauman, E. Bruce, 2007. Chemical reactor design, optimization, and scaleup, 2nd ed. Wiley.

[4] Sattar, Al-Jibbouri., 2006. Scale-up of chromatographic ion-exchange processes in biotechnology. J. Chromatogr. A. 1116, 135-142.

Chapter 8

Suggested future work

8.1 Myo-inositol and phosphate recovery from the dry milling process. Dry-milling process accounts for 82% of current US ethanol production, and all planned expansion in capacity will also utilize this process. As P concentration in DDGS is high (0.9% DM), DDGS could be an abundant resource for the production of myo-inositol and P.

8.2 Recovery of more valuable co-products from both dry and wet milling process : 1) corn fiber oils; 2) proteins; 3) vitamins, such as carotenroids, tocopherols, and tocotrienols etc.4) other chemicals, such as phytosterols.

8.3 Development of separation and analytical methods for valuable chemicals in corn.